



## **Thesis declaration**

I, Emily Taljaard, verify that in submitting this thesis;

The thesis is my own account of the research conducted by me, except where other sources are fully acknowledged in the appropriate format,

the extent to which the work of others has been used is documented by a percent allocation of work and signed by myself and my Principal Supervisor,

the thesis contains as its main content work which has not been previously submitted for a degree at any university,

the University supplied plagiarism software has been used to ensure the work is of the appropriate standard to send for examination,

any editing and proof-reading by professional editors comply with the standards set out on the Graduate Research School website, and

that all necessary ethics and safety approvals were obtained, including their relevant approval or permit numbers, as appropriate.

Signed:

Date 07/12/2023

,

## **Acknowledgments**

There were many people who helped me throughout this project, however, it would take me years to name everyone individually, but I am extremely grateful to everyone. I would like to thank the following people who have supported and helped me with this study and without whom this project would not have been completed.

I would like to thank all my supervisors, Dr James Tweedley, Dr Alan Cottingham, Dr Danielle Johnston, and Dr Kerry Trayler, for not only providing me with the opportunity to conduct this research but also for their ongoing support, feedback, and guidance. Without your invaluable knowledge and supervision, I would not have been able to make it through this Accelerated Masters program or discover my love for this species.

I would also like to acknowledge the Department of Primary Industries & Regional Development (DPIRD) and the Department of Biodiversity, Conservation, & Attractions (DBCA) for funding this project and supplying staff to make this study possible. Thank you to the commercial fisher, who provided specimens to conduct studies on. This project would be impossible without your assistance and participation.

To Chalie Maus, thank you for skippering the boat and allowing me out in the field. Despite a few cold and rainy nights of catching nothing, I have thoroughly enjoyed my time in the field. Your support on land and insight into commercial fisheries and their policies has been immensely helpful, and without it, this thesis would still be in an editorial state. I would also like to thank all those who assisted in sampling, including Kurt Krispyn, Jake Watsham, David Oberstein, and other DPIRD and DBCA staff members.

I would also like to express my appreciation for Daniel Cox, for not only editing my images, but also allowing me to use unpublished data for the diets of the Southern Eagle Ray in Cockburn Sound. Without this data, comparisons would not be possible, leaving a portion of this thesis incomplete.

To my partner Patrick, thank you for your continuous support throughout this process and for helping me be a normal person compared to just a Masters' student. Thank you for reading through my work when there were so many other things you could be doing. You have been amazing, and I cannot thank you enough.

Lastly, to my dear friends and family, I appreciate you all immensely for all your support, as well as listening to all my facts about the Southern Eagle Ray and Taylor Swift. You have all kept me slightly sane and have helped me make it through this year. I would like to acknowledge Annika Weibel, Ben Roots, and Emma West, who supported me when things did not go right while also undertaking this degree and making it slightly more bearable.

### **Attribution statement**

In accordance with the Murdoch University Graduate Degrees Regulations, it is acknowledged that this thesis represents the work of the Candidate with contributions from their supervisors and, where indicated, collaborators. The Candidate is the majority contributor to this thesis, with no less than 75% of the total work attributed to their efforts.

Emily Taljaard  
Candidate

Dr James Tweedley  
Principal Supervisor

## **Publications**

As of March 2024, the following publications have been derived from information contained in this thesis.

### ***Journal article***

Trayler, K., Taljaard, E., Maus, C., Cottingham, A., Johnston, D. & Tweedley, J. (2024). Ray of white. *Landscape* 39(3): 25-27

### ***Oral presentation***

Taljaard, E., Tweedley, J., Cottingham, A., Johnston, D., Trayler, K. (2023). Abundance and biological characteristics of the Southern Eagle Ray. Australian Marine Science Association (AMSA) Marine Science Student Workshop 2023. Rottneest Island, Australia.

## Abstract

The Southern Eagle Ray, *Myliobatis tenuicaudatus* (Hector, 1877), is the only extant myliobatid species located on the southern coast of Australia and New Zealand. Anecdotal evidence suggests that the abundance of this species has increased in the Swan-Canning Estuary in recent years, likely due to declining streamflow and marinization. As there is little information on this species, which is fished commercially within the estuary, the aim of this study was to determine key biological parameters to assist with future management. Individuals were found in the estuary year-round, with the highest catches in autumn and the lowest in winter. Similar to other myliobatids, there were strong relationships between the measures of disk width (DW) and weight, body length, and total length ( $P = <0.01$  for all regressions). Females reached a larger size and an older age than males (DW = 1,181 vs. 816 mm; Age = 15.9 vs. 9.9 years, respectively), consistent with other members of the Myliobatidae. Females also reached a greater  $DW_{\infty}$  value and grew at a slower rate. The estimated  $DW_{\infty}$  was lower for *M. tenuicaudatus* than other myliobatids. Females matured at a larger size than males ( $DW_{50} = 833$  vs. 595 mm). Gonadosomatic indices peaked in the summer for females and in spring for males, indicating breeding occurs in spring and females release birth young during summer. Unlike other myliobatids, both uteri were found to be fully functional in *M. tenuicaudatus*. As is typical for myliobatids, *M. tenuicaudatus* is a durophagous generalist mesopredator feeding predominantly on polychaetes, crustacean (mainly prawns and brachyurans), and molluscs. An ontogenetic shift in dietary composition was recorded with an increase of molluscs and larger crustaceans at sizes  $>600$  mm DW. The biological data collected in this project will be used to inform future management practices of *M. tenuicaudatus* within Western Australian estuaries.

## Table of contents

Thesis declaration.....	2
Acknowledgments.....	3
Abstract.....	6
1. Introduction.....	13
1.1 Taxonomy.....	13
1.2 Geographical and spatial distribution.....	14
1.3 Biological characteristics.....	16
1.3.1 Morphology.....	16
1.3.2 Age and growth.....	17
1.3.3 Reproduction.....	18
1.3.4 Dietary composition.....	19
1.4 Study aims.....	20
1.5 Study significance.....	21
2. Methods.....	23
2.1 Study site.....	23
2.2 Sampling regime.....	24
2.3 Laboratory processing.....	25
2.3.1 Initial Processing.....	25
2.3.2 Age and growth.....	25
2.3.3 Reproduction.....	27
2.3.4 Dietary composition.....	28
2.4 Data analysis.....	28
2.4.1 Environmental Conditions and ray catches.....	28
2.4.2 Morphology.....	29
2.4.3 Age and growth.....	29
2.4.4 Reproduction.....	30
2.4.5 Dietary comparisons.....	30
3. Results.....	34
3.1 Environmental variables and ray catches.....	34
3.2 Size and morphometrics.....	38
3.3 Age and growth.....	40
3.4 Reproduction.....	43
3.5 Dentition and dietary composition.....	46
4. Discussion.....	56
4.1 Environmental variables and <i>Myliobatis tenuicaudatus</i> catch rates.....	56
4.2 Morphometrics.....	58
4.3 Age and growth.....	60
4.4 Reproduction.....	63
4.5 Diets.....	67
4.6 Limitations.....	73
4.7 Implications and further research.....	74
5. Conclusion.....	75
6. References.....	76
7. Appendices.....	84

## List of figures

<b>Figure 1.4.1.</b> Total number of <i>Myliobatis tenuicaudatus</i> caught during Fish Community Index samples in the Swan-Canning Estuary in each year between 2012 and 2023. ....	20
<b>Figure 2.1.1.</b> Satellite image of the six sites in the Swan-Canning Estuary sites sampled monthly between November 2022 and October 2023. Image sourced from Google Earth. ....	23
<b>Figure 2.2.1.</b> <i>Myliobatis tenuicaudatus</i> with annotated morphological measures used in this study. ....	24
<b>Figure 2.3.3.1.</b> Vertebrae of two <i>Myliobatis tenuicaudatus</i> aged (a) 0.87, and (b) 5.26, respectively, indicating age bands. The first band noted (B) is the band allocated at age 0. The scale bar indicates 1 mm. ....	27
<b>Figure 3.1.1.</b> Average ( $\pm$ SE) values for (a) water temperature, (b) salinity, and (c) dissolved oxygen concentration across all sites in the Swan-Canning Estuary in each month between November 2022 and October 2023. The blue line indicates surface measurements while the grey line indicates bottom measurements. ....	34
<b>Figure 3.1.2.</b> Number of <i>Myliobatis tenuicaudatus</i> caught and Blue Swimmer Crabs ( <i>Portunus armatus</i> ) caught per net in the Swan-Canning Estuary-Canning Estuary between November 2022 to October 2023. ....	35
<b>Table 3.1.2.</b> Mean squares (MS), Sum of squares (SS), Pseudo- <i>F</i> ( <i>pF</i> ), and significance level ( <i>P</i> ) derived using PERMANOVA of the catch of <i>Myliobatis tenuicaudatus</i> between months and sites. <i>df</i> = degrees of freedom. Note the Month x Site interaction was used to calculate the residual. ....	36
<b>Figure 3.1.4.</b> Average number ( $\pm$ SE) and total catch of <i>M. tenuicaudatus</i> among (a) months and (b) sites in the Swan-Canning Estuary. ....	37
<b>Figure 3.2.1.</b> Disk width distribution of the <i>Myliobatis tenuicaudatus</i> caught within the Swan-Canning Estuary from November 2022 to October 2023. ....	38
<b>Figure 3.2.2.</b> Scatter plot and linear regressions for natural log disk width compared to weight for (a) males ( <i>df</i> = 94, $R^2$ = 0.98, $P$ = <0.01) (b) and females ( <i>df</i> = 81, $R^2$ = 0.96, $P$ = <0.01); body length for (c) males ( <i>df</i> = 130, $R^2$ = 0.92, $P$ = <0.01) (d) and females ( <i>df</i> = 137, $R^2$ = 0.92, $P$ = <0.01); and total length of (e) males ( <i>df</i> = 118, $R^2$ = 0.66, $P$ = <0.01) (f) and females ( <i>df</i> = 123, $R^2$ = 0.88, $P$ = <0.01) <i>Myliobatis tenuicaudatus</i> in the Swan-Canning Estuary. ....	39
<b>Figure 3.3.1.</b> Mean marginal incremental analysis ( $\pm$ SE) for the <i>Myliobatis tenuicaudatus</i> caught in the Swan-Canning Estuary. ....	40

<b>Figure 3.3.2.</b> Age class distribution for <i>Myliobatis tenuicaudatus</i> caught in the Swan-Canning Estuary .....	41
<b>Figure 3.3.3.</b> Von Bertalanffy growth curves for (a) male and (b) female <i>Myliobatis tenuicaudatus</i> in the Swan-Canning Estuary. ....	42
<b>Figure 3.4.2.</b> Monthly reproductive parameters calculated for the <i>Myliobatis tenuicaudatus</i> in the Swan-Canning Estuary between November 2022 to October 2023. Gonadosomatic Index (GSI) and mean gonad weight ( $\pm$ SE) for (a) male and (b) female, and (c) Heptasomatic Index (HSI; $\pm$ SE) for male and females (n = 21 and 24, respectively). ....	44
<b>Figure 3.4.3.</b> (a) Clasper length (males; n=125) and (b) uterus mass (females; n=87) in comparison to disk width for <i>Myliobatis tenuicaudatus</i> caught in the Swan-Canning Estuary.....	46
<b>Figure 3.4.4.</b> Maturity curve, and 95% confidence intervals for (a) male and (a) female <i>Myliobatis tenuicaudatus</i> with their respective DW50 (red) values and DW95 (blue) values.....	46
<b>Figure 3.5.1.</b> Photographs of the jaws of <i>Myliobatis tenuicaudatus</i> of different sizes. a) 243, b) 384, c) 428 d) 611, e) 794, f) 862 and g) 1,045 mm disk width. ....	47
<b>Figure 3.5.4.</b> Metric MDS plots for a) dietary composition of <i>M. tenuicaudatus</i> in 200 mm disk width classes; and b) centroid plot for 200 mm disk width classes. ....	52
<b>Figure 3.5.4.</b> Shade plot of prey items by 200 mm length classes of <i>M. tenuicaudatus</i> in the Swan-Canning Estuary. ....	53
.....	54
<b>Figure 3.5.5.</b> (a) mMDS ordinations and (b) nMDS centroid plot of the diet of <i>Myliobatis tenuicaudatus</i> in the Swan-Canning Estuary in Summer (SU; ■), Autumn, (A; ■), Spring (SP; ■) and Winter (W; ■). ....	54
<b>Figure 3.5.6.</b> Shade plot with additional cluster analyses for the dietary composition of <i>Myliobatis tenuicaudatus</i> from the Swan-Canning Estuary in each season where sufficient numbers of samples were collected, i.e. in Summer (SU; ■), Autumn, (A; ■), Spring (SP; ■) and Winter (W; ■). ....	55
<b>Figure 4.3.1.</b> DW $\infty$ in comparison to growth rate of various myliobatids and allies from various sources. Males (●), females (▲), unknown sex (■). <i>M. californica</i> (Martin, 1982); <i>Myliobatis tenuicaudatus</i> (This study); <i>Aetomylaeus bovinus</i> (Başusta & Aslan, 2018); <i>Aetobatus flagellum</i> (Yamaguchi et al., 2005); <i>Aetobatus narinari</i> (Dubick, 2000); <i>Rhinoptera bonasus</i> (Fisher et al., 2013); <i>Rhinoptera seindachneri</i> (Pabón-Aldana et al.,	

2022); <i>Mobula mobular</i> (Cuevas-Zimbrón et al., 2013); <i>Mobula japonica</i> (Pardo et al., 2016). .....	61
<b>Figure 4.5.1.</b> Means values ( $\pm 1$ SE) of (a) the number of prey items and (b) Shannon diversity as a proxy for dietary breath the four families belonging to the Myliobatiformes order. Data taken from papers listed in Fig 4.5.4. ....	68
<b>Figure 4.5.2.</b> (a) non-metric and (b) metric MDS plots of dietary composition of various Myliobatid and allied species; i.e. Myliobatidae (●), Aetobatidae (▲), Rhinopteridae (▼) and Mobulidae (■). Data taken from papers listed in Fig. 4.5.4. ....	69
<b>Figure 4.5.3.</b> Prey items categorised by (a) hardness level and (b) habitat for the four Myliobatiformes families. Data taken from papers listen in Fig 4.5.4. ....	70
<b>Figure 4.5.4.</b> Shade plot indicating different prey items consumed by species in each family i.e. Myliobatidae (▲), Aetobatidae (▼), Rhinopteridae (■) and Mobulidae (◆). <i>Myliobatis aquila</i> (Jardas et al., 2004; Gül & Demirel, 2020), <i>M. californica</i> (Talent, 1982; Gray et al., 1997; Fernández-Aguirre et al., 2022; Reyes-Ramírez et al., 2022), <i>M. chilensis</i> (Gonzalez-Pestana et al., 2021), <i>M. freminvilii</i> (Szczepanski & Bengtson, 2014), <i>M. tenuicaudatus</i> (Sommerville et al., 2011). <i>Aetoylaeus bovinus</i> (Capapé, 1977), <i>A. narinari</i> (Schluessel et al., 2010; Ajemian et al., 2012). <i>Rhinoptera bonasus</i> (Collins, 2005; Ajemian et al., 2012), <i>R. steindachneri</i> (Ehemann et al., 2019; Simental-Anguiano et al., 2022)., <i>M. birostris</i> (Medeiros et al., 2022), <i>Mobula mobular</i> (Notarbartolo-di-Sciara, 1988; Coasaca-Céspedes et al., 2018), <i>Mobula munkiana</i> (Notarbartolo-di-Sciara, 1988; Coasaca-Céspedes et al., 2018). ....	71
<b>Appendix 2.</b> (a) Water temperature, (b) salinity, and (c) dissolved oxygen concentrations at the bottom of the water column at each sample site in the Swan-Canning Estuary in each month between November 2022 and October 2023. ....	86
<b>Appendix 3.</b> Count of male (■) and female (■) <i>Myliobatis tenuicaudatus</i> of various disk widths in the Swan-Canning Estuary each month sampled. ....	87
<b>Appendix 4.</b> Species accumulation curve for each (a) 200 mm disk width class and (b) season for dietary items of <i>Myliobatis tenuicaudatus</i> . ....	88

## List of tables

<b>Table 3.1.1.</b> Results from Pearson’s correlations for bottom water temperature, salinity, dissolved oxygen concentration, and Blue Swimmer Crabs ( <i>Portunus armatus</i> ) abundance in relation to the number of <i>Myliobatis tenuicaudatus</i> caught within the Swan-Canning Estuary.....	35
<b>Table 3.3.1.</b> Von Bertalanffy growth parameters ( $DW_{\infty}$ , k, t0) for male and female <i>Myliobatis tenuicaudatus</i> in the Swan-Canning Estuary. ....	42
<b>Table 3.5.2.</b> Percentage frequency of occurrence (%F) and average percentage by volume (%V) of dietary categories and major taxa (bolded) in stomach contents of <i>Myliobatis tenuicaudatus</i> in the Swan-Canning Estuary. ....	50
<b>Table 3.5.3.</b> R values derived from ANOSIM test of dietary composition in 200 mm disk width classes. Significant differences ( $P < 0.05$ ) are shaded in grey.....	52
<b>Table 3.5.4.</b> Dietary categories that typified (grey) and distinguished (white) the diet of <i>M. tenuicaudatus</i> within 200 mm disk width class based on SIMPER. The length class in which each dietary category was most frequent is provided in superscript for each pairwise comparison. Insignificant comparisons are noted as N/S. Bray-Curtis similarity (Sim) and dissimilarity (Dsim) values are also provided.....	53
<b>Table 3.5.5.</b> R values derived from ANOSIM test of dietary composition in each season. Significant differences ( $P < 0.05$ ) are shaded in grey.....	54
<b>Table 3.5.6.</b> Dietary categories that typified (grey) and distinguished (white) the diet of <i>M. tenuicaudatus</i> within each season based on SIMPER. The season in which each dietary category was most frequent is provided in superscript for each pairwise comparison. Bray-Curtis similarity (Sim) and dissimilarity (Dsim) values are also provided.....	55
<b>Table 4.2.1.</b> Reported ranges of disk width (DW) of various myliobatid and allied species from the scientific literature. ....	59
<b>Table 4.3.1.</b> Maximum age and Von Bertalanffy growth parameters ( $DW_{\infty}$ , k and t0) for various myliobatids and allied species. ....	62
<b>Table 4.4.1.</b> Reproductive characteristics for various species of myliobatids and allies, including disk width at maturity ( $DW_{50}$ ), age at maturity, litter size, gonadosomatic index (GSI), gestation period and functionality of the uterus.....	65
<b>Table 4.5.1.</b> Dietary categories that typified (grey) and distinguished (white) of species in each of the families within the Myliobatiformes based on SIMPER. The family in which each dietary category was most frequent is provided in superscript for each pairwise comparison. Bray-Curtis similarity (Sim) and dissimilarity (Dsim) values are	

also provided. LBC denotes large benthic crustacean, SPC represents small pelagic crustaceans. ....72

**Appendix 1.** Species and maximum size of each species in each family as well as common names and taxonomic authority. Common names and images taken from (Last et al., 2016; Jabado et al., 2022). \* indicates species that originally was part of *Manta* genus before becoming part of the *Mobuila* genus. .... 84

## 1. Introduction

Chondrichthyans are a diverse group of cartilaginous fishes, including sharks and batoids (rays), that play a variety of vital ecological roles within marine and coastal ecosystems (Molina & Cazorla, 2015). Due to their vulnerability to a range of anthropogenic factors such as fishing and urbanisation, understanding their biological characteristics is essential for effective management (Molina & Cazorla, 2015; Davey et al., 2023). Batoids are the most diverse group of chondrichthyans, with 663 valid named species spanning 23 families. However, they are also noted as the most endangered group, with over 20% of all species categorised as critical, endangered or vulnerable listed in the International Union for Conservation of Nature (IUCN) Red List (Dulvy et al., 2014; Kyne, 2016; Martins et al., 2018; Dulvy et al., 2021). Due to their dorsoventrally flattened body and feeding habits, batoids are bioturbators that disturb soft sediments increasing oxygen penetration and nutrient cycling, and provide benefits to other mesopredators by exposing buried prey items (Martins et al., 2018). Moreover, their movement facilitates the transfer of nutrients between habitats and ecosystems, and as a mesopredator (trophic level 3.1 to 4.5), they are predated upon by a range of higher-level consumers, such as sharks (e.g. Tiger Sharks), mammals (e.g., Killer Whales) and birds (Visser, 1999; Flowers et al., 2021). The main predators of batoids are other elasmobranchs, with other rays, usually acting opportunistically responsible for 39.1%, followed by sharks at 24.1% and mammals 18.4% (Flowers et al., 2021).

### 1.1 Taxonomy

The Myliobatiformes are one of four orders within the superorder Batoidea. This order was considered to be taxonomically stable, however, contemporary molecular and morphological analyses have resulted in several families and genera being redefined (White, 2014; Jabado et al., 2022). The Myliobatiformes currently comprises twelve families (Fricke et al., 2020), with the species of interest in this study, the Southern Eagle Ray, *Myliobatis tenuicaudatus*, belonging to the Myliobatidae. This family previously contained three subfamilies, i.e. Myliobatinae (four genera i.e. *Aetobatus*, *Myliobatis*, *Aetomylaeus*, and *Pteromylaeus*), Rhinopterinae (one genus *Rhinoptera*) and Mobulinae (one genus, *Mobula*), which some authors, such as Nelson (2016), still follow. However White and Naylor (2016) revised the taxonomy and divided the Myliobatinae into four families, i.e., Myliobatidae (True Eagle Rays), Aetobatidae (Pelagic Eagle Rays), Rhinopteridae (Cownose Rays), and Mobulidae (Devil Rays). The above four-family

scheme is recognised by Eschmeyer's Catalog of Fishes and the World Register of Marine Species and is supported by differences in the size range, head and body shape and feeding habits (Eschmeyer et al., 2021; Froese & Pauly, 2023).

Before the above taxonomic revision, the Myliobatidae contained four genera, which has now been reduced to two as members of the *Aetobatus* are now recognised as belonging to a different family (Aetobatidae), while species within the genus *Pteromylaeus* have been amalgamated into the genus *Aetomylaeus* (Aschliman, 2014; Last et al., 2016; White & Naylor, 2016). The Myliobatidae currently comprises 19 species, and the Aetobatidae family contains five species (Appendix 1). The Rhinopteridae did not undergo major taxonomic revision and is represented by seven morphologically similar species that are often difficult to distinguish (Last et al., 2016). Mobulids were previously separated due to the location of their mouth, with *Manta* species possessing a terminal mouth and *Mobula* species a subterminal mouth. Due to genetic similarities, these two genera have now been combined and the number of species reduced from eleven to eight (White et al., 2018). In the current study, the four-family approach is utilised, and for brevity and convenience, the Aetobatidae, Rhinopteridae, and Mobulidae are considered to be “allies” of the Myliobatidae, as previously each family comprised part of the Myliobatidae.

## **1.2 Geographical and spatial distribution**

Myliobatids and allies occur in temperate and/or tropical waters with the factors influencing the distribution of these species poorly documented (Weir et al., 2012; Davey et al., 2023). There are hotspots of species richness with species from each of the four families occurring in coastal waters off South America, including, but not limited to *Myliobatis goodei*, *Aetobatus narinari*, *Rhinoptera brasiliensis*, and *Mobula hypstoma* (Last et al., 2016). Similarly, various species are located around the African coast, including *Myliobatis aquila*, *Aetomylaeus bovinus*, *Rhinoptera marginata*, and *Mobula kuhlii*. Most species that occur around the Australian coastline and others, such as *Aetomylaeus vespertilio*, *Mobula alfredi* and *Mobula birostris*, typically have a circumglobal distribution in equatorial waters.

As the most speciose family, members of the Myliobatidae occur in a range of continents and habitats. Seven species are found around the coast of South America, six in the Indo-West Pacific and Australia and two off the northern coast of Africa (Last et al., 2016). They are mainly found over sandy and mud substrates in coastal waters

including estuaries, with some species have been noted to occur in depths of 60 m (i.e., *Myliobatis longirostris*, and *Aetomylaeus maculatus*). In comparison, others have been documented in waters >100 m deep (*M. aquila*, *Myliobatis chilensis*, *A. bovinus*, and *Aetomylaeus caeruleofasciatus*). Two myliobatids, *Myliobatis tenuicaudatus* and *Myliobatis hamlyni* (Purple Eagle Ray) are found in Australian waters (Last et al., 2016). The former species occurs across 20,000 km<sup>2</sup> including southern Australia, Norfolk Island and New Zealand. Individuals typically inhabit inshore sand flats seagrass beds, and estuaries, and although they rarely exceed depths of 85 m individuals have been recorded in offshore waters as deep as 422 m (Last & Stevens, 2009). *Myliobatis hamlyni* has a patchy known distribution but has been recorded in more tropical waters along the Western Australia coast, specifically Shark Bay and Forestier Island region, as well as along Swains Reefs in Queensland and extending northward until Okinawa in Japan (Last et al., 2016). This species is believed to exhibit demersal behaviour, primarily inhabiting continental shelves and upper slopes at depths ranging from 120 to 350 m.

Among the aetobatids, five species reside in the Indo-West region spanning from the Persian Gulf to Japan and two species occur in each of on the north coast of South America and Africa (Last et al., 2016). A single species in this genus, i.e., *Aetobatus ocellatus* is found in Australia along its northern coastline. Individuals are commonly found in inshore coastal waters down to 60 m in depth. It has been noted that movement patterns of species in this family, including migration, are influenced by water temperature (Yamaguchi et al., 2005; Last et al., 2016).

Rhinopterids have been recorded in waters off the northern coast of Africa, America and the Indo-Pacific. The single extant Rhinopteridae species, *Rhinoptera neglecta* is distributed along the Northern Territory and Queensland coast of Australia (Last et al., 2016; Tagliafico et al., 2020). Most species are noted to be benthopelagic and move in large schools (fegers) or aggregations. There are some congeneric differences in habitat preference with *R. brasiliensis* found in shallow (< 20 m) waters with sandy bottoms, while *Rhinoptera marginata* occurs in waters ~100 m deep on the continental shelf (Last et al., 2016).

There are six species of mobulids, including the Reef Manta Ray *Mobula alfredi*, that are located in the tropical region north of Australia. These pelagic species reside in coastal waters but can also be found offshore. The two species previously considered part of the *Manta* genus, i.e., *Mobula alfredi* and *Mobula birostris*, are often located in and around coral and rocky reefs (Last et al., 2016).

Environmental conditions, including water temperature and salinity has been found to influence the movement of several species of myliobatids and their allies. For example, the Longhead Eagle Ray (*Aetobatus flagellum*) was found along the coast of Ariake Bay and Seto Island Sea in Japan during the spring and summer months, however, during the cooler winter months, they moved to oceanic regions (Yamaguchi et al., 2005). Moreover, Davey et al. (2023) detected similar movement patterns in *M. tenuicaudatus* in South Australia, in which individuals disappeared from Coffin Bay between June and August (Austral winter). These movements were likely caused by water temperature due to the absence of rays within the bay when water temperatures reached 10.6°C. Salinity is thought to influence the movement patterns of *M. tenuicaudatus* as no individuals were recorded in the Walpole-Nornalup Estuary on the south coast of Western Australia when salinity was <25 ppt (Potter & Hyndes, 1994). However it cannot be conclusively determined that salinity was a driver of movement, as the decrease in salinity as a result of winter rainfall coincides with a decline in water temperature. Meloni et al. (2002) mentioned that assessing salinity-related cues such as Na<sup>+</sup> and Cl<sup>-</sup> would assist in determining what environmental factors conclusively affect the presence and movement of this family.

### **1.3 Biological characteristics**

#### **1.3.1 Morphology**

Disk width (DW), i.e. as the stretched linear distance between the tips of the pectoral fins, is a standard measurement to assess the size of batoids due to strong positive relationships between DW and other morphological measures, and that as other metrics may be subjected to inaccuracies due to damage or dysmorphia of the specimen (Serra-Pereira et al., 2010). Among the four families, the mobulids contain species reaching a maximum size range of 1,100 to 9,100 mm (Last et al., 2016). Myliobatid species have the second largest range of maximum disk widths (590 to 3500 mm) with *M. tenuicaudatus* has been documented to reach a maximum disk width of 1600 mm with a birth size of 200 to 300 mm (Last et al., 2016). A study conducted in New Zealand using 200 mm mesh sized gill nets documented the maximum size for this species to be 1,300 mm (Marcotte, 2013). In comparison, aetobatids have a maximum size range of 900 to 3000 mm, while rhinopterids have the smallest maximum size range at between 900 and 1,650 mm.

Unlike disk width, there is limited data available on total weights for the myliobatid and allied species. The available data does however show that *Myliobatis tobijei* attain the heaviest maximum weight and *Myliobatis ridens* has the lightest maximum weight (33,600 g and 2,730 g, respectively) (White & Dharmadi, 2007; Araújo et al., 2016). *Aetobatus narinari* is the heaviest aetobatid with a maximum weight of (119,200 g) (Boggio-Pasqua et al., 2022), while the maximum weight of only one rhinopterids species, *Rhinoptera bonasus* is documented (22,780 g) (Fisher et al., 2013). No weights for mobulids have been reported.

### 1.3.2 Age and growth

Determining the age (longevity) and growth rates of fish species is vital for effective management, particularly for species exploited by fishing activities (Khan & Khan, 2020). Due to the lack of calcium phosphate-enriched structures in chondrichthyans, traditional methods of aging such as those using teleost otoliths (ear stones) are not able to be undertaken and as such, central vertebrae are used instead (Martin & Cailliet, 1988; Başusta & Aslan, 2018). Similar to otoliths, vertebrae contain opaque bands, that form in the summer months when growth is faster as well as translucent rings that form during winter months (Martin & Cailliet, 1988; Cailliet et al., 2006). It is common amongst myliobatid species and their allies that females reach an older age than males (Martin, 1982; Başusta & Aslan, 2018). The largest recorded difference in maximum ages occurs in *Myliobatis californica* where females live for up to 23 years but the males only 6 (Martin, 1982). Similarly, female *Aetobatus narinari* reach 25 and males 21 years (Dubick, 2000), while among the rhinopterids *Rhinoptera bonasus* females reach a greater age than males, i.e., 21 vs 18 years (Fisher et al., 2013).

The von Bertalanffy parameters are commonly used to assess the growth of fish species (Essington et al., 2001). These parameters estimate the asymptotic length/ disk width ( $L_{\infty}/DW_{\infty}$ ), growth coefficient ( $k$ ), and theoretical age when the species was 0 mm ( $t_0$ ). Amongst studied species, females have been consistently found to have a larger  $DW_{\infty}$  than males. For example, in both *M. californica* and *A. narinari* documented major  $DW_{\infty}$  variances between males and females (*M. californica* 1,004 mm, 1,566 mm; and *A. narinari* 1,465 mm, 2,459 mm, respectively) (Martin & Cailliet, 1988; Dubick, 2000). However, despite reaching a larger  $DW_{\infty}$ , females typically have a lower  $k$  and  $t_0$ . For example, *M. californica* females display this trait with a growth coefficient of 0.229 and 0.099, and  $t_0$  values of -1.58 and -1.94 years, for males and females, respectively. Similar

trends have been recorded in *A. narinari*, i.e.  $k = 0.087$  vs  $0.031$  and  $t_0 = -4.09$  mm and  $-7.04$  mm, for males and females, respectively (Last et al., 2016). The only species studied where females exhibit a larger  $t_0$  than males is *A. bovinus*, i.e.  $-1.90$  mm and  $-2.98$  mm, respectively (Başusta & Aslan, 2018).

It has been documented that water temperature positively correlates with both growth and developmental rates in the rajid, *Raja microocellata* (Hume, 2019). Furthermore, Schieber et al. (2023) hypothesises that temperature influences endocrine system, further influencing the growth and reproduction patterns of the urotrygonid *Urobatis jamaicensis*. Many myliobatid and allied species that have documented von Bertalanffy growth parameters have a circumglobal distribution, where temperatures are warmer, causing a greater growth rate but a lower DW. No studies have been done to assess the von Bertalanffy parameters on such species residing in temperate waters and as such comparisons between distributions for these parameters are yet to be made.

### 1.3.3 Reproduction

All members of the Myliobatiformes are viviparous, where mothers hold their embryos in the uterus and give birth to live young (Carrier et al., 2012; Araújo et al., 2016). Unlike some Myliobatiformes, myliobatid and allied species have two ovaries and two uteri (Walker, 2020; Yamaguchi et al., 2021). This allows the mother to either develop the embryos or hold the eggs until fertilised (García-Salinas et al., 2021; Yamaguchi et al., 2021). While species within these four families typically possess two uteri, both may not always be fully utilised. For example, in species such as *Myliobatis goodei* and *Aetobatus narinari*, the uteri may become fused or only one may be actively utilised, while the other remains notably reduced, indicative of a vestigial organ (García-Salinas et al., 2021).

Due to their vivipary, the fecundity produced can be accurately determined. Yamaguchi et al. (2021) compared the number and size of pups between ten myliobatids, four aetobatids, seven rhinopterids, and eight mobulids species. These authors found that myliobatids had the highest fecundity with, for example, *M. aquila*, and *M. californica*, recording over 12 pups per mother. In contrast, mobulids had the lowest number of pups, with a maximum of two pups per female. The largest maximum fecundity for an aetobatids was seven pups found in *A. narutobiei* (Yamaguchi et al., 2021). In most myliobatids, the gestation period is typically between nine and twelve months (Last et al.,

2016). Batoids are noted to be prone to abortion (Wosnick et al., 2019; Wosnick et al., 2023). A study conducted by Adams et al. (2018) found that batoids contributed >54% to all documented elasmobranch abortions caused by a range of fishing methods. Elasmobranch abortions are noted to be caused as a stress response.

Age and disk width at 50% maturity ( $A_{50}$ ,  $DW_{50}$ ) are also important biological characteristics to understand for fisheries management. However, there is limited literature documenting the  $DW_{50}$  of myliobatid and allied species for males and females, noting that sample size is often a limiting factor. This is typically due to the biomass of individuals and limited number of individuals found within a population. In order to maintain a healthy population, management and ethical practices must be taken into consideration, and as such, fewer specimens for scientific studies can be taken. Jones et al. (2010) estimated the  $DW_{50}$  female and male *M. tenuicaudatus* to be 879 and 689 mm, respectively. In the congeneric *M. goodei*, female  $DW_{50}$  was ~683 mm, while males matured at ~555 mm (Araújo et al., 2016).

#### 1.3.4 Dietary composition

Despite all being once considered, at one point, to belong to the same family, there are differences between feeding methods and prey consumed by myliobatids, rhinopterids, aetobatids and mobulids. The former two families are recognised as durophagous benthic feeders, characterised by the presence of rigid jaws containing hard, fused grinding plates composed of flat teeth. These teeth interlock to efficiently crush hard-shelled organisms (Summers, 2000; Kolmann et al., 2015). They are deemed generalist feeders that predate on a variety of organisms, including molluscs, teleosts, echinoderms and crustaceans (Szczepanski & Bengtson, 2014; Gonzalez-Pestana et al., 2021; Fernández-Aguirre et al., 2022). For example, the main dietary composition of *M. tenuicaudatus* in coastal waters off south-western Australia is molluscs, particularly gastropods, 40.9%, 28.3% percentage volume, respectively, as well as crustaceans (Sommerville et al., 2011).

Despite the pelagic nature of aetobatids, the main prey items they consume on are predominantly benthic, and similar to myliobatids and rhinopterids they are durophagous. In contrast to species in these families, aetobatids have a specialised diet, feeding predominantly on molluscs (~76%), with a smaller portion of the diet comprising crustaceans (~18-22%) (Schlüssel et al., 2010; Jacobsen & Bennett, 2013). Furthermore,

some species in this family, e.g. *A. narinari*, have been documented to feed on only one type or species of prey (Chan et al., 2022).

In comparison to benthic feeders, mobulids typically feed on pelagic prey such as small crustacean with studies finding > 90% of their diet to be Euphausiids (krill) or other zooplankton (Jacobsen & Bennett, 2013; Coasaca-Céspedes et al., 2018). While they have a tooth plate, it is not used in feeding. Their tooth plates have been broken into three dental morphologies, cobblestone, comb-like and peg-like dependent on evolutionary histories (Adnet et al., 2012). Mobulids have been documented to filter feed and use cephalic lobes to guide prey into their mouths (Rohner et al., 2017).

#### 1.4 Study aims

*Myliobatis tenuicaudatus* (Hector, 1877; previously referred to as *Myliobatis australis*) was first recorded as a single sighting in the Swan-Canning Estuary (Perth, Western Australia) in 1977 (Chubb, 1979). However, in recent years, anecdotal sightings, including that of an albino juvenile (Trayler et al., 2024) have increased. This is supported by the results of a regular monitoring program (Tweedley et al., 2022), where the number of individuals recorded increased from 15 to 153 over the last 11 years (one-tailed Pearson correlation,  $R = 0.770$ ;  $P = 0.003$ ; Fig. 1.4.1). The postulation this species has increased in abundance is consistent with anecdotal reports of increased interactions with commercial fishing operations within the estuary (DPIRD, pers. comm.). However, to evaluate the sustainability of fishing operations of *M. tenuicaudatus* in the Swan-Canning Estuary, there is a need to determine the biological characteristics of this species.

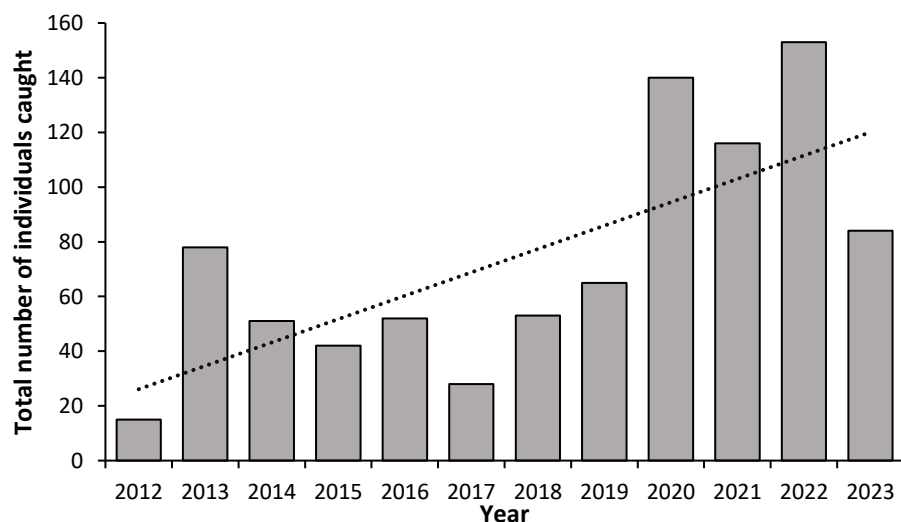


**Figure 1.4.1.** Total number of *Myliobatis tenuicaudatus* caught during Fish Community Index samples in the Swan-Canning Estuary in each year between 2012 and 2023.

While there is limited biological information, such as the disk width and weight, of several myliobatid and allied species, there are many knowledge gaps. In regard to the presence of the *M. tenuicaudatus* in the Swan-Canning Estuary, it is not known whether individuals are present in the estuary year-round and, if so, if their catch rate is affected by environmental variables such as salinity and water temperature. While reproductive and dietary studies have been conducted previously by Jones et al. (2010) and Sommerville et al. (2011), were carried out in coastal rather than estuarine waters, where environmental conditions and prey availability are different (Campbell et al., 2021).

The overarching aims of this study was to determine the biological characteristics and catch rates of *Myliobatis tenuicaudatus* in the Swan-Canning Estuary. The specific aims were to i) assess the spatial and temporal pattern of abundance within the Estuary; ii) estimate the size, age range and growth parameters; iii) determine if breeding occurs in the estuary and when spawning occurs; and iv) document the dietary composition of *M. tenuicaudatus* and determine if it varies with ontogeny and among seasons.

The following hypotheses were proposed.

1. *Myliobatis tenuicaudatus* will be more abundant in summer than in winter due to the increase in temperature and salinity.
2. Like other batoid species, females will have a longer longevity and slower growth coefficient ( $k$ ) than males.
3. Parturition and copulation will occur during summer with females reaching a larger size at maturity than males; and
4. *Myliobatis tenuicaudatus* will exhibit a generalist diet, feeding on a variety of benthic prey items and, with larger prey consumed by larger-bodied rays.

### ***1.5 Study significance***

Understanding the spatial and temporal distribution of *M. tenuicaudatus* is vital as it can be used to identify preferable environmental conditions, including salinity, water temperature, and dissolved oxygen concentrations. Determining spatial distributions are important to assess where *M. tenuicaudatus* reside and if there are any overlaps in terms of where they reside and where commercial fishing pressures occur. Temporal abundances can be used to assess migration patterns as well as feeding movements. Limited studies have been conducted on the abundance of batoids within estuaries,

however, some have shown that rays decline in winter as individuals leave the estuary or move in to deeper, more saline waters (Bishop et al., 2016).

Disk width and weight, age, and reproduction are important parameters used to generate stock assessments and to assess mortality rates. Determining the dietary composition is vital in understanding the food web of an ecosystem, particularly for large-bodied mesopredators, such as batoids. Furthermore, if *M. tenuicaudatus* are consuming Blue-Swimmer Crabs (*Portunus armatus*) as part of their diet, this information could be communicated to fishers and provide an explanation indication as to why rays are be increasing caught as bycatch in nets targeting crabs. Similarly, this can provide the basis of advice to fishers on areas to avoid in order to minimise bycatch.

Effective policies and management of a species and ecosystem are vital to ensure the ecosystem remains stable and healthy and that levels of fishing are sustainable. Data generated by this research will provide the basis for appropriate management strategies for the *M. tenuicaudatus* in the Swan-Canning Estuary potentially altering and improving current policies which are currently based on limited data. The current exemption allowing commercial fishers in the Swan-Canning Estuary and Peel-Harvey Estuary to retain 1 tonne annually over a three-year period, is a conservative approach due to limited information on this species in south Western Australia. Finally, the data generated in this study will increase the understanding of this species and the family, both locally and globally. As noted previously, there is minimal information regarding the biological characteristics of *M. tenuicaudatus* and many other myliobatid and allied species.

## 2. Methods

### 2.1 Study site

The Swan-Canning Estuary is ~50km in length, and covers an area of ~55km<sup>2</sup>, and flows through Western Australia's capital city, Perth. It is permanently connected to the ocean via a narrow entrance channel at the Port of Fremantle and extends upstream through two basins (Melville Water and Perth Water), and tidal portions of the Swan and Canning rivers. Although the deepest point of the estuary is found at the entrance of the channel at 20 m, over half the estuary is < 2 m in depth (Hogan-West et al., 2019). As south-western Australia experiences a Mediterranean climate, the Swan-Canning Estuary is influenced by warm, dry summers and wet winters with ~80% of the annual rainfall occurring between May and September (Hodgkin & Hesp, 1998; Hallett et al., 2018). Due to the highly seasonal rainfall and microtidal amplitudes (tidal range of ~0.6 to 0.8 m) present within the estuary, physio-chemical aspects of the water, in particular salinity, and water temperature undergo seasonal changes (Tweedley et al., 2016).

The Swan-Canning Estuary has been subjected to a range of anthropogenic pressures (Brearley, 2005). A monitoring project, the Fish Community Index (FCI), was developed by the Department of Biodiversity, Conservations & Attractions and Murdoch University to assess the ecological condition of the estuary (Hallett et al., 2019). Records from annual monitoring of 24 sites across the estuary since 2012 showed that 94% of all *M. tenuicaudatus* caught during that project were recorded within six sites in the Melville Water basin and, as such, sampling of those same sites has been undertaken for this study (Tweedley, unpublished data; Fig 2.1.1).

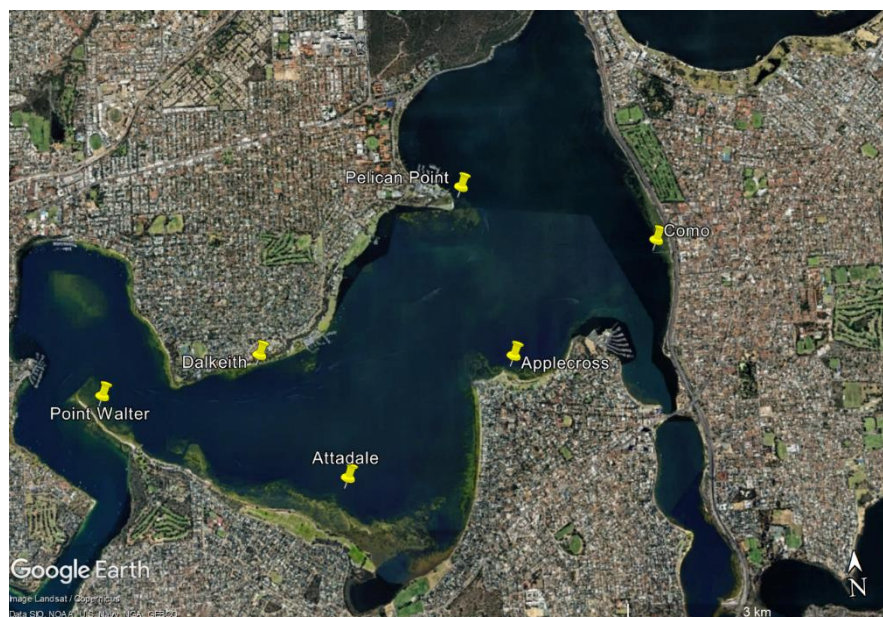


**Figure 2.1.1.** Satellite image of the six sites in the Swan-Canning Estuary sites sampled monthly between November 2022 and October 2023. Image sourced from Google Earth.

## 2.2 Sampling regime

Gill netting was conducted by staff from the Department of Primary Industries & Regional Development (DPIRD) at six sites in the Swan Canning Estuary monthly between November 2022 and October 2023. Each gill net was 160 m long and comprised eight 20 m panels of different mesh sizes (i.e., 25, 51, 63, 76, 89, 102, 115, and 127 mm). The nets which are negatively buoyant were deployed from a boat parallel to the shoreline between depths of 2 m and 6 m after sunset and were set for three hours before being retrieved. The capture per unit effort (CPUE) remained consistent between each site and month. All individuals of *M. tenuicaudatus* and the portunid *P. armatus* caught were counted and sexed. Prior to release, a range of morphometric measurements, i.e. disk width, disk length, body length, and total length (Fig 2.2.1), were also measured (to the nearest 1 mm) and the individual weighed to the nearest 5 g. All individuals were also sexed based on the presence of claspers in males. The sexual maturity of all males was determined by measuring and assessing the calcification of the copulatory organ, the clasper (see section 2.3.3). As the reproductive structures for females are internal, sexual maturity was not determined in the field. Among the monthly catches of *M. tenuicaudatus*, ~15 individuals of various sizes and stages of maturity were randomly selected and euthanised using blunt force trauma as it is deemed one of the most ethical and effective method for batoids (Holmes et al., 2022). The samples collected by DPIRD, and additional frames (n= 45) were donated from the commercial fisher were provided to Murdoch University under Animal Ethics Cadaver permit #974. Upon receipt of the specimens, they were transported to the laboratory where they were frozen at -20 °C before being processed.

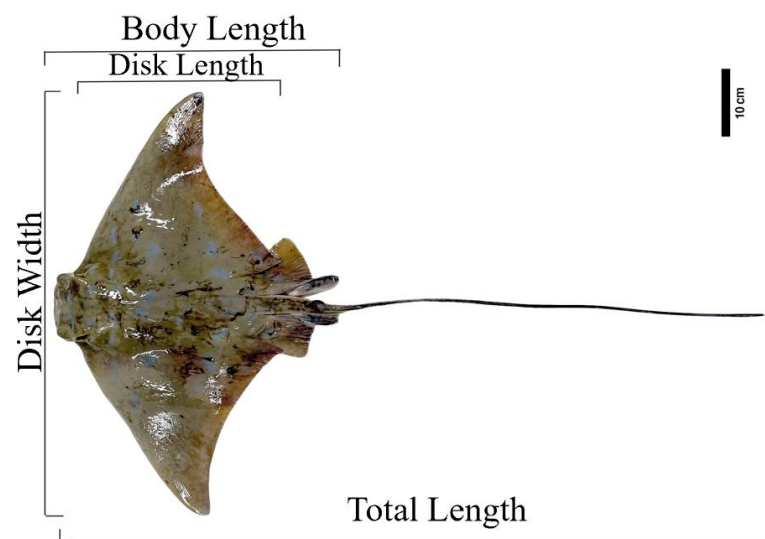


**Figure 2.2.1.** *Myliobatis tenuicaudatus* with annotated morphological measures used in this study.

The salinity (ppt), water temperature (°C) and dissolved oxygen concentration ( $\text{mgL}^{-1}$ ) at both the surface and bottom of the water column was recorded at each site on each sampling occasion using a ProSolo Digital Water Quality Meter (Yellow Springs Instrument, Ohio, USA).

## ***2.3 Laboratory processing***

### ***2.3.1 Initial Processing***

In the laboratory, each specimen was weighed, with morphometric measurements recorded as those released alive during field sampling (Fig. 2.2.1). Secateurs and surgical scissors were then used to open the cavity of the body from the cloaca to the pectoral girdle. The liver was removed and weighed to be used for calculating the hepatosomatic index (HSI) and the reproductive tract was examined (see section 2.3.3). The stomach and intestines were then removed, with the stomach being preserved in a vial containing 100% ethanol. The gonads were also removed and weighed to be used for the gonadosomatic index (GSI; see 2.3.3). A section of the last five to ten precaudal vertebrae able to be access from the lower cavity were removed and frozen at  $-20^{\circ}\text{C}$ . Finally, the jaws from 14 individuals ranging from 243 to 1,045 mm DW were extracted using a scalpel and immersed in boiling water. Softened flesh was removed using a range of forceps and toothbrushes.

### ***2.3.2 Age and growth***

The vertebrae were removed from the freezer and thoroughly cleaned by manually removing the soft tissue and notochord. Individual vertebrae were separated before being soaked in hypochlorite (4%) for a maximum of 20 minutes before being rinsed in water. This limit was employed as hypochlorite can decalcify cartilage if exposed for too long (Başusta & Aslan, 2018). The vertebrae were then air-dried for a minimum of 48 hours.

Vertebrae were cast in Fibreglass & Resin branded resin and sectioned to a width of  $11\mu\text{m}$ , using an IsoMet low-speed single diamonds bladed. The sections were then mounted on microscopic slides using a DPX neutral mounting medium before being examined under a microscope with a reflected light source after drying for a minimum of three days.

To verify that the bands present in vertebrae are formed annually, marginal increment analysis was employed. Verification was conducted using ImageJ (Schneider

et al., 2012) by counting how many rings were present on the vertebrae and calculating the radius of the edge of the opaque ring to the edge of the vertebrae. The radius of the vertebrae was also measured. The marginal increment analysis was calculated using the following equation:

$$MIR = VR - Rn,$$

where *MIR* is the marginal increment ratio,

*VR* is the vertebral radius; and

*Rn* is the radius of the ultimate band (Cailliet et al., 2006; Lessa et al., 2006).

The age of each specimen was derived from the bands on a vertebra, with one growth band considered a pairing of an opaque and translucent band, i.e., representative of the warmer and colder seasons, respectively. The first band was defined as age 0. The level of delineation was also considered and allocated into three major categories; near, edge (when a new band appears on the edge of the vertebrae) or wide (when there is a large zone between the large band and edge of the vertebrae). It was determined that the birthdate of *M. tenuicaudatus* was 1 February (Austral summer) and age estimated using the following equation:

$$\text{Age} = (m + (d/30) + (x \times 12)) / 12$$

Where *m* is the number of months of capture after the designated birthdate (e.g., March would be month 1),

*d* is the day of capture and

*x* is the number of zones present on the vertebrae.

However, if delineation was considered as “wide” zone within two months either side of the birthdate (i.e., December to April), an additional year was included to account for the upcoming delineation.

A second reader was also employed to verify the ages of all individuals (n= 124). It was determined that most ages were calculated to be the same age, while only eight vertebrae (6.5%) varied between readers and then typically by only 1 to 2 years, allowing a percentage of agreement (PA) of 93.5%. Further vertebral readings were conducted until the variances were resolved.

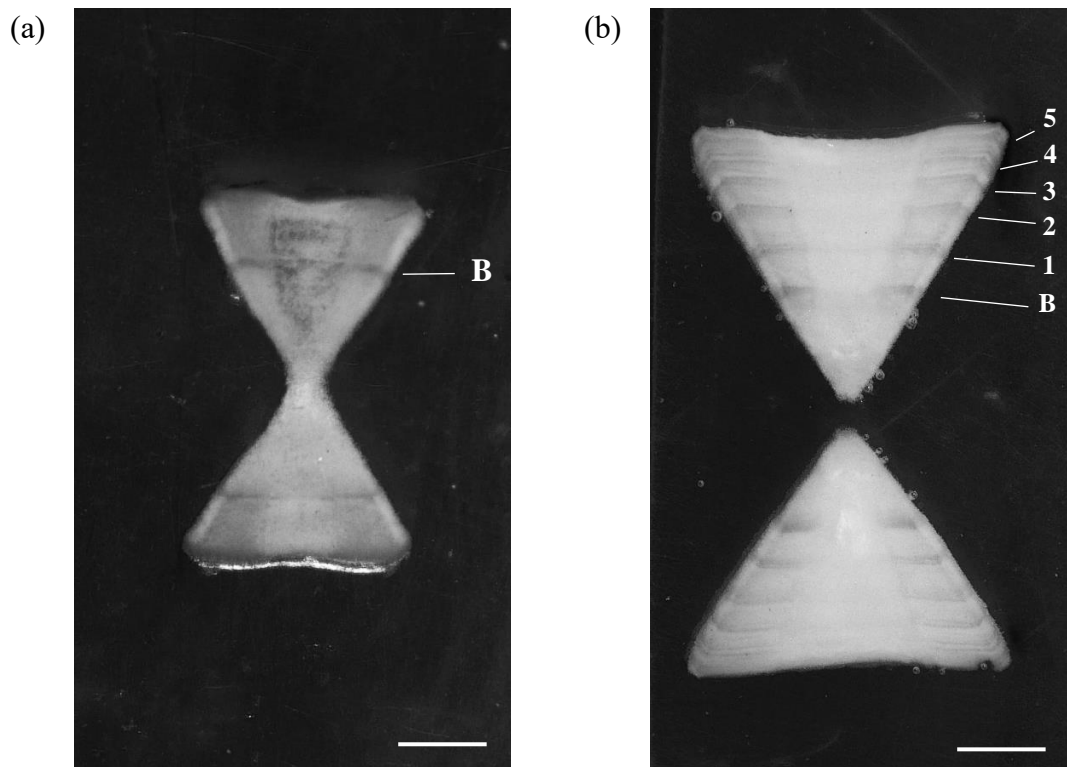


**Figure 2.3.3.1.** Vertebrae of two *Myliobatis tenuicaudatus* aged (a) 0.87, and (b) 5.26, respectively, indicating age bands. The first band noted (B) is the band allocated at age 0. The scale bar indicates 1 mm.

### 2.3.3 Reproduction

Maturity in males was determined by measuring and assessing the size of the claspers and their extent of calcification as per the ICES guidelines for males (Valetta, 2010). Stage 1 (immature): clasper smaller than the pelvic fin and not calcified. Stage 2 (developing): clasper of the same size or slightly larger than the pelvic fin and slightly calcified. Stage 3 (mature): clasper longer than the pelvic fin and fully calcified. Testes were removed and weighed individually and as a whole to calculate the gonadosomatic index (GSI).

As female Myliobatiformes have two ovaries and two uteri, each ovary was removed and weighed. When present, eggs were measured with calipers to the nearest 0.01 mm. The uteri are located on the spinal cord in the lower portion of the cavity with a fused wall. After separation, each uterus was weighed individually before all epigonal organs (ovaries, uteri, and oviductal gland) were weighed to calculate the GSI. The development level of any foetus was also determined using the criteria in Yamaguchi et al. (2021). The stage of maturity was determined following the ICES guidelines (Valetta, 2010). Stage 1 and 2 females (immature and developing, respectively): two thin, underdeveloped uteri and pale ovaries, potentially with small, yellow eggs. Stage 3

(mature) females: two developed uteri and the presence of yellow eggs within the dark pink ovaries. Stage 4 females (mature/ pregnant) were classed in three substages, indicating the differing stages of embryonic development, i.e. fertilised egg, embryo developing, and embryos fully developed with no egg sacs. Stage 5 (mature/ postpartum): similar characteristics to stage 2 females, however the uteri are darker in colour with a wider cloaca. Individuals that were measured below 300 mm were identified to be neonates due to the determined age at this size to be less than one year old.

#### *2.3.4 Dietary composition*

The stomach from each specimen was removed and placed in a vial containing 100% ethanol for at least seven days to ensure preservation prior to identification which does not negatively influence the identification of prey items or the volumetric contributions (Sommerville et al., 2011). After this period, the stomachs were dissected, and the fullness of the stomach was estimated between 0 (empty) and 10 (full). Each prey item was examined under a Nikon SMZ745T dissecting microscope and its percentage volume was visually estimated to the nearest 1%. This method has been widely accepted and utilised in recent dietary studies and is considered reliable representations of the dietary composition of this species (Sommerville et al., 2011; Platell et al., 2024). Each new prey item found was documented, photographed, and saved within a reference collection. Prey items were then identified to the lowest taxonomic resolution possible using taxonomic experts and reference books and keys, with added descriptions to ensure accurate taxonomic resolution (Grey et al., 1983; Jones & Morgan, 1994).

### **2.4 Data analysis**

#### *2.4.1 Environmental Conditions and ray catches*

Using Microsoft Excel (Microsoft Corporation, 2018), values for all environmental conditions (salinity, water temperature and dissolved oxygen concentration) were averaged and used to construct a line graph with associated standard error bars. The same software was employed to construct a scatterplot between the abundance of *M. tenuicaudatus* and a potential prey item *P. armatus*. Pearson's correlation tests were used to explore whether relationships existed between the above abiotic and biotic variables and catches of *M. tenuicaudatus*. These analyses were conducted in R version 4.3.1 using the "tidyverse", "ggplots2" and "dplyr" packages (Wickham, 2016; Wickham et al., 2019; R Core Team, 2023; Wickham et al., 2023).

A heat map of the total number of *M. tenuicaudatus* recorded at each site was produced by overlaying circles onto Google Earth (2023) satellite image. These points were then colour-scaled using the conditional formatting function in Excel to identify the site with the highest and lowest catches. Two-way univariate Permutational Analysis of Variance (PERMANOVA) was performed to determine whether the abundance of *M. tenuicaudatus* differed significantly ( $P < 0.05$ ) among site (six levels) and Month (12 levels). As there was no replication at the site level in a month, the Site  $\times$  Month interaction term was employed as the PERMANOVA residual, thus providing a sound and conservative basis for assessing the statistical significance of the two main effects (Tweedley et al., 2015). This analysis was conducted using Primer v7 using the PERMANOVA+ add in (Anderson, 2008; Clarke & Gorley, 2015). Significant main effects identified by PERMANOVA were visualised using means plots with associated standard errors bars.

#### 2.4.2 Morphology

The number of individuals in each DW class (50 mm) was plotted in R version 4.3.1. The extent of any relationships between DW and each of total weight, body length and total length were plotted and subjected to linear regression in Excel. To assess whether there was a relationship between weight and DW, both measures were log<sub>e</sub> transformed to ensure they conform to normality assumptions before being plotted. The defleshed jaws were photographed using a Nikon D7000 digital camera with 16.9-million-pixel resolution and the number of tooth rows counted. The width and depth of each jaw were measured to the nearest 0.01 mm using 150 mm digital, vernier callipers (Kincrome, Melbourne, Australia) and the oral gape shape (i.e. mouth depth / mouth width) calculated (Karpouzi & Stergiou, 2003). Relationships between these variables were also examined using linear regression.

#### 2.4.3 Age and growth

As previously mentioned, marginal incremental analysis was calculated using the equation VR-Rn. All values were averaged and plotted by month with associated standard error bars. With a similar method as the disk width distribution, an age distribution was constructed in one-year classes (Cerrato, 1990). The von Bertalanffy growth model was fitted to the disk widths (*DW*) and ages (*t*) of male and female *M. tenuicaudatus* caught in the Swan-Canning Estuary. The von Bertalanffy growth curve follows:

$$DW_t = DW_\infty (1 - \exp[-k(t-t_0)]),$$

Where  $DW_t$  = the estimated disk width at age  $t$  (years)

$DW_\infty$  = the asymptotic length

$k$  = the growth rate; and

$t_0$  = the hypothetical age at which the fish would have a zero length

This was calculated in R, using the FSA packages (Ogle et al., 2023).

#### 2.4.4 Reproduction

The GSI, i.e., the ratio of gonad weight to body weight, and HSI, i.e., the ratio of liver weight to body weight was calculated for each individual *M. tenuicaudatus* processed in the laboratory. Mean monthly GSI ( $\pm 1SE$ ) for mature *M. tenuicaudatus* ( $>DW_{50}$ ) were plotted with mean gonad weight. Similarly, the HSI for both males and females were averaged and plotted together on a line graph with associated standard error bars. The clasper length and uterus mass were plotted against disk width, and colour coded based on the maturity stage. Using the R packages, “ggplot2”, “car”, “MASS”, “psyphy”, “RCurl”, “SizeMat”, “tidyverse” and “dplyr”, the  $DW_{50}$ , where 50% of the population is mature, was calculated for both males and females (Venables & Ripley, 2002; Torrejon-Magallanes, 2020; Knoblauch, 2023; Lang, 2023). The  $DW_{95}$ , at which 95% of the population is mature was also calculated. Using these packages, and calculated values, maturity curves were plotted.

#### 2.4.5 Dietary comparisons

##### *Myliobatis tenuicaudatus*

A total of 106 dietary items were identified from the stomach contents of *M. tenuicaudatus* obtained from the Swan-Canning Estuary, due to mastication and variable states of digestion these ranged from unidentifiable material to species-level identification. For comparison to existing data from Cockburn Sound (Daniel Cox, unpublished data) and the marine waters in lower-west Western Australia Sommerville et al. (2011) all dietary items were aggregated to the dietary categories used in the latter study and the percentage volumetric contribution (%V) and frequency of occurrence (%F) of each calculated. To assess broad changes in the diet of *M. tenuicaudatus* with increasing DW, individuals were allocated to ten 100 mm DW categories ranging from  $< 200$  to  $> 1,100$  mm DW and the percentage contribution of prey at the phyla-level, i.e. annelids, arthropods, molluscs, and chordates calculated. The presence of changes in the

percentage contribution of prey belonging to the first three categories with increasing DW classes were tested using one-way Pearson's correlations using SPSS v29 ( $P < 0.05$ ).

For multivariate statistical analyses, each dietary item was assigned to one of nine dietary categories based on taxonomy (see Platell et al., 2024). Multivariate analyses of dietary composition were conducted in Primer v7 with the PERMANOVA+ extension (Anderson, 2008; Clarke & Gorley, 2015). Firstly, all stomachs from *M. tenuicaudatus* obtained from the Swan-Canning Estuary that contained no contents (i.e., empty) or solely unidentified prey were removed from the dataset. Prey that was not considered a direct dietary item ingested deliberately, e.g. macrophytes and parasites, were removed and the data standardised so that the total of the dietary categories for each individual summed to 100.

Prey accumulation curves were constructed using all samples and the samples collected from each 200 mm DW class (i.e. < 200, 200-399, 400-599, 600-799, 800-999 and >1,000) and seasons (i.e. spring, summer, autumn, and winter). The curves for all samples and DW classes except for the smallest and largest classes all reached an asymptote, as did those for each season (Appendix 4).

As the dietary composition of individual *M. tenuicaudatus* may contain a limited number of the dietary categories this variability can be masked by “real” trends in dietary composition (Lek et al., 2011). To reduce this potential effect, stomachs were sorted into random groups and the data averaged; a practice commonly-used when analysing dietary data of various aquatic-feeding organisms (Greenwell et al., 2019; Maschette et al., 2020; Campbell et al., 2021). This procedure was first undertaken by averaging between two and five individual stomachs from the same DW class and pooling across seasons thus removing the influence of the latter factor. It was repeated again only this time averaging between two and six individuals for each season and pooling across DW classes.

The data for DW classes were square-root transformed to balance the contribution of dietary categories and used to construct a Bray-Curtis resemblance matrix. This matrix was then subjected to a one-way Analysis of Similarities (ANOSIM) test (Clarke & Gorley, 2015) to assess if the dietary composition varied significantly ( $P < 5\%$ ) among the six 200 mm DW classes. Trends in dietary composition were explored visually using Bootstrapped metric Multidimensional Scaling (Bootstrapped mMDS) using the Bootstrapped Averages routine. This used the averages of repeated bootstrap samples

(bootstrapped averages) for each DW class were used to construct an mMDS ordination plot. Superimposed on the plot was a point representing the group average (i.e., the average of the bootstrapped averages) and the associated, smoothed, and marginally bias-corrected 95% bootstrap region, in which 95% of the bootstrapped averages fall. The Bray-Curtis resemblance matrix was used to calculate a distance-among-centroid matrix, which creates an average in the 'Bray-Curtis space' for each DW class (Lek et al., 2011). This matrix was, then used to generate an nMDS ordination plot and a trajectory added to show the linear change in diet with increasing size class. In addition, RELATE was used to ascertain whether the dietary composition changed significantly in a serial manner through sequential length classes (Platell et al., 2022). In this test, the test statistic rho ( $\rho$ ), reflects the strength of the seriation with values ranging from  $\sim 0$  (little correlation) to  $\sim 1$  (near-perfect correlation).

The shade plot (Clarke et al., 2014) and Similarity Percentages (SIMPER; Clarke & Gorley, 2015) routines were used to elucidate the dietary categories that were responsible for the differences in diet among *M. tenuicaudatus* in different DW classes. A shade plot, derived from the square-root transformed percentage volumetric contribution data averaged across replicates for each of the DW classes, was constructed. This plot is a simple visualization of the frequency matrix, where a white space for a dietary category demonstrates that it was not consumed by individuals that DW class. At the same time, the depth of shading from grey to black is linearly proportional to the volumetric contribution of that dietary category to the overall diet. DW classes (*x*-axis) and dietary categories (*y*-axis) were arranged based on separate dendrogram derived from hierarchical agglomerative clustering using resemblance matrixes constructed using the Index of Association. As the shade plot visualised averaged data for each DW class, they do not account for the frequency of occurrence of prey, SIMPER used the replicate level data and identified those dietary categories that typified the diet in one DW class and those that were responsible for distinguishing between each pair of DW classes.

The entire process, i.e. one-way ANOSIM, bootstrapped mMDS, centroid nMDS, shade plot and SIMER, was repeated for the data grouped according to season (pooling across length classes). The only exception was that a RELATE test was not conducted as seasonal data are not serial.

A meta-analysis of the diet of myliobatids, aetobatids, rhinopterids and mobulids was conducted to see how similar the diet of *M. tenuicaudatus* in the Swan-Canning Estuary was to other myliobatid and also compare differences among families globally. A total of 20 scientific publications were found providing data on 17 species, noting that some papers documented the diet of multiple species, and the same species were the focus of multiple papers, e.g. the four separate studies on *A. narinari*. To ensure consistency of taxonomic resolution among the published studies, the 53 different dietary items were allocated to 22 dietary categories. These were based on a combination of taxonomy, functional features such as position in the water column and body size, and the level of identification (see Platell et al., 2024 for full rationale). For example, benthic and pelagic tunicates were distinguished, and crustaceans were identified as either i) small pelagic (e.g. euphausiids, copepods), ii) small benthic (e.g. amphipods, isopods), iii) large benthic (e.g. penaeids, stomatopods) or iv) crustaceans (e.g. unidentified/distinguished crustaceans). In addition to being allocated to dietary categories, dietary items were also assigned to a broad hardness, i.e. soft (e.g. annelids, teleosts), medium (e.g. crustaceans) and hard (e.g. gastropod molluscs) and habitat, i.e. benthic (e.g. annelids), demersal (e.g. penaeids) and pelagic (e.g. copepod) category. Dietary items were recorded as either percentage mass (%M) or volume (%V) or number (%N) or frequency of occurrence (%F). Following Greenwell et al. (2019), only those studies recording data as either %M or %V were included in the meta-analysis. This reduced the number of samples (i.e. a species from a particular study) from 31 to 25, i.e. 9 myliobatids, 5 aetobatids, 5 rhinopterids and 6 mobulids.

A data matrix was constructed from the %V or %W of catch dietary category to the total diet of a species in a study. As with the analyses of the diet of *M. tenuicaudatus* in the Swan-Canning Estuary, non-prey categories such as macrophytes, parasites and totally unidentifiable prey were excluded, the values in the remaining categories re-standardised to 100. The DIVERSE routine was used to calculate the prey richness (i.e. number of dietary categories a species consumed) and dietary breadth, i.e. Shannon diversity (Svanbäck et al., 2008)). Value for each matrix were used to create a Euclidean distance matrix and each matrix subjected to one-way PERMANOVA to determine if the values differed among the four families. The dietary composition data matrix was square-root transformed, used to construct a Bray-Curtis resemblance matrix, which was, in turn, subjected to one-way ANOSIM and used to create nMDS and bootstrapped mMDS ordination plots. The transformed data were then used to create a shade plot and subjected to SIMPER.

### 3. Results

#### 3.1 Environmental variables and ray catches

Water temperatures in the Swan-Canning Estuary varied among months but was similar between the surface and bottom of the water column (Fig 3.1.1.a). The average temperature was higher in summer months (December to February) reaching a maximum of 25.2 °C in February and declined during winter (June to August) to a minimum of 15.3 °C in July. Salinity changed between water depths (Fig 3.1.1.b), months, and sites (Appendix 2b). Polyhaline conditions were present in November (30.2 ppt), and they increased sequentially to a maximum of 37.5 ppt in March, before declining to a minimum of 23.7 ppt in June. No stratification was present except in August, bottom salinity increased to 29.6, but the surface salinity dropped to 20.0 ppt. Dissolved oxygen concentrations remained stable between 6.5 and 7.5 mgL<sup>-1</sup> from November to March, after which the values diverged, with the bottom reaching lower levels than the surface, i.e. <6.2 mg/L in August (Fig 3.1.1.c). Most individual sites followed the described trend for temperature and salinity, however there were large variations in dissolved oxygen concentrations (Appendix 2c).

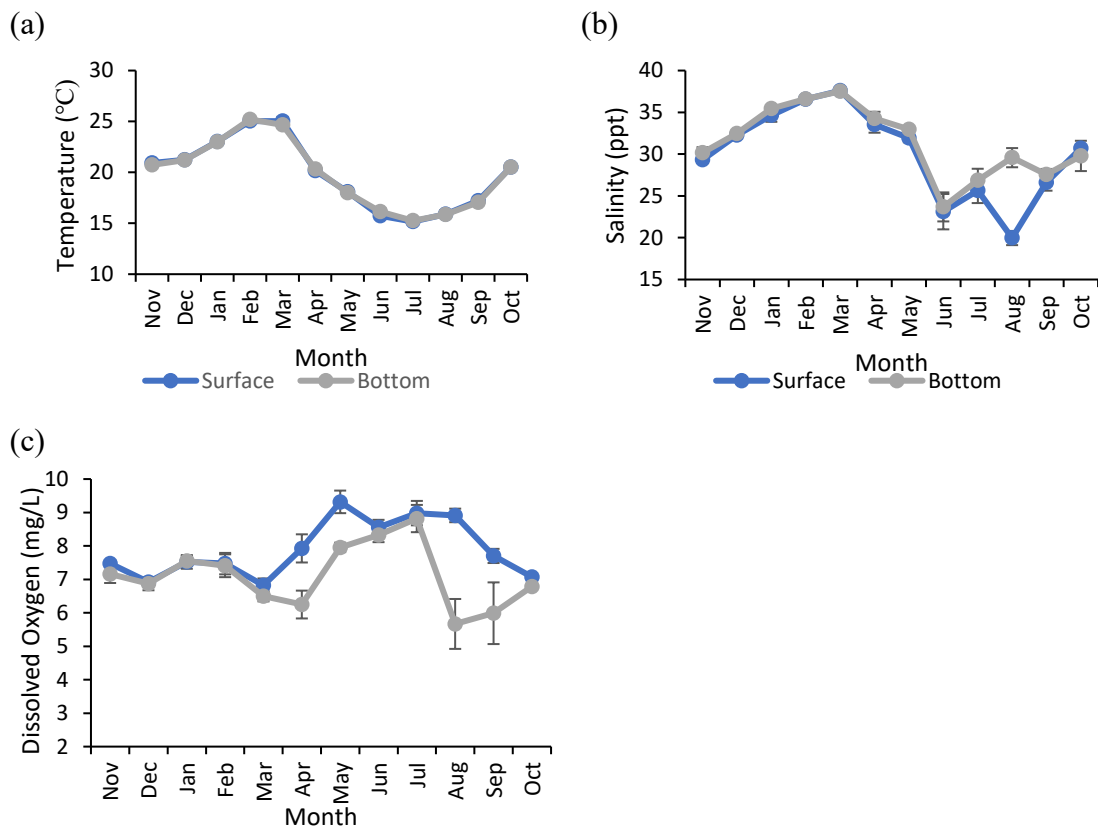


**Figure 3.1.1.** Average ( $\pm$  SE) values for (a) water temperature, (b) salinity, and (c) dissolved oxygen concentration across all sites in the Swan-Canning Estuary in each month between November 2022 and October 2023. The blue line indicates surface measurements while the grey line indicates bottom measurements.

A total of 323 *M. tenuicaudatus* were caught in the Swan-Canning Estuary between November 2022 and October 2023. There was no significant correlation between catch rate and any of the environmental parameters (Table 3.1.1). Between the three water quality measures, salinity had the least non-significant value ( $P= 0.066$ ) and positive correlation ( $R = 0.22$ ,  $R^2 = <0.01$ ). There was, however, a significant positive correlation between the abundance of *M. tenuicaudatus* and that of *P. armatus* ( $R= 0.28$ ,  $R^2= 0.08$ ,  $P = 0.017$ ; Fig. 3.1.2).

**Table 3.1.1.** Results from Pearson’s correlations for bottom water temperature, salinity, dissolved oxygen concentration, and Blue Swimmer Crabs (*Portunus armatus*) abundance in relation to the number of *Myliobatis tenuicaudatus* caught within the Swan-Canning Estuary.

Factor	df	R	R <sup>2</sup>	P
Water temperature	70	0.129	0.017	0.281
Salinity	70	0.218	0.048	0.066
Dissolved oxygen concentration	66	-0.089	0.008	0.468
<i>Portunus armatus</i>	70	0.280	0.079	0.017

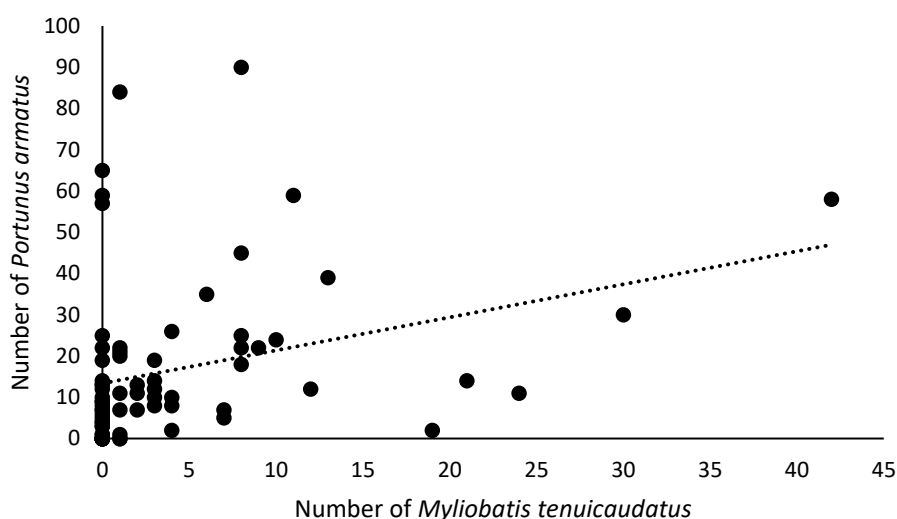


**Figure 3.1.2.** Number of *Myliobatis tenuicaudatus* caught and Blue Swimmer Crabs (*Portunus armatus*) caught per net in the Swan-Canning Estuary-Canning Estuary between November 2022 to October 2023.

Among sites, the most individuals were caught at Attadale (93), with intermediate catches at Como, Point Walter and Pelican Point (55-67) and the lowest at Dalkeith and Applecross (19-22; Fig 3.1.3). Catch rates were significantly greater at Point Walter than either Dalkeith and Applecross ( $P= 0.02$  and  $0.01$ , respectively) as well as Attadale when compared to Dalkeith and Applecross ( $P= <0.01$  for both; Fig 3.1.3, Fig 3.1.4b).

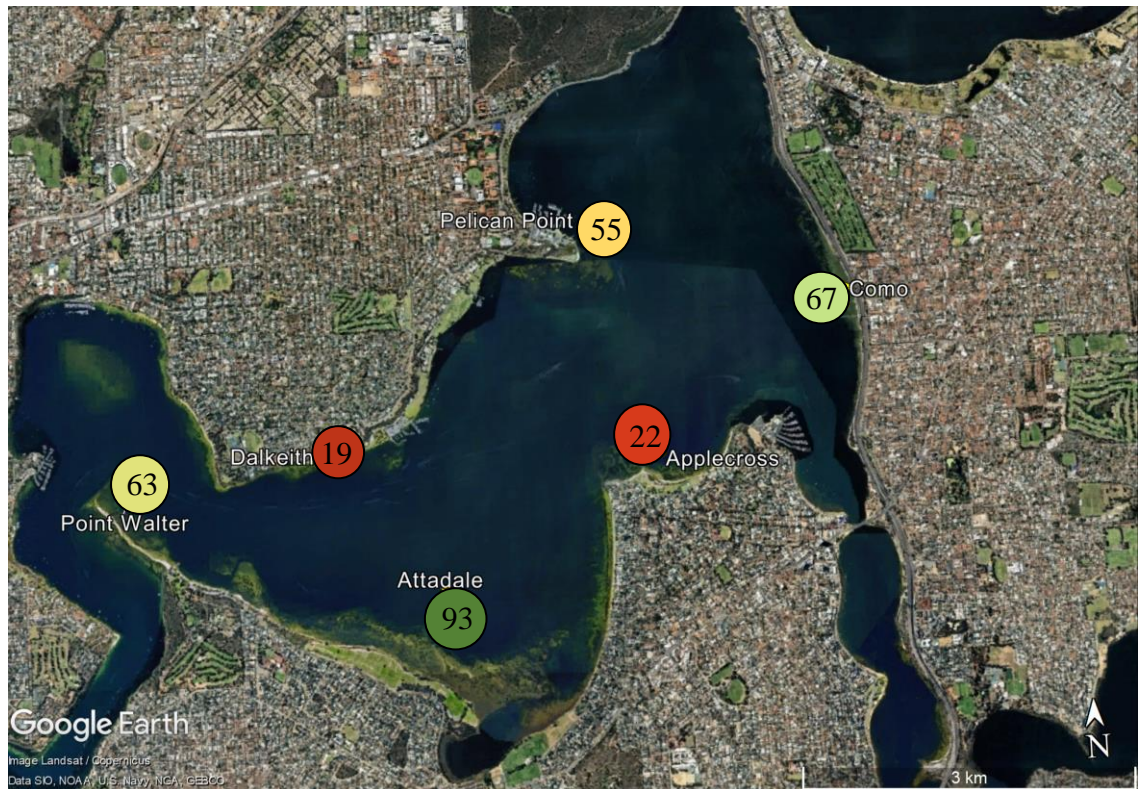


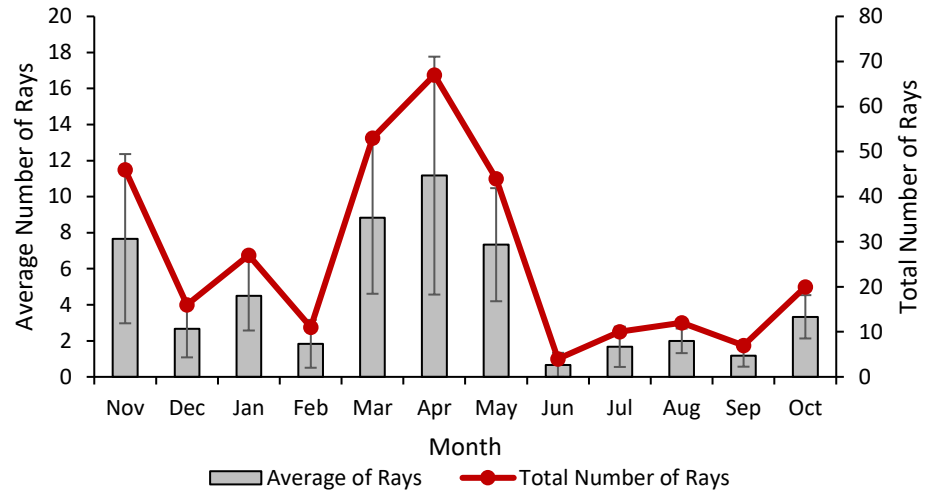
**Figure 3.1.3.** Total catch of *Myliobatis tenuicaudatus* at each site using 160m gill nets in the Swan-Canning Estuary from November 2022 to October 2023.

Catch rates of *M. tenuicaudatus* differed significantly among sites only, with no significance noted between months (Table 3.1.2). The total catch was highest in April (67 individuals) and lowest in June (4 individuals; Fig. 3.1.3.a). On an average basis, catches fluctuated during November to March before peaking in April and declining in June. From June the average catch rate remained consistently low before rising slightly in October. The population was inflated by the abundance of immature pups from March to May.

**Table 3.1.2.** Mean squares (MS), Sum of squares (SS), Pseudo-*F* (*pF*), and significance level (*P*) derived using PERMANOVA of the catch of *Myliobatis tenuicaudatus* between months and sites. *df* = degrees of freedom. Note the Month x Site interaction was used to calculate the residual.

Factor	<i>df</i>	SS	MS	<i>pF</i>	<i>P</i>
Month	11	31,936	290	1.435	0.170
Site	5	39,194	7,839	3.875	0.005
Residual	55	11,111	2,023		

(a)



(b)

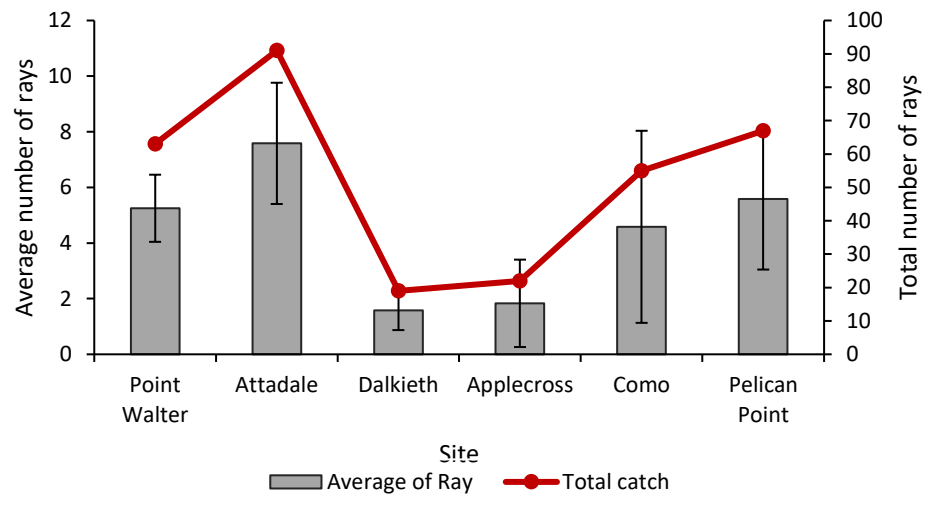


**Figure 3.1.4.** Average number ( $\pm$ SE) and total catch of *M. tenuicaudatus* among (a) months and (b) sites in the Swan-Canning Estuary.

### 3.2 Size and morphometrics

Male *M. tenuicaudatus* had an average DW of  $550 \pm 13$  mm (range = 235 to 816 mm) and an average weight of  $3,745 \pm 223$  g (range = 180.6 to 9,980 g; Fig 3.2.1). Females had a larger average DW of  $612 \pm 21$  mm (range = 243 - 1,181 mm) with an average weight of  $7,102 \pm 637$  g (range = 259.1 to 34,260 g). The largest female was 1.4 times the DW of the largest male and 2.1 times the weight. Two main size range cohorts were identified in the male population, at 300 mm and 550 – 650 mm. Two main cohorts were seen in the female population at 250 mm as well as 600 mm. Females at 800 – 950 mm were also identified.

Neonates (individuals <300mm DW) were found within the estuary every month except January and September. Individuals >900 mm were caught every month other than June (Appendix 3).

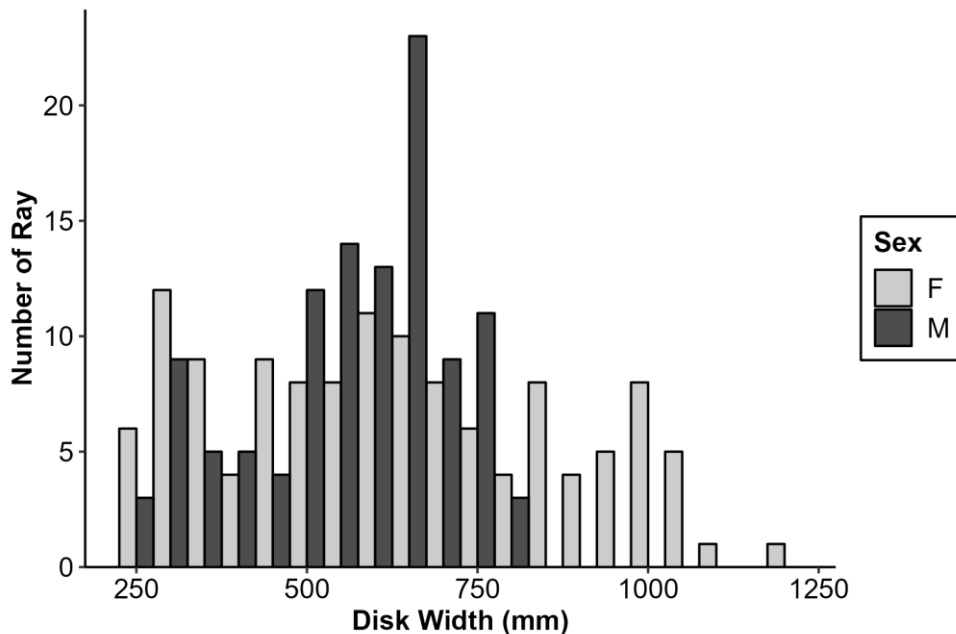


**Figure 3.2.1.** Disk width distribution of the *Myliobatis tenuicaudatus* caught within the Swan-Canning Estuary from November 2022 to October 2023

DW was had a strong relationship with all other body measures for both male and females, and as such, was used as the prominent body size measure (Fig 3.2.2). There was a significantly positive linear relationship between the natural log of disk width and weight for both male and females ( $R^2 = 0.96$ , and  $0.99$ ; Fig 3.2.2 a,b). There was also a strong positive linear relationship between disk width and body length with  $R^2$  values ( $0.92$  for both sexes; Fig 3.2.2, c,d). Despite the strong relationships between the above measures, that for disk width and total length was less marked for both males and females ( $R^2 = 0.65$ , and  $0.78$ , respectively; Fig 3.2.2. d,e).

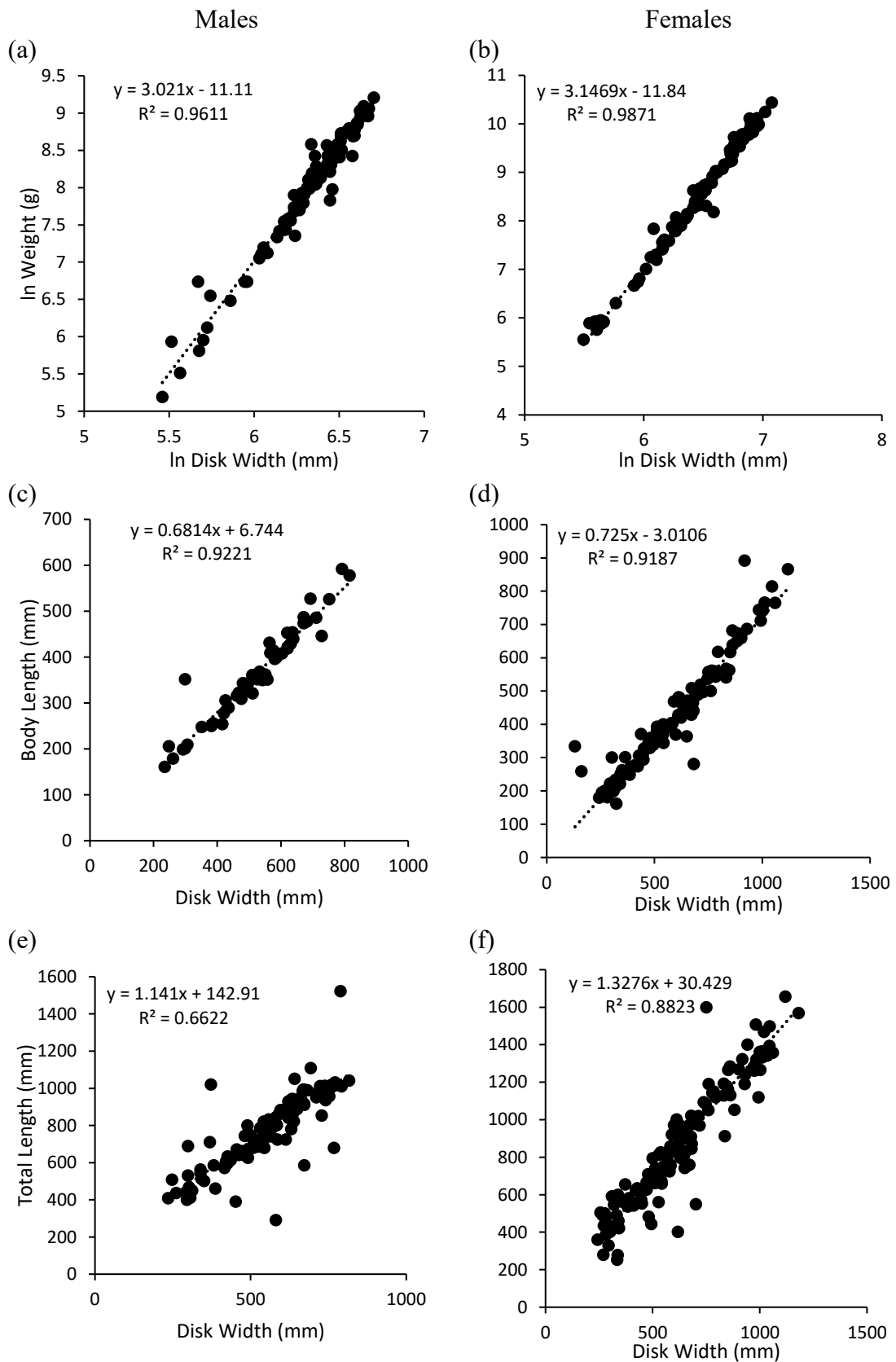


**Figure 3.2.2.** Scatter plot and linear regressions for natural log disk width compared to weight for (a) males ( $df= 94$ ,  $R^2= 0.98$ ,  $P= <0.01$ ) (b) and females ( $df= 81$ ,  $R^2= 0.96$ ,  $P= <0.01$ ); body length for (c) males ( $df= 130$ ,  $R^2= 0.92$ ,  $P= <0.01$ ) (d) and females ( $df= 137$ ,  $R^2= 0.92$ ,  $P= <0.01$ ); and total length of (e) males ( $df= 118$ ,  $R^2= 0.66$ ,  $P= <0.01$ ) (f) and females ( $df= 123$ ,  $R^2= 0.88$ ,  $P= <0.01$ ) *Myliobatis tenuicaudatus* in the Swan-Canning Estuary.

### 3.3 Age and growth

In elasmobranch species, and also *M. tenuicaudatus*, opaque bands tend to form in summer, while translucent bands occur in winter (Goldman, 2005). Marginal incremental analysis (MIA) of the produced an increasing trend from February to a peak in June (Fig 3.3.1), however there was a high degree of variability in this month due to the limited number of samples caught ( $n = 4$ ; see above). The lowest incremental data was in February (1.58 MIA). Under these conditions, it can be stated that the formulation of bands tend to occur during winter with the highest MIA value; therefore, it was be assumed one band-pair is formed annually on the vertebral centra and becomes delineated in February.

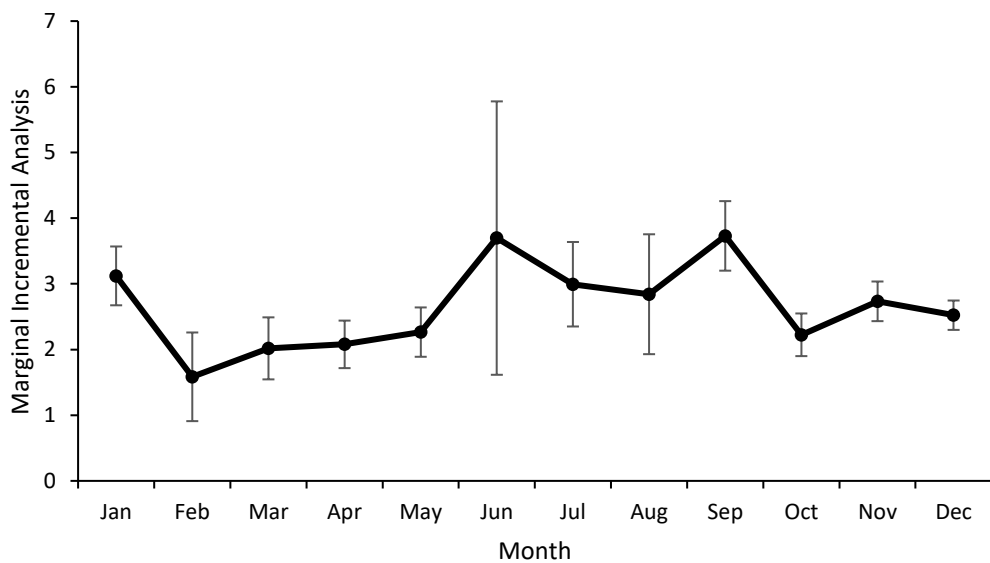


**Figure 3.3.1.** Mean marginal incremental analysis ( $\pm$ SE) for the *Myliobatis tenuicaudatus* caught in the Swan-Canning Estuary.

The age of *M. tenuicaudatus* caught in the Swan-Canning Estuary ranged between 0.1 and 15.9 years (i.e., females= 0.1 - 15.9 and males= 0.3 - 9.9). The results indicate that the age classes are uniform until ~10 years of age, after which there is an absence of males and a decline in females (Fig 3.3.2). Despite the maximum age documented as 9.9 years, these were found in ray frames provided by the commercial fisher, and as such do not have a calculated disk width.

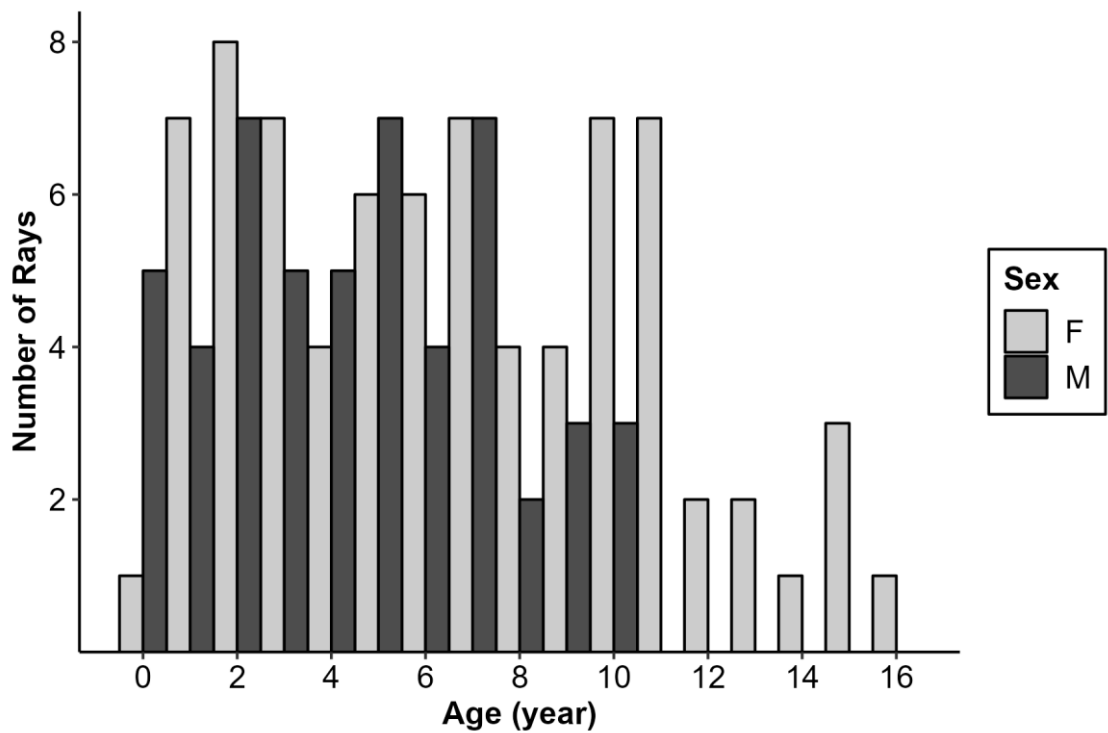


**Figure 3.3.2.** Age class distribution for *Myliobatis tenuicaudatus* caught in the Swan-Canning Estuary

The asymptotic disk width, or  $DW_{\infty}$  was greater in females than males, with higher variability in females, i.e., 1,033 mm and 1,836 mm, for males and females, respectively (Fig 3.3.3, Table 3.3.1). Growth rate ( $k$ ) and theoretical age when the disk width approaches 0 ( $t_0$ ) were greater in males than females (males= 0.12 mm and  $-2.4 \text{ year}^{-1}$ ; females= 0.05 mm and  $-3.4 \text{ year}^{-1}$ ; Table 3.3.1).

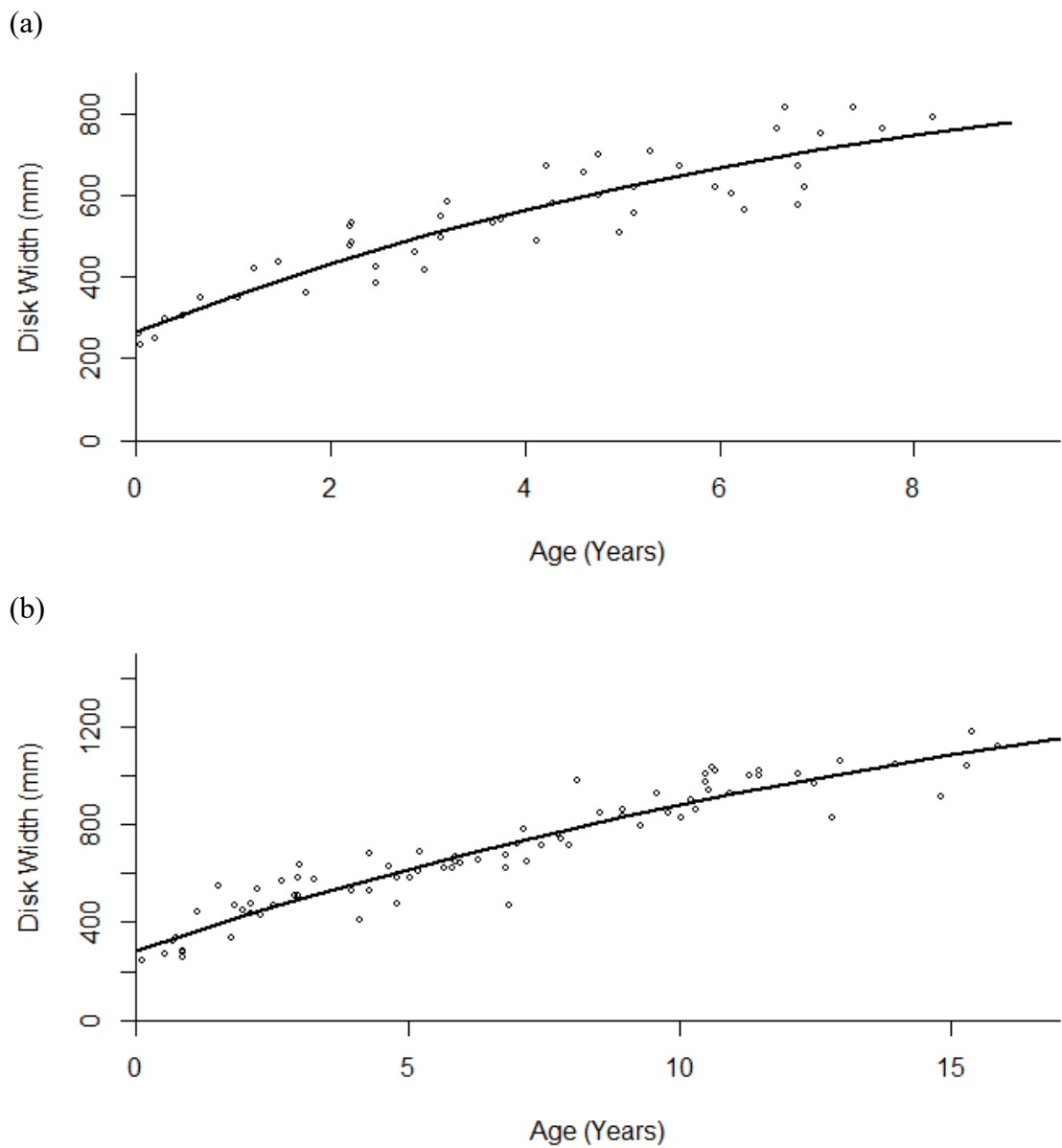


**Figure 3.3.3.** Von Bertalanffy growth curves for (a) male and (b) female *Myliobatis tenuicaudatus* in the Swan-Canning Estuary.

**Table 3.3.1.** Von Bertalanffy growth parameters ( $DW_{\infty}$ ,  $k$ ,  $t_0$ ) for male and female *Myliobatis tenuicaudatus* in the Swan-Canning Estuary.

	Estimate	2.5% CL	97.5% CL
<b>Male</b>			
$DW_{\infty}$ (mm)	1033.38	754.26	2671.93
$k$ (year <sup>-1</sup> )	0.12	0.03	0.26
$t_0$ (year)	-2.40	-4.15	-1.51
<b>Female</b>			
$DW_{\infty}$ (mm)	1836.47	1308.28	4546.71
$k$ (year <sup>-1</sup> )	0.05	0.02	0.09
$t_0$ (year)	-3.43	-5.31	-2.29

### 3.4 Reproduction

In female *M. tenuicaudatus*, the left ovary was fully functional while the right had limited functionality with one female noted to display ova in the right ovary (Fig 3.4.1). Both uteri were determined to be fully functional with eggs present in both. A total of 20 of the 27 mature females examined were pregnant, of which two contained one uterine egg in each uterus. Despite most females holding one or two uterine eggs, there was one female that was observed to present three aborted fetuses. During sampling it was observed that 14 females had aborted uterine eggs, with this being more prevalent during the winter months. Males were found to contain a functional left and right testis and an epigonal organ (Fig 3.4.1).

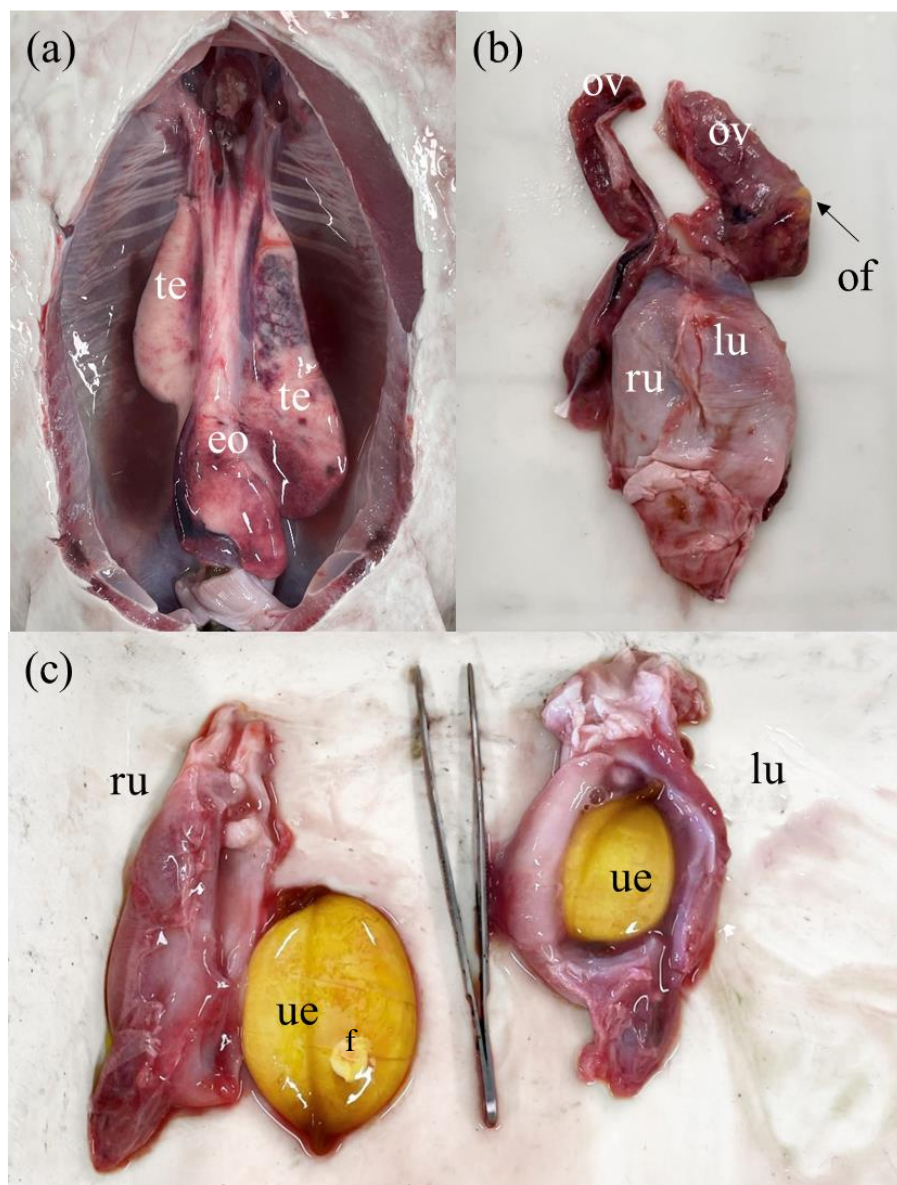


**Figure 3.4.1** Mature (a) male, (b) female reproductive structures; and (c) two fully functional uteri with uterine eggs. Important reproductive structures are labelled, testes (te), epigonal organ (eo), ovary (ov), the right and left uterus, (ru, lu, respectively), ovarian follicle (of), uterine eggs (ue), and fetus (f).

A total of 21 mature males and 27 mature females were analysed for a GSI and HSI. Based on the limited number of samples, a seasonal trend was apparent in the GSI for males with an increase from July to October, reaching a maximum of 1.09 % followed by a decrease in December to May, with a trough at 0.37 % in the latter month (Fig 3.4.2). In contrast, female GSI was stable from March to November with a sharp increase in GSI in December (3.14 %) decreasing to 0.83 % in February. Monthly HSI indicated a similar trend for both sexes with a slight decline in December to February (2.60 % and 5.07 %, for males and females, respectively). This was followed by an increase in July to September (8.06 % and 10.07 %, for males and females, respectively).

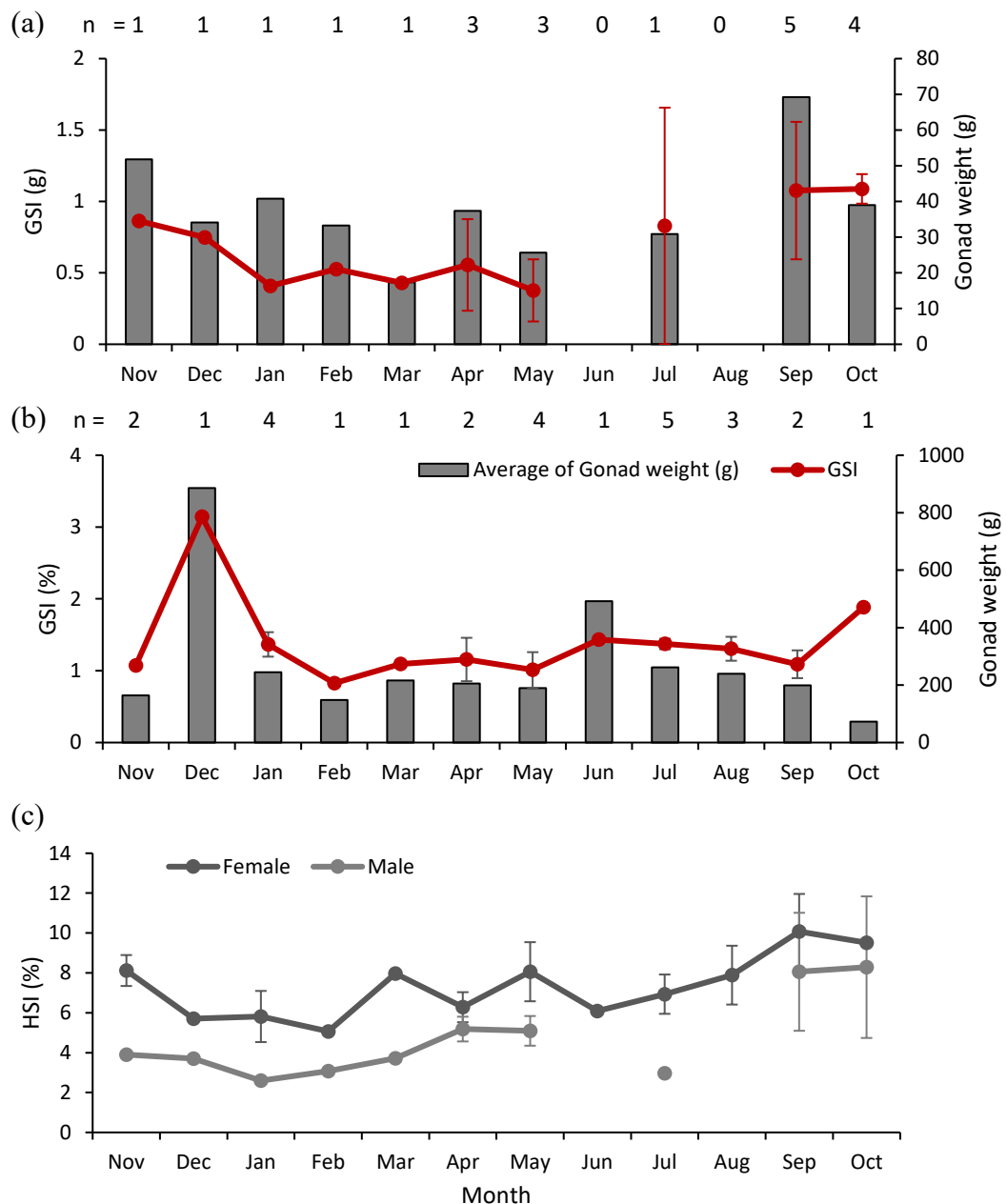


**Figure 3.4.2.** Monthly reproductive parameters calculated for the *Myliobatis tenuicaudatus* in the Swan-Canning Estuary between November 2022 to October 2023. Gonadosomatic Index (GSI) and mean gonad weight ( $\pm$  SE) for (a) male and (b) female,

and (c) Heptasomatic Index (HSI;  $\pm$  SE) for male and females (n = 21 and 24, respectively).

Clasper length increased significantly at approximately 450 mm DW with increases less marked at ~700 mm (Fig 3.4.3). The smallest male to attain sexual maturity was measured at 561 mm and the largest immature male had a DW of 728 mm. For stage one males, the average clasper size was 29.4 mm, while the average clasper size for stage two (immature) and three (mature) were 87.2 and 114.1 mm, respectively. For stage one females there was a limited increase in the uterine mass before a significant increase at 650 mm DW, at which most females were documented at stage two development Fig 3.4.3b). This increase continued throughout all other stages. The smallest female to attain sexual maturity and pregnancy was at 832 mm DW, while the largest immature female was recorded at 862 mm DW.

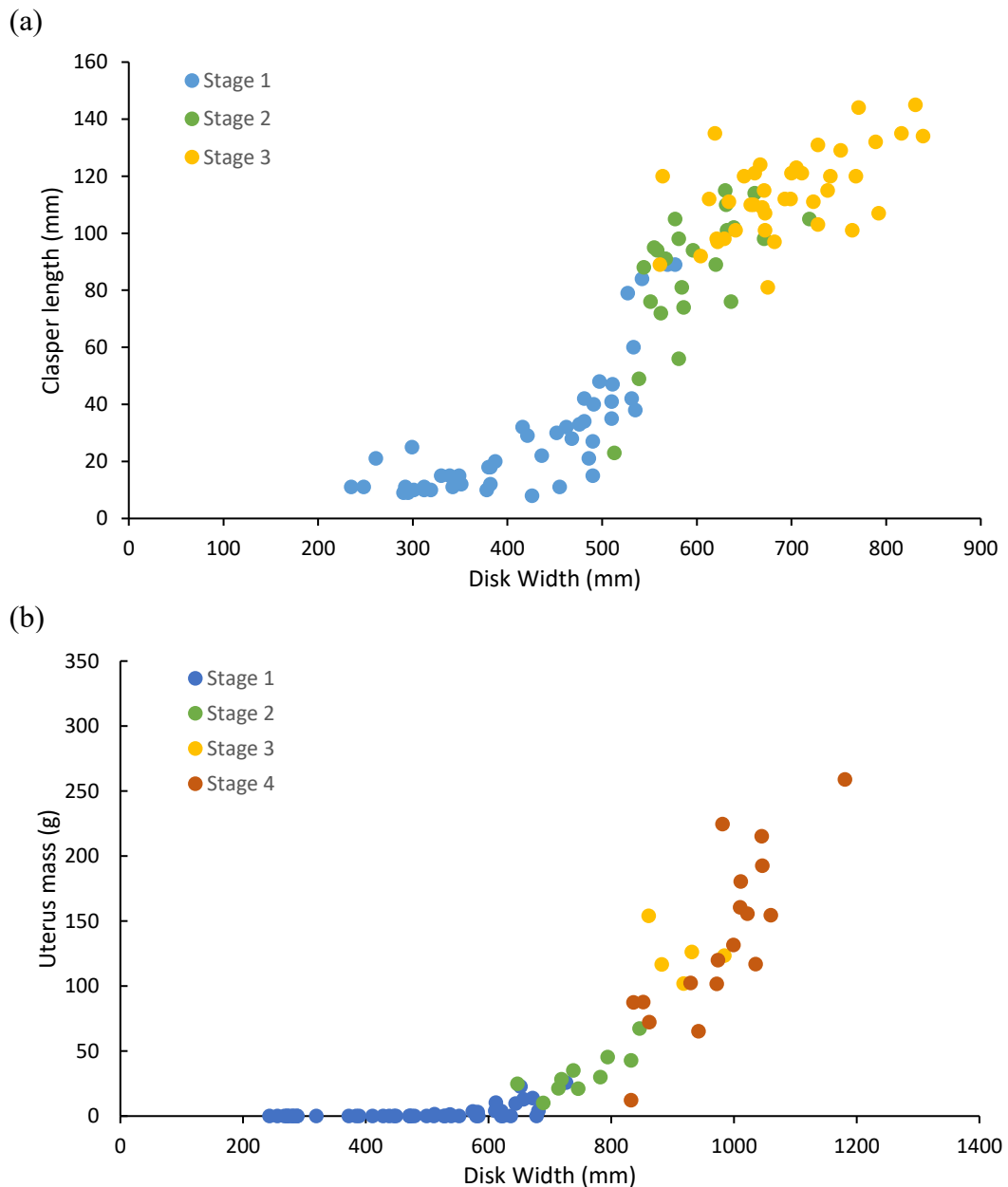


**Figure 3.4.3.** (a) Clasper length (males; n=125) and (b) uterus mass (females; n=87) in comparison to disk width for *Myliobatis tenuicaudatus* caught in the Swan-Canning Estuary

At sexual maturity ( $DW_{50}$ ), male disk width was less than that of females (Fig 3.4.4). The predicted median  $DW_{50}$  and age ( $A_{50}$ ) at 50% maturity for males was 595 mm and 5.1 years. The  $DW_{50}$  for females was 833 mm at 8.9 years.

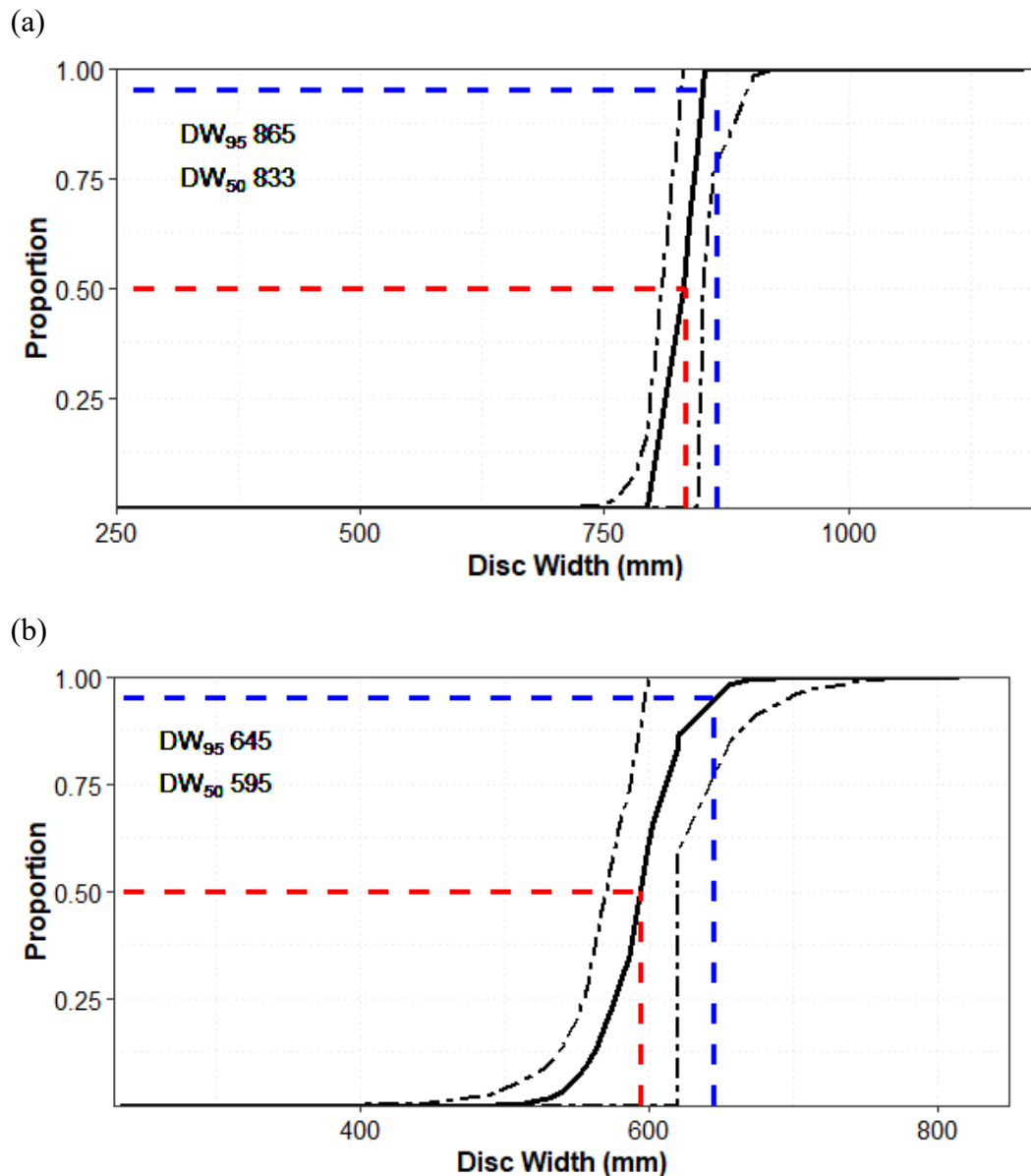


**Figure 3.4.4.** Maturity curve, and 95% confidence intervals for (a) male and (a) female *Myliobatis tenuicaudatus* with their respective  $DW_{50}$  (red) values and  $DW_{95}$  (blue) values.

### 3.5 Dentition and dietary composition

The mouth of *M. tenuicaudatus* located on the ventral surface, rather than being terminal as in mobulids. The jaws, which are surrounded by large adductor muscles, are relatively short and thick, and comprises a top jaw that curves upwards and a relatively

flat bottom jaw (Fig. 3.5.1). The teeth are thick, flattened and hexagonal and interlock into a pavement-like tooth plate. This extends across the full width of the mouth with an elongated central tooth with three small teeth on either side in a diagonal arrangement. Teeth are formed at the dorsal margin of the mouth and are lightly calcified with those situated further forward (ventral) are more mineralised. These become scratched and scoured and, in larger individuals, there was a noticeable depression of wear, particularly in the lower jaw, where prey is crushed (Fig. 3.5.1f). The bottom plate extends slightly more ventrally than the upper, beyond the point of contact with the upper jaw and are lost, typically from the outside inwards. This results in their being different numbers of rows of teeth, ranging from 11 to 17 rows in the bottom jaw and 9 to 15 rows on the top jaw.

Both jaw width and depth increased with larger disk width ( $R^2= 0.94$ , and  $0.85$ , respectively;  $P= <0.01$ ; Fig 3.5.2). There was a significant positive relationship between the jaw width and depth ( $R^2= 0.74$ ,  $P= <0.01$ ). The oral shape decreases, i.e. mouth becomes more oval-shaped, as individuals increase in size ( $R^2= 0.32$ ,  $P= 0.03$ ).

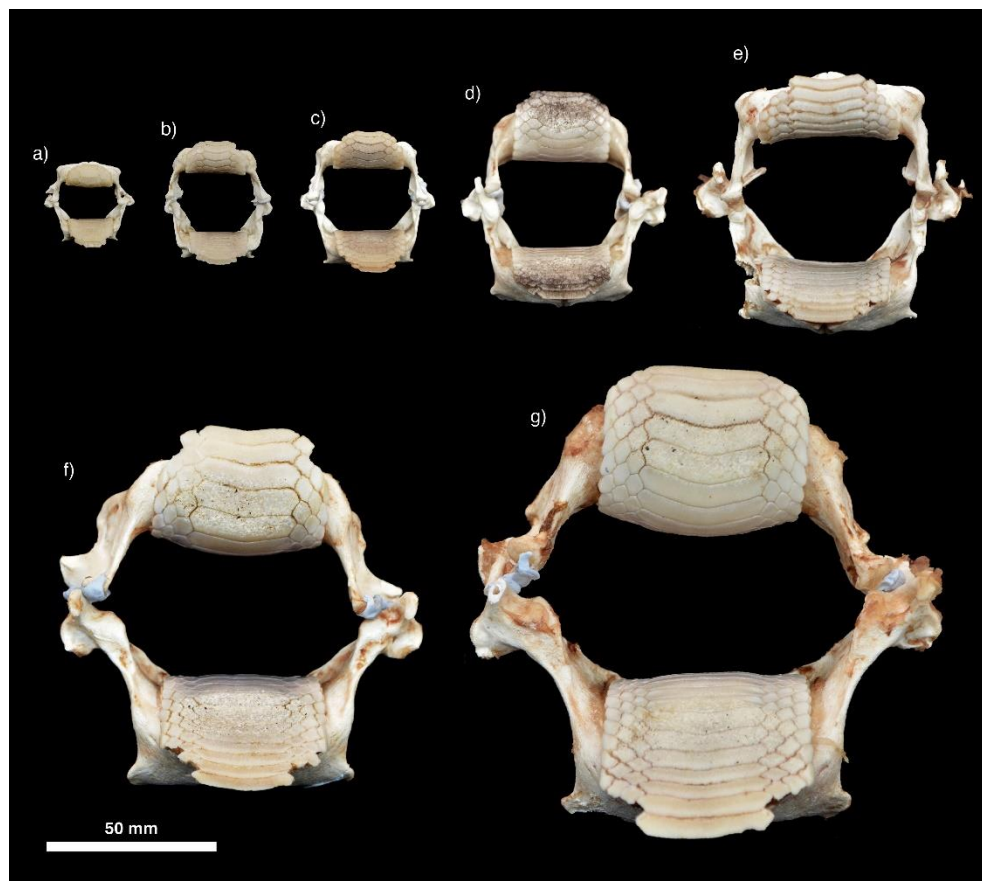


**Figure 3.5.1.** Photographs of the jaws of *Myliobatis tenuicaudatus* of different sizes. a) 243, b) 384, c) 428 d) 611, e) 794, f) 862 and g) 1,045 mm disk width.

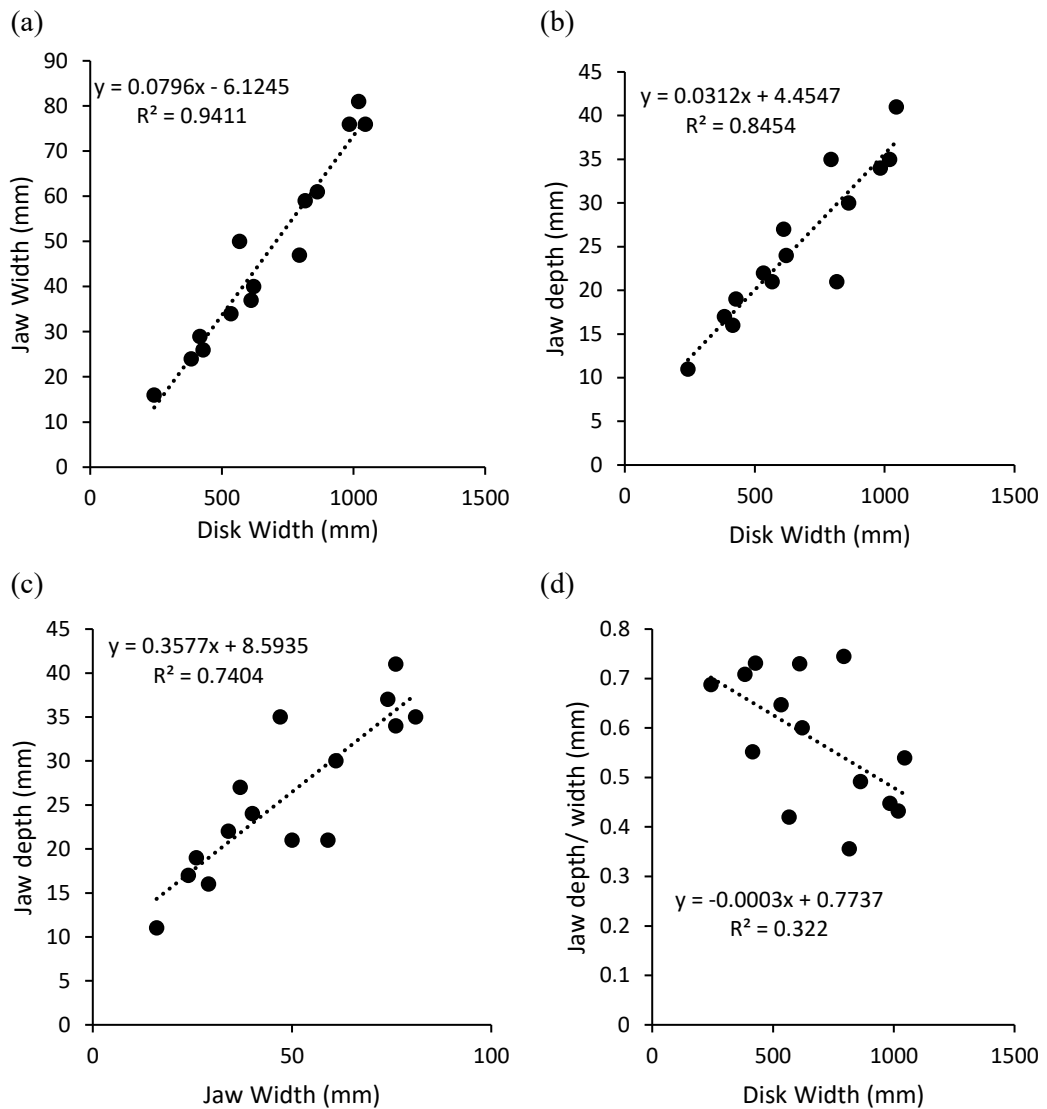


**Figure 3.5.2.** Disk width and jaw (a) width ( $df= 12$ ,  $R^2= 0.94$ ,  $P= <0.01$ ), (b) depth ( $df= 12$ ,  $R^2= 0.85$ ,  $P= <0.01$ ), (c) jaw width and depth ( $df= 12$ ,  $R^2= 0.74$ ,  $P= <0.01$ ), as well as (d) oral shape (depth/width) in comparison to DW ( $df= 12$ ,  $R^2$ ,  $P= 0.03$ ) of *M. tenuicaudatus* from the Swan-Canning.

The stomachs of 157 *M. tenuicaudatus* caught within the Swan-Canning Estuary were analysed with 107 found to contain prey items. Of the 157 stomachs analysed 24 were from frames provided by the commercial fisher, all of which were found to be empty. The main volumetric items found were crustaceans with the majority being penaeid prawns (45.0% and 25.8%, respectively; Fig. 3.5.3; Table 3.5.2). While crustaceans composed a large portion of prey items, on a limited number of brachyurans were recorded present, most of which were small species, likely *Thalamita* sp. The large portunid, *P. armatus* was only recorded in nine stomachs of the 107 stomachs containing food (8.4%) in low volumes (5.6 %V). These samples all came from large female, i.e. 1,050 DW mm. Molluscs and polychaetes comprised a large volume of identifiable dietary components (14.6% and 18.0%, respectively). Frequency of occurrence of each prey item, also document similar trends, with crustaceans present in over 41.0% of

samples. Molluscs were found in more stomachs than polychaetes (20.3% and 18.0%, respectively), despite polychaetes maintaining a higher percentage volume (Table 3.5.2). At the 100 mm DW classes, the volumetric contribution of arthropods increased significantly with body size ( $R= 0.773$ ;  $P=0.004$ ), those of annelids decreased significantly ( $R = -0.868$ ;  $P=<0.001$ ), while those of molluscs remained similar ( $r = 0.315$ ;  $P=0.180$ ): Fig. 3.5.4).

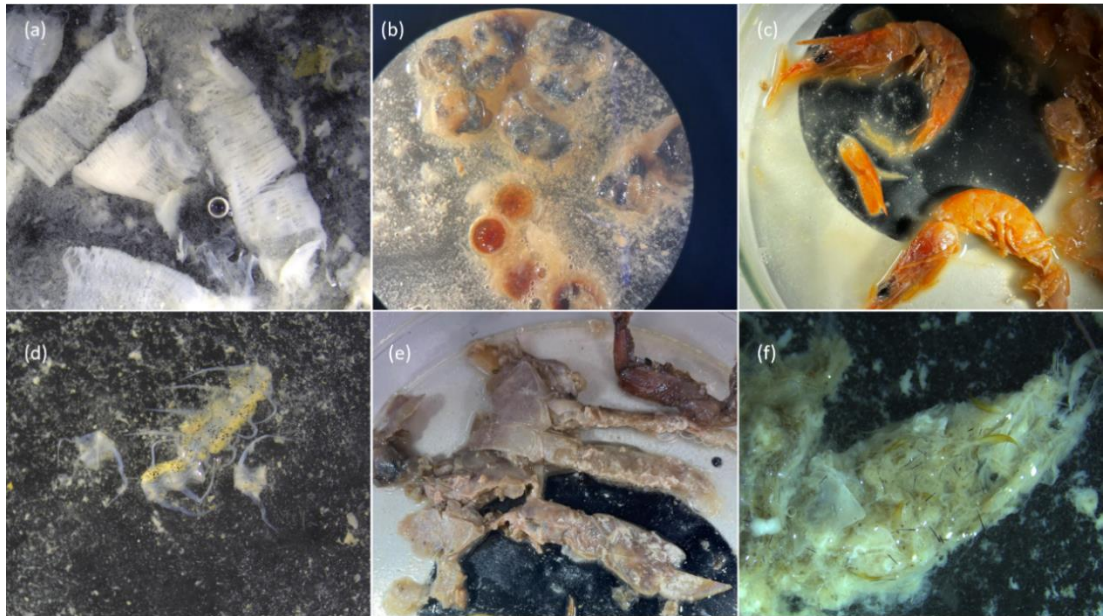


**Figure 3.5.3.** Examples of dietary items from *Myliobatis tenuicaudatus* in the Swan-Canning Estuary including: (a) bivalve siphon; (b) gastropod with operculum and body segments; (c) the penaeids *Penaeus latisulcatus* and *Metapenaeus dalli*; (d) backbone of a teleost; (e) *Portunus armatus* body segments; and (f) Nereididae sp. polychaete with jaws.

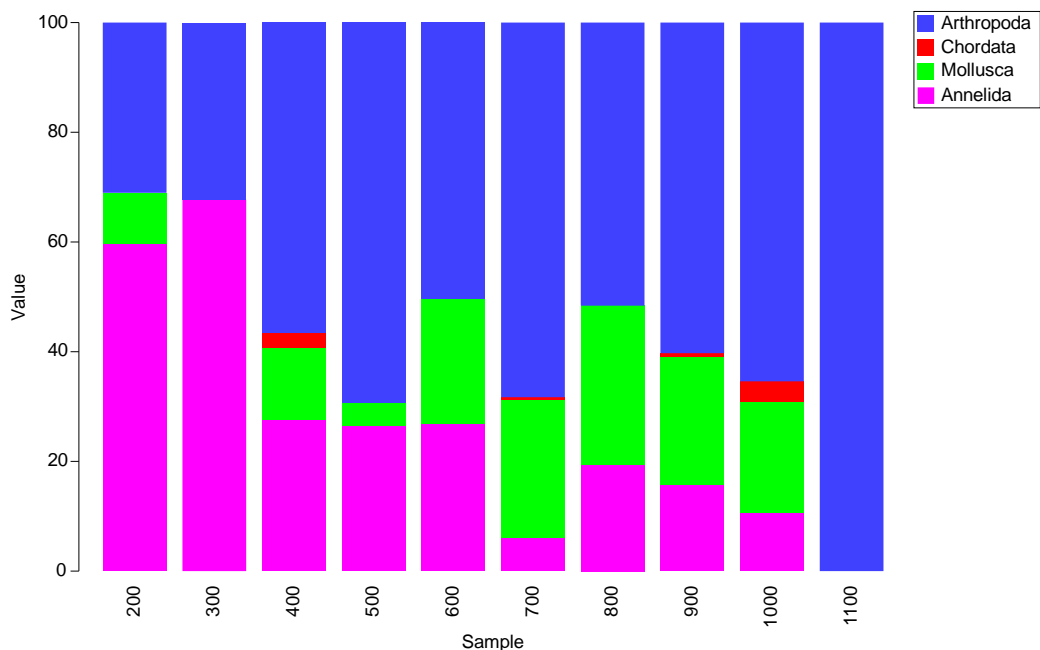


**Figure 3.5.4.** Stacked bar graph of the volumetric contribution of phyla-level prey to the diet of increasing sizes of *Myliobatis tenuicaudatus*.

**Table 3.5.2.** Percentage frequency of occurrence (%F) and average percentage by volume (%V) of dietary categories and major taxa (bolded) in stomach contents of *Myliobatis tenuicaudatus* in the Swan-Canning Estuary.

	Swan-Canning Estuary		Cockburn Sound		Lower west coast	
	%F	%V	%F	%V	%F	%V
<b>Polychaeta</b>	<b>14.3</b>	<b>18.0</b>	<b>22</b>	<b>14.6</b>	<b>52.7</b>	<b>22</b>
Opheliidae					1.2	0.4
Onuphidae					2.3	1.1
Nereididae	2.3	4.4	9	3.3	2.3	1.2
Unid.	12.0	13.6	17	11.3	47.7	19.2
Polychaeta						
<b>Other Worms</b>	<b>1.5</b>	<b>1.1</b>	<b>1</b>	<b>0.6</b>	<b>3.5</b>	<b>1</b>
Sipunculans			1	0.6	1.2	0.2
Nemertean					0.6	0.5
Echiurans	1.5	1.1			1.7	0.3
<b>Mollusca</b>	<b>20.3</b>	<b>14.6</b>	<b>33</b>	<b>39.7</b>	<b>79.1</b>	<b>40.9</b>
Bivalvia	9.0	7.04	2	1.3	18	8.4
Gastropoda	10.9	7.5	33	37.9	64	28.3
Polyplacophora					2.9	1.1
Scaphopoda					4.7	1.5
Cephalopoda					2.9	1.4
Unid. Mollusca			2	0.4	0.6	0.2
<b>Crustacea</b>	<b>41.0</b>	<b>45.0</b>	<b>26</b>	<b>33.1</b>	<b>68</b>	<b>29.2</b>
Brachyura	12.0	11.2	16	17.5	20.3	6.4
<i>Portunus armatus</i> *	3.4	5.6				
Penaeidae	22.9	25.8	3	1	27.3	8.1
Pleocyemata	6.0	8.0	16	7.2		
Stomatopoda			10	6.9		
Cumacea					0.6	<0.1
Tanaidacea					0.6	<0.1
Isopoda					1.2	0.1
Amphipoda					19.2	9.1
Unid.			3	0.7	18.6	5.3
Crustacea						
<b>Echinodermata</b>			<b>1</b>	<b>0.4</b>	<b>5.8</b>	<b>2.1</b>
Ophiuroidea			1	0.4	2.3	1.1
Echinoidea					0.6	0.1
Holothuroidea					2.9	0.9
<b>Teleostei</b>	<b>1.9</b>	<b>0.7</b>	<b>8</b>	<b>4.1</b>	<b>6.4</b>	<b>3</b>
Tetradontidae	0.4	0.3				
Sillaginidae			1	0.9		
Clupeidae					0.6	0.2
Plotosidae					0.6	0.2
Unid. Teleost	1.5	0.5	7	3.2	5.2	2.6
<b>Macrophyta</b>	<b>0.4</b>	<b>0.2</b>			<b>5.2</b>	<b>1.9</b>
Ascidiacea			<b>1</b>	<b>0.6</b>		
<b>Unidentified material</b>	<b>21.1</b>	<b>20.5</b>	<b>15</b>	<b>6.8</b>		
n	157		34		193	
n with food	107		34		173	
Avg fullness	4.3 (± 0.23)		3.7 (± 0.32)		4.6 (± 0.2)	

\* *Portunus armatus* has been included within the Swan-Canning Estuary as it was a targeted dietary item. As it can be identified as brachyuran, it may also be present in Cockburn Sound and Lower west coast samples.

Comparing the data from the Swan-Canning Estuary to other studies on this species in Western Australia, it was clear that the individuals from Cockburn Sound consumed mainly molluscs (33%F and 39.7%V, respectively; Table 3.5.1). However, crustaceans and polychaetes were still noted as major contributors to the dietary composition. Despite being in close proximity to the Swan-Canning Estuary, there was a greater diversity of species found in Cockburn Sound with sipunculids, echinoderms (brittle stars) and ascidians (sea squirts) present in these samples. Sommerville et al. (2011) conducted their study along the coast of Western Australia including near the mouth of the Swan-Canning Estuary and Cockburn Sound. This study also documents similar trends in which molluscs, crustaceans and polychaetes were the three most abundant prey groups. Among the three studies and locations, individuals from the Swan-Canning Estuary consumed the largest volume and frequency of occurrence of penaeid prawns, while simultaneously having the lowest volume and frequency of brachyurans. Teleosts were predated on by individuals from all studies.

One-way ANOSIM detected a difference in the dietary content between disk width classes of *M. tenuicaudatus* (Global  $R = 0.38$ ;  $P = 0.1\%$ ). At a pairwise level the diets of individuals in the 200 mm class significantly different prey items in comparison to all other size classes ( $R = 0.34-0.73$ ;  $P = 0.1-2.8\%$ ; Table 3.5.3). This is shown on the nMDS plot and particularly the centroid nMDS plot where the point(s) representing the smallest size class lie to the left (Fig 3.5.3). Individuals in the 200 mm size class was fed predominantly on polychaetes (Fig 3.5.4). The diets between individuals in the 400 vs 600 mm and 400 vs 800 mm disk width classes were not significantly different ( $P = 8.9\%$ , and  $13.7\%$ , respectively), as they both consumed large volumes of penaeid prawns. Individuals of 400 mm and 600 mm disk width, however, found to significantly differentiate from larger individuals at 1,000 mm (both  $P = 0.4\%$ ). Individuals at 800 mm were noted to feed on penaeids, gastropods and polychaetes and those at 1,000mm on crabs and gastropods.

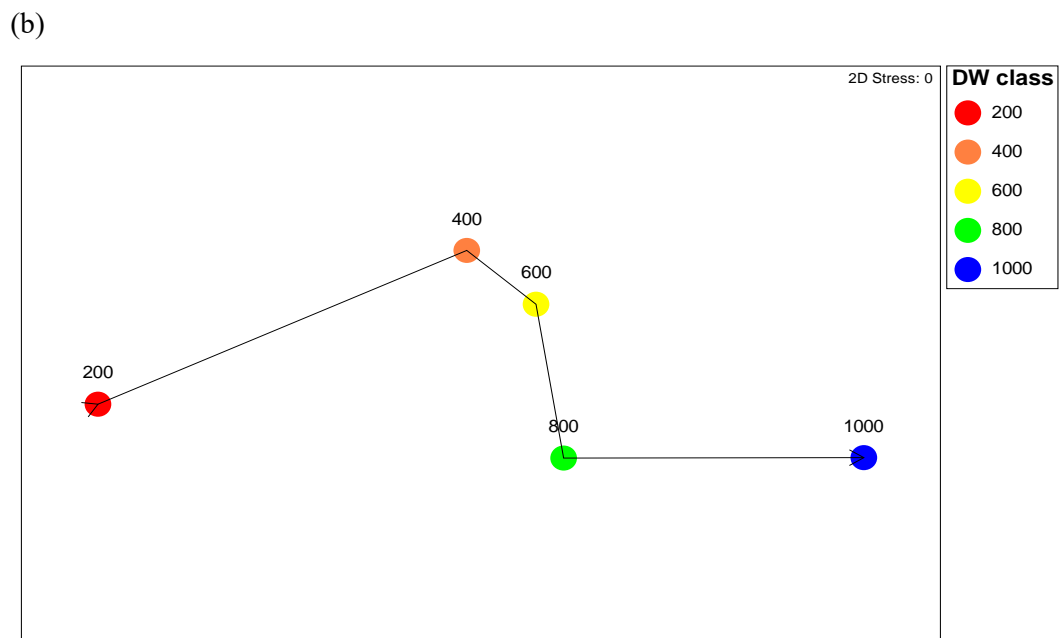
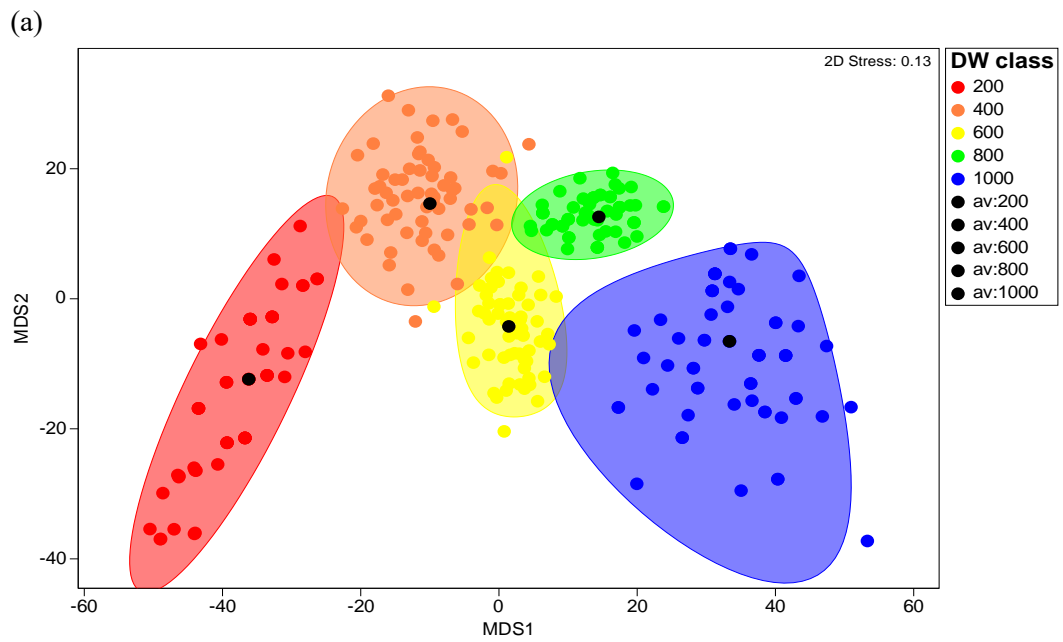


**Figure 3.5.4.** Metric MDS plots for a) dietary composition of *M. tenuicaudatus* in 200 mm disk width classes; and b) centroid plot for 200 mm disk width classes.

**Table 3.5.3.** R values derived from ANOSIM test of dietary composition in 200 mm disk width classes. Significant differences ( $P < 0.05$ ) are shaded in grey.

	200	400	600	800
400	0.338			
600	0.725	0.148		
800	0.652	0.157	0.279	
1000	0.574	0.550	0.512	0.268

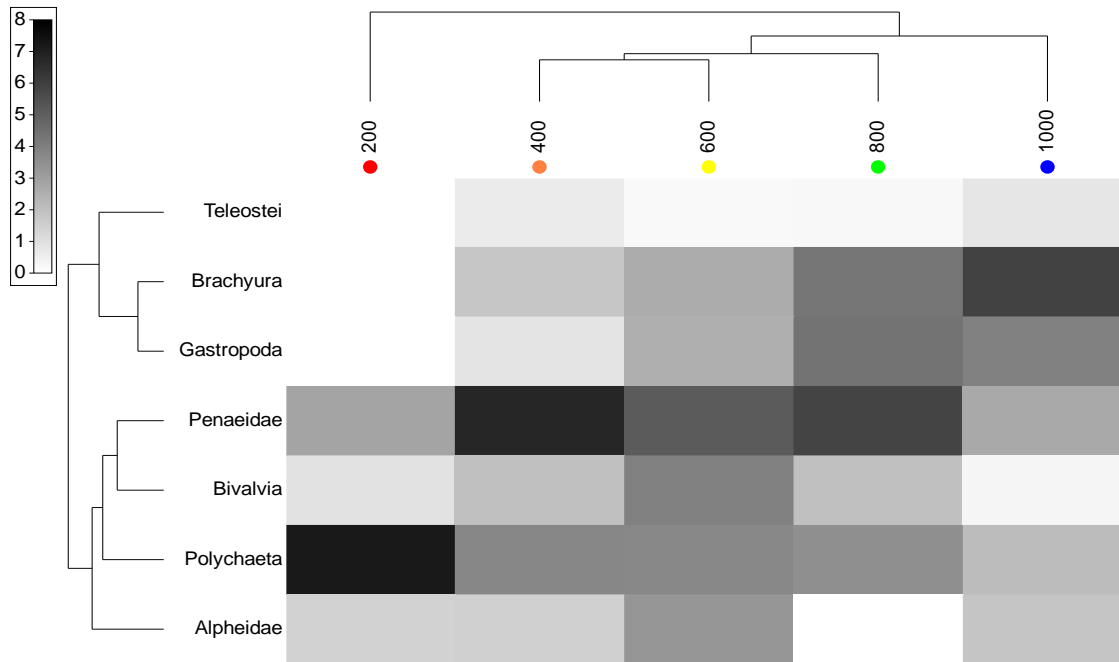


**Figure 3.5.4.** Shade plot of prey items by 200 mm length classes of *M. tenuicaudatus* in the Swan-Canning Estuary.

**Table 3.5.4.** Dietary categories that typified (grey) and distinguished (white) the diet of *M. tenuicaudatus* within 200 mm disk width class based on SIMPER. The length class in which each dietary category was most frequent is provided in superscript for each pairwise comparison. Insignificant comparisons are noted as N/S. Bray-Curtis similarity (Sim) and dissimilarity (Dsim) values are also provided.

	200	400	600	800	1000
200	Sim: 47.13 Polychaeta				
400	Dsim: 59.30 Polychaeta <sup>200</sup> Penaeidae <sup>400</sup>	Sim: 54.59 Penaeidae Polychaeta			
600	Dsim: 61.96 Penaeidae <sup>200</sup> Penaeidae <sup>600</sup> Bivalvia <sup>600</sup> Alpheidae <sup>600</sup>	Dsim: 43.34 N/S	Sim: 66.16 Penaeidae Bivalvia Polychaeta		
800	Dsim: 66.87 Polychaeta <sup>200</sup> Gastropoda <sup>800</sup> Brachyura <sup>800</sup>	Dsim: 43.00 N/S	Dsim: 35.95 Alpheidae <sup>600</sup> Bivalvia <sup>600</sup> Gastropoda <sup>800</sup> Brachyura <sup>800</sup>	Sim: 74.33 Penaeidae Brachyura Gastropoda	
1000	Dsim: 80.56 Brachyura <sup>1000</sup> Polychaeta <sup>200</sup> Gastropoda <sup>1000</sup>	Dsim: 64.30 Brachyura <sup>1000</sup> Penaeidae <sup>400</sup> Gastropoda <sup>1000</sup>	Dsim: 53.35 Brachyura <sup>1000</sup> Bivalvia <sup>600</sup> Alpheidae <sup>600</sup> Penaeidae <sup>600</sup>	Dsim: 44.84 Brachyura <sup>1000</sup> Penaeidae <sup>800</sup>	Sim: 49.34 Brachyura Gastropoda

The dietary composition of the population of *M. tenuicaudatus* significantly differed between seasons (Global  $R = 0.36$ ;  $P = 0.1\%$ ), with that in summer and autumn differing significantly from spring ( $P = 0.4\%$  and  $0.9\%$ , respectively; Fig 3.5.5). Diet in spring comprised mainly polychaetes and penaeid prawn (Fig. 3.5.6), while in summer the volume of penaeids increased (average abundance 3.91 and 7.02, respectively) and polychaetes decreased (average abundance 6.21 and 4.42). Penaeids were also a prominent prey item in autumn along with brachyurans and bivalves. Winter noted the highest abundance of brachyurans as well as a large presence of penaeid prawns.

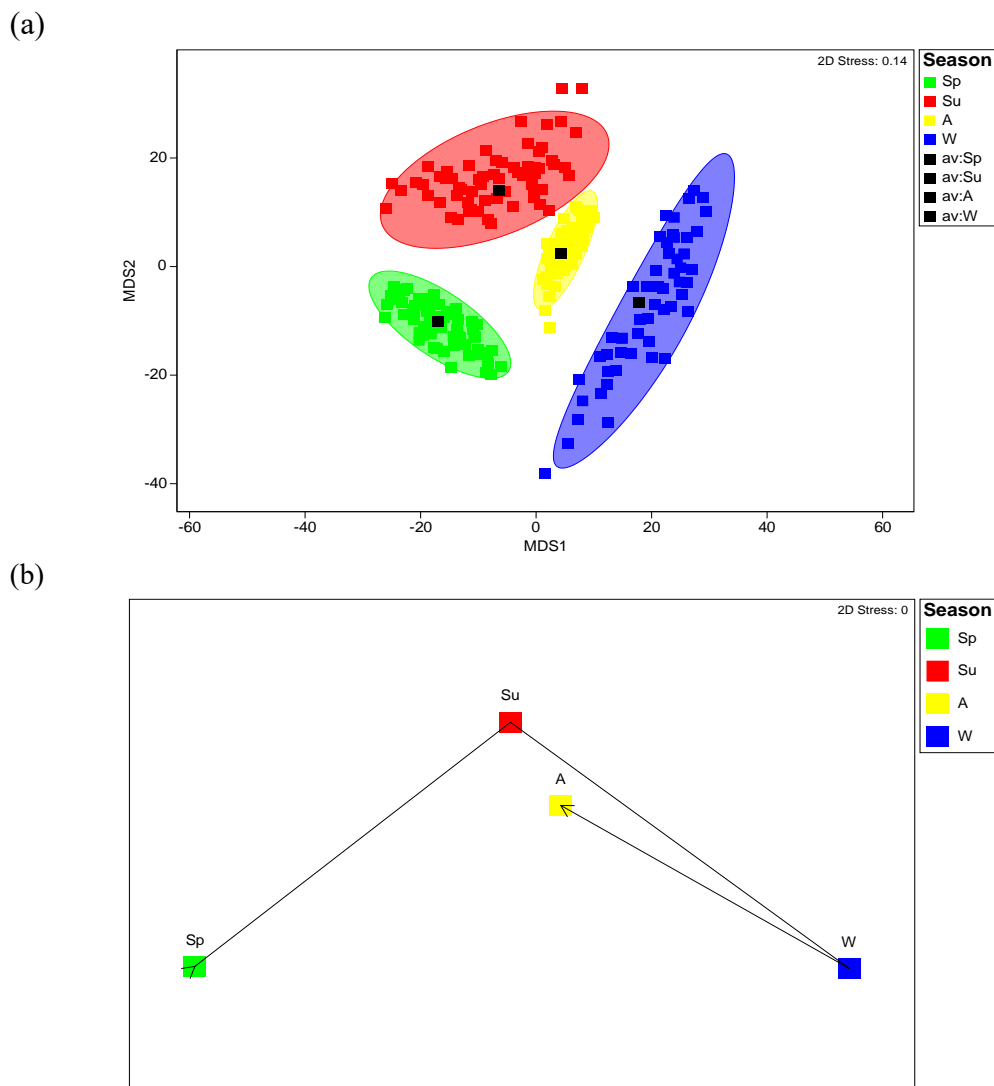


**Figure 3.5.5.** (a) mMDS ordinations and (b) nMDS centroid plot of the diet of *Myliobatis tenuicaudatus* in the Swan-Canning Estuary in Summer (SU; ■), Autumn (A; ■), Spring (SP; ■) and Winter (W; ■).

**Table 3.5.5.** R values derived from ANOSIM test of dietary composition in each season. Significant differences ( $P < 0.05$ ) are shaded in grey.

	Summer	Spring	Autumn
Spring	0.348		
Autumn	0.219	0.574	
Winter	0.256	0.592	0.341

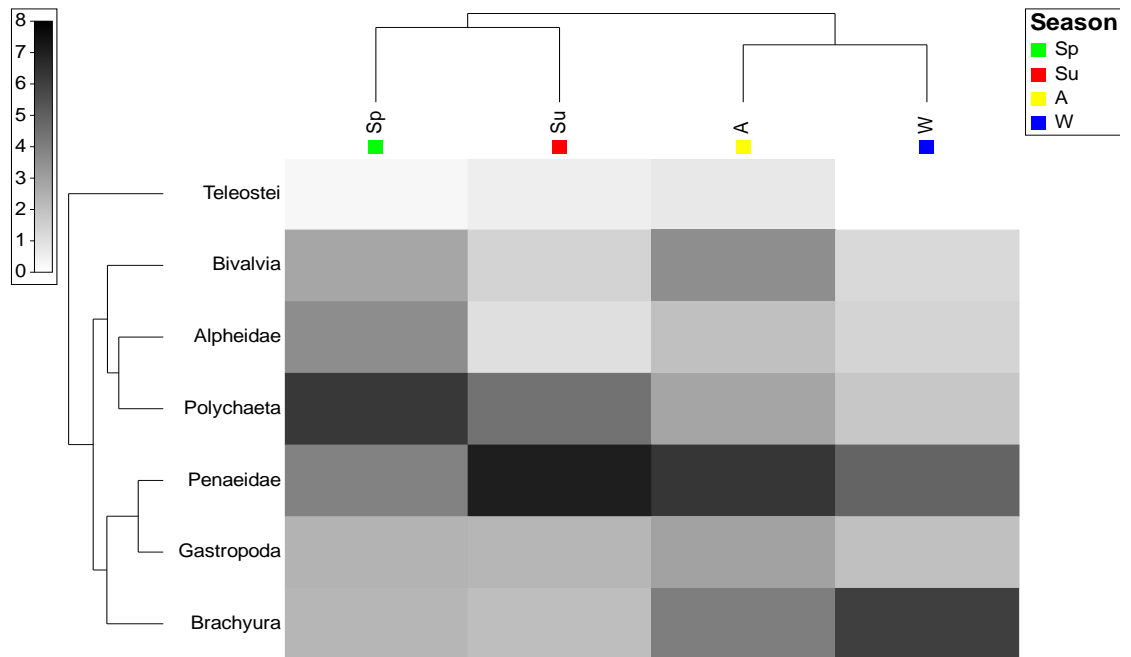


**Figure 3.5.6.** Shade plot with additional cluster analyses for the dietary composition of *Myliobatis tenuicaudatus* from the Swan-Canning Estuary in each season where sufficient numbers of samples were collected, i.e. in Summer (SU; ■), Autumn, (A; ■), Spring (SP; ■) and Winter (W; ■).

**Table 3.5.6.** Dietary categories that typified (grey) and distinguished (white) the diet of *M. tenuicaudatus* within each season based on SIMPER. The season in which each dietary category was most frequent is provided in superscript for each pairwise comparison. Bray-Curtis similarity (Sim) and dissimilarity (Dsim) values are also provided.

	Spring	Summer	Autumn	Winter
Spring	Sim: 72.64 Polychaeta Penaeidae Alpheidae			
Summer	Dism: 39.73 Penaeidae <sup>Su</sup> Alpheidae <sup>Sp</sup> Bivalvia <sup>Sp</sup>	Sim: 63.18 Penaeidae Polychaeta		
Autumn	Dsim: 34.16 Polychaeta <sup>Sp</sup> Alpheidae <sup>Sp</sup> Penaeidae <sup>Au</sup> Brachyura <sup>Au</sup>	Dsim: 34.15 Bivalvia <sup>Au</sup> Polychaeta <sup>Su</sup> Brachyura <sup>Au</sup>	Sim: 77.26 Penaeidae Brachyura Bivalvia	
Winter	Dsim: 50.15 Polychaeta <sup>Sp</sup> Brachyura <sup>W</sup> Alpheidae <sup>Sp</sup> Penaeidae <sup>W</sup>	Dsim: 48.32 Brachyura <sup>W</sup> Polychaeta <sup>Su</sup> Penaeidae <sup>Su</sup>	Dsim: 39.01 Polychaeta <sup>Au</sup> Bivalvia <sup>Au</sup> Penaeidae <sup>Au</sup>	Sim: 54.04 Brachyura Penaeidae

#### **4. Discussion**

Determining and understanding the biological characteristics of fisheries species such as morphology, growth and reproduction are vital for an effective management and stock assessments. This study was the first to estimate several biological characteristics for *Myliobatis tenuicaudatus*, as well as determine the spatial and temporal abundance and distribution of this species in an estuary. The dietary composition of *M. tenuicaudatus* was determined analyses to see if it changes with increasing body size and among seasons. As this thesis centres on a single species in a single environment, all findings are discussed, and comparisons made to other species in the Myliobatidae and their allies.

##### ***4.1 Environmental variables and Myliobatis tenuicaudatus catch rates***

Environmental variables typically influence the spatial and temporal distribution of batoid species (Meloni et al., 2002). However, the catch rates of *M. tenuicaudatus* in the Swan-Canning Estuary was not found to be correlated with either water temperature, salinity or dissolved oxygen, despite being noted previously (Davey et al., 2023). One possible explanation is that the range in those parameters were less than those in comparable studies where shifts in abundance have occurred. For example, Davey et al. (2023) noted that *M. tenuicaudatus* were prominent in Coffin Bay (South Australia) during summer before disappearing during the winter period when water temperatures dropped to 10.6 °C. Similarly, it was noted that *M. tenuicaudatus* was not recorded in the Walpole-Nornalup Estuary (southern Western Australia) when the temperature reached 5 °C but was abundant in summer when temperatures reached 25 °C (Potter & Hyndes, 1994). Both lower values as far smaller than the minimum temperature of 14.5°C recorded at Point Walter in the Swan-Canning Estuary, thus the observed temperature may be with the organism's tolerance envelope.

Salinity was also expected to influence the distribution and abundance *M. tenuicaudatus* as typically elasmobranchs are stenohaline (Ballantyne & Fraser, 2012) and that Potter and Hyndes (1994) did not catch this species in the Nornalup-Walpole Estuary when salinities were < 25 ppt. While this was true in the Swan-Canning Estuary in June 2023 (when salinity reached 24 ppt), as sampling was conducted in the bottom waters of the lower reaches of the estuary, salinities may not have declined enough to elicit a response. However, the fact that 94% of the *M. tenuicaudatus* individuals recorded at part of the Fish Community Index (Hallett et al., 2019), which samples from the basin area of the Lower Swan-Canning Estuary to the Upper Swan-Canning Estuary region,

have been recorded from the six sites sampled in the current study in the lower reaches indicates that the salinity regime across the estuary as a whole influences the distribution of this species. Similar to the findings noted, most marine species that are found in estuaries are recorded in lower reaches (Valesini et al., 2017).

Dissolved oxygen concentration was also shown not to be influential. Similar trends have been reported by others (Potter & Hyndes, 1994; Meloni et al., 2002; Davey et al., 2023). It should be noted that *M. tenuicaudatus* might be influenced if oxygen levels became hypoxic or anoxic levels, but this did not occur and the bottom waters of the area where sampling occurred were normoxic (>2mgL).

There was, however, a significant correlation between the abundances of *M. tenuicaudatus* and *Portunus armatus*. It has been suggested by commercial fishers across the southern Western Australia, that *M. tenuicaudatus* are present year-round and predate on *P. armatus* (DPIRD, pers. Comm. 2023). That being said, *P. armatus* was not found to be an important prey item for *M. tenuicaudatus* in this or previous studies where samples were obtained from commercial fishers operating in marine waters (Sommerville et al., 2011). The correlation recorded in the current study may reflect the fact that *M. tenuicaudatus* could be attracted to the nets due to the movements of captured prey (fish) and/or blood from injured fish creating a burley trail and attracting other taxa. Alternatively, *M. tenuicaudatus* and *P. armatus* may also have higher activities in the shallows in warmer water temperatures, having a higher probability of capture. (Poh et al., 2019) notes that as marine species, *P. armatus* prefer saline waters and restricted to downstream subregions, overlapping the preferred sites of *M. tenuicaudatus*.

Catches of *M. tenuicaudatus* were not significantly influenced by month, however there were with lower numbers of individuals caught during winter, which was expected. However, there were limited individuals caught in summer than autumn and spring. As most elasmobranch species are stenohaline, and rainfall is least in summer (Hodgkin & Hesp, 1998) the lower catch rates of *M. tenuicaudatus* are unusual. In various studies globally, it has been noted that batoids species move into protected areas during birthing and breeding seasons, which is typically during summer, before moving into deeper oceanic areas during winter (Davy et al., 2015; Martins et al., 2018; Yamaguchi et al., 2021; Davey et al., 2023). It was noted that this species gave birth (parturition) during the austral summer months, however, this time of year could also be the time of copulation where males and females move into deeper waters to reproduce (Yamaguchi et al., 2021). The increase in catch rates in autumn is likely due to the inflation of the population by

neonates after birth in summer. It has been documented in various myliobatid and allied species, such as *R. javanica* and *R. bonasus* that copulation starts at the mid-depth before continuing to the bottom of deeper areas (Uchida, 1990; Pratt & Carrier, 2001).

Site was also a significant influence on the catches of *M. tenuicaudatus*, with four sites yielding relatively high catch rates and two sites with lower. There were no environmental parameters noted to cause these variances, and as such may be caused by site preferences. Both Applecross and Dalkeith were closer to the shoreline than other sites, and as such may be unpreferred sites.

#### **4.2 Morphometrics**

The maximum DW of the *M. tenuicaudatus* documented in this study was 1,181 mm, which is less than a previous maximum size reported of 1,300 mm DW in specimens collected in New Zealand (Marcotte, 2013) and the estimate of 1,600 mm DW stated by (Last et al., 2016). The size variance may be due to the distribution of specimen (Western Australia in comparison to New Zealand) and differing size of gill net mesh sizes used in the two studies (multimesh with a maximum size of 127 mm vs 200 mm mesh).

*Myliobatis tenuicaudatus* <300 mm DW were recorded within the Swan-Canning Estuary in all months except January and September. All such individuals were less than one year old. Nursery areas, are regions where parturition occurs and juveniles are present in high densities, reside (Springer, 1967; Beck et al., 2001; Martins et al., 2018). In such areas, food is plentiful, allowing for relatively fast growth rates, with limited predation risks (Martins et al., 2018). Due to these characteristics, estuaries, and shallow marine ecosystems are often considered as nursery areas for batoid species. Due to the large numbers of juvenile and neonate individuals found within this study, as well as the presence of various prey items and limited number of predators, it is likely that the Swan-Canning Estuary could act as a nursery area for *M. tenuicaudatus*.

Similar to most myliobatid and allied species, female *M. tenuicaudatus* grows to a larger size than males. Most myliobatids have a similar size at birth (210-295 mm DW), however grow to various sizes (Table 4.2.1). *M. tenuicaudatus* is among the largest myliobatid species, together with *M. californica* (1,300 mm DW), while this study documented the second largest individual (1,180 mm DW). Male *M. tenuicaudatus* remain central between other species with the *M. ridens* reaching the lowest maximum disk width and *M. freminvillei* the greatest (590mm and 1,180mm, respectively) (Araújo et al., 2016; Tagliafico et al., 2016). *Myliobatis freminvillei* is also the only Myliobatidae

**Table 4.2.1.** Reported ranges of disk width (DW) of various myliobatid and allied species from the scientific literature.

	Male DW (mm)	Female DW (mm)	Male weight (g)	Female weight (g)	Sample size
<b>Myliobatidae</b>					
<i>Myliobatis aquila</i> <sub>1</sub>	210-720	240-1,140	116-5,250	190-29,400	73
<i>Myliobatis californica</i> <sub>2</sub>	322-920	310-1,300			
<i>Myliobatis freminvillei</i> <sub>3</sub>	228-1,180	240-960	200-19,000	200-12,000	187
<i>Myliobatis goodei</i> <sub>4</sub>	450-650	433-1,150	1,360-3,560	1,820-25,800	95
<i>Myliobatis ridens</i> <sub>4</sub>	366-590	243-980	1,300-2,730	183-13,080	175
<b><i>Myliobatis tenuicaudatus</i></b>	<b>235- 839</b>	<b>243-1,181</b>	<b>180.6-9,980</b>	<b>259.1-34,260</b>	<b>323</b>
<i>Aetomylaeus bovinus</i> <sub>5</sub>	295-1,290		270-33,600		94 *
<b>Aetobatidae</b>					
<i>Aetobatus flagellum</i> <sub>6</sub>	?-1,000	?-1,500	?-14,400	?-50,000	**
<i>Aetobatus narinari</i> <sub>7</sub>	420-1,912	414-2,144	1,100-108,400	1,300-11,920	609
<i>Aetobatus narutobiei</i> <sub>8</sub>	298-1,038	297-1,536	409.3-17,350	411.6-60,000	1189
<b>Rhinopterae</b>					
<i>Rhinoptera bonasus</i> <sub>9</sub>	300-980	300-1,105	327-14,530	325-22,780	694
<i>Rhinoptera brasiliensis</i> <sub>10</sub>	468-1,019				*
<i>Rhinoptera steindachneri</i> <sub>11</sub>	418-825	401-942			276
<b>Mobulidae</b>					
<i>Mobula alfredi</i> <sub>12</sub>	2,330-3,850	2,330-3,800			7
<i>Mobula hypostoma</i> <sub>13</sub>	552-773				9 *
<i>Mobula kuhl</i> <sub>14</sub>	1,009-1,197				*

\* = studies that combined sexes, \*\* = studies with only a maximum value; and ? = number not provided in source document.

1. (Capapé, 1977), 2. (Martin & Cailliet, 1988), 3. (Tagliafico et al., 2016), 4. (Araújo et al., 2016), 5. (Başusta & Aslan, 2018), 6. (Yamaguchi et al., 2005), 7. (Boggio-Pasqua et al., 2022), 8. (Yamaguchi et al., 2021), 9. (Fisher et al., 2013), 10. (Jones et al., 2017), 11. (Pabón-Aldana et al., 2022), 12. (Marshall et al., 2009), 13. (Moral-Flores et al., 2020), 14. (White & Dharmadi, 2007). This study is bolded

species where males attain a larger size than females (Tagliafico et al., 2016). *Myliobatis tenuicaudatus* is smaller than most allied species, with the exception of *R. steindachneri* (Pabón-Aldana et al., 2022).

### 4.3 Age and growth

Marginal incremental analyses demonstrated that the growth rings on the vertebrae of *M. tenuicaudatus* are annual, with a delineation in February. If, in the current study, more samples were collected, the marginal increment analysis would be less variable and show a clearer trend, however these were consistent with studies on other elasmobranch (Lessa et al., 2006).

As with other batoid species, there was a notably large difference between maximum ages of male and female *M. tenuicaudatus*, with the oldest documented males (10 years) being six years younger than that of females (16 years). Females of various batoid species typically live to an older age (Yamaguchi et al., 2005; White & Dharmadi, 2007; Başusta & Aslan, 2018). Between myliobatid species, *M. tenuicaudatus* reaches the maximum age for males (9.9 years), while *M. californica* reaches the greatest age for females (23 years; Table 4.3.1) (Martin, 1982). In comparison to allied species, *A. narinari* attains the oldest age for both males and females (21 and 25 years, respectively), while male *A. bovinus* has the lowest documented maximum age (5 years) (Başusta & Aslan, 2018).

Growth of *M. tenuicaudatus* also varied significantly between females and males. For example, asymptotic disk width ( $DW_{\infty}$ ) was estimated to be just under two times greater for females (1,836 mm) than males (1,033 mm). As both  $DW_{\infty}$  values exceeded the maximum DW recorded in the study, more samples and/or larger mesh sizes may be required to improve parameter estimates (Pardo et al., 2016). Conversely, females grew at a slower rate ( $k=0.05$ ) than males ( $k=0.12$ ). The theoretical age at which the disk width is 0 mm, commonly referred to as  $t_0$  for varied between males and females ( $t_0=-2.4$  and  $-3.43$  years, respectively). This differs from spawning teleost species, which typically have small negative values rather than large negative values exhibited by the viviparous myliobatid and allied species (Musick et al., 2005).

A major parameter of the von Bertalanffy growth curve is the  $DW_{\infty}$ , the asymptotic disk width in which the growth rate approaches zero. It can be noted that as  $DW_{\infty}$  increases, the growth ( $k$ ) decreases in most myliobatids, with the exception of the mobulids (Fig 4.3.1). Rhinopterids are documented to reach the lowest  $DW_{\infty}$  and highest

growth value, followed by the aetobatids (Fig 4.3.1). Meanwhile, the myliobatid species are scattered intermediately. *Myliobatis tenuicaudatus* resides in the midrange of all values with the lowest  $DW_{\infty}$  for both males and females in comparison to other myliobatid species. Both *Mobula mobular* and *Mobula japanica* do not follow the trend, however likely as the parameters were not calculated for separate sexes (Cuevas-Zimbrón et al., 2013; Pardo et al., 2016). It is noteworthy that the latter study was unable to attain larger specimens, and which would have influenced the growth parameters they estimated. Relative to their body size, mobulids, such as *M. mobular*, possess a larger gill area affording them the ability to utilise higher oxygen levels (Başusta & Özbek, 2017), which may explain their higher growth rates. Other than the mobulids, *Aetobatus narinari* and *Aetomylaeus bovinus* grow to the largest  $DW_{\infty}$  size (Dubick, 2000; Başusta & Aslan, 2018).

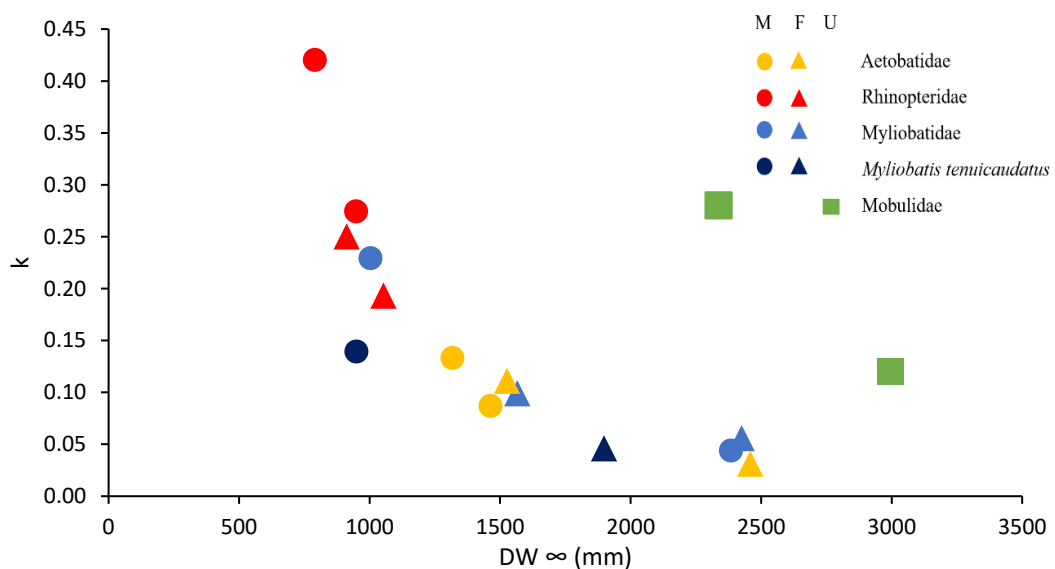


**Figure 4.3.1.**  $DW_{\infty}$  in comparison to growth rate of various myliobatids and allies from various sources. Males (●), females (▲), unknown sex (■). *M. californica* (Martin, 1982); *Myliobatis tenuicaudatus* (This study); *Aetomylaeus bovinus* (Başusta & Aslan, 2018); *Aetobatus flagellum* (Yamaguchi et al., 2005); *Aetobatus narinari* (Dubick, 2000); *Rhinoptera bonasus* (Fisher et al., 2013); *Rhinoptera seindachneri* (Pabón-Aldana et al., 2022); *Mobula mobular* (Cuevas-Zimbrón et al., 2013); *Mobula japanica* (Pardo et al., 2016).

Despite there being >40 species in the myliobatid and allies, the maximum ages of only seven species are currently documented in the scientific literature (Table 4.3.1). Among these, female *M. californica* in Central California were found to reach up to 23 years in age, while males only aged up to 5 years (Martin & Cailliet, 1988). Female *Aetobatus flagellum* were also noted to grow to an older age compared to males i.e. 19 vs 9 years (Yamaguchi et al., 2021). Similarly, *Aetomylaeus bovinus*, displayed a greater maximum age of 14 years for females and 5 years for males (Başusta & Aslan, 2018). This indicates that for many species, females tend to attain an older age than males. It was

**Table 4.3.1.** Maximum age and Von Bertalanffy growth parameters ( $DW_{\infty}$ ,  $k$  and  $t_0$ ) for various myliobatids and allied species.

	Male age	Female age	Male Von Bertalanffy parameter			Female Von Bertalanffy parameter		
			$DW_{\infty}$ (mm)	$k$	$t_0$	$DW_{\infty}$ (mm)	$k$	$t_0$
<b>Myliobatidae</b>								
<i>Myliobatis californica</i> <sub>1</sub>	6	23	1004.0	0.229	-1.58	1566.0	0.099	-1.94
<b><i>Myliobatis tenuicaudatus</i></b>	<b>9.9</b>	<b>15.9</b>	<b>1033.4</b>	<b>0.120</b>	<b>-2.40</b>	<b>1836.5</b>	<b>0.050</b>	<b>-3.43</b>
<i>Aetomylaeus bovinus</i> <sub>2</sub>	5	14	2384.0	0.044	-2.98	2425.9	0.056	-1.90
<b>Aetobatidae</b>								
<i>Aetobatus flagellum</i> <sub>3</sub>	9	19	1318.0	0.133	-2.09	1527.0	0.111	-2.10
<i>Aetobatus narinari</i> <sub>4</sub>	21	25	1465.0	0.087	-4.09	2459.0	0.031	-7.04
<b>Rhinopterae</b>								
<i>Rhinoptera bonasus</i> <sub>5</sub>	18	21	949.8	0.2741	-2.14	1053.4	0.193	-2.64
<i>Rhinoptera steindachneri</i> <sub>6</sub>	7.67	10.75	791.0	0.420		912.1	0.25	
<b>Mobulidae</b>								
<i>Mobula mobular</i> <sub>7</sub>		14				2338.0*	0.28*	-1.68*
<i>Mobula japonica</i> <sub>8</sub>		15-20*				2995*	0.12*	

1. (Martin, 1982), 2. (Başusta & Aslan, 2018), 3. (Yamaguchi et al., 2005), 4. (Dubick, 2000), 5. (Fisher et al., 2013), 6. (Pabón-Aldana et al., 2022), 7. (Cuevas-Zimbrón et al., 2013), 8. (Pardo et al., 2016). This study is bolded.

\* denotes studies where sexes have been combined.

also determined that female *M. californica* obtained a larger size at a slower growth coefficient ( $k$ ) ( $DW_{\infty} = 1,587$  mm,  $k = 0.0995$ ) than males ( $DW_{\infty} = 1,004$  mm,  $k = 0.229$ ). This may be due to females reaching a larger age at maturity and being required to give birth while males provide sperm in the reproductive exchange (Frisk, 2010; Fricke et al., 2020). Following a similar growth trend, *A. bovinus* displayed a greater growth coefficient for females (0.056) than males (0.044) (Başusta & Aslan, 2018).

The greater growth coefficient and larger maximum  $DW_{\infty}$  of *M. mobular* may be due to the circumglobal distribution of the ray in the warmer equatorial waters. However, it is unknown if there are any external factor that assist the growth rate and  $DW_{\infty}$ . The two rhinopterids were found along the coast of the equatorial region of both North and South America, while the aetobatids were situated in the Indo-Pacific region in warmer waters (15.9- 22.3 °C compared to 25-28 °C, respectively). The two myliobatids were found along the coast of Africa (*A. bovinus*) and the southern coast of North America (*M. californica*). The metabolic theory of ecology notes that fish species found in warmer water typically have a faster metabolism, in turn allowing species to maintain a faster a growth rate (Brown et al., 2004).

#### **4.4 Reproduction**

*Myliobatis tenuicaudatus* is recorded as a matrotrophic viviparous species that holds young within the uterus before giving live birth (Araújo et al., 2016; Yamaguchi et al., 2021). Because of this, understanding the reproduction of this species is vital for fisheries management.

The gonadosomatic index (GSI) is used in many elasmobranch and teleost species to determine the timing of the breeding season and maturity (Hismayasari et al., 2015). Female *M. tenuicaudatus* had a higher GSI than males (range of 0.8-3.4 and 0.4-1.1 %, respectively). Although it is difficult to draw conclusions from the limited number of sexually mature individuals, GSI was greatest in December indicating the development of foetuses before releasing pups in January and February, as noted by the sharp GSI decline in February. In the following months, the GSI remained consistently between 1.0 and 1.4 %. Other myliobatid species (eg. *M. goodei*, *M. ridens*) have a peak of GSI in spring, when water temperatures rise, while the *Aetobatus narutobiei* showed a similar trend to *M. tenuicaudatus* (Table 4.4.1). This indicates that it is common for species to

develop embryos during warmer months potentially due to higher food availability and more favourable environmental conditions.

The heptasomatic index (HSI) is used predominantly in chondrichthyans species to determine energy reserves within the liver, which is typically shown as an inverse trend to the GSI (Hismayasari et al., 2015). Similar to GSI, females have a greater HSI value than males. The female peak in winter indicates that the energy reserve increases during winter, potentially due to a lack of food availability (Hismayasari et al., 2015). The fluctuation of female HSI between February and June may be accounted for by the limited sample sizes. Most species have the HSI peak in the inverse season (i.e., winter), with the exception of *M. ridens* which peak in summer (Araújo et al., 2016). Rossouw (1987) noted that an increase in HSI indicated an increase in lipids and that these levels were low when embryos were near on full development. This would explain the lower HSI values in February for females as it has been determined that this is the end of the parturition season for females, similar to the stingray *Dasyatis chrysonota* (Ebert & Cowley, 2009).

The disk width at which 50% of the population is mature ( $DW_{50}$ ) is lower in males than in females (595 mm, and 833 mm, respectively). These values were broadly consistent with the previous study conducted on this species along the southern coast of Western Australia, which documented the  $DW_{50}$  to be 689 mm for males and 879 mm for females (Jones et al., 2010). However, the slight variance may be caused by the lower sample size of the study (148 vs. 110 in the current study) as well as the location of the study. While both being conducted in Western Australia, focused on the coastal area beginning at the Swan-Canning Estuary around to the south coast, while this study only focused on the estuarine system at the northern end of the other studies' sample range. Following the metabolic theory of ecology, the colder waters in the southern region allow larger sizes at slower growth rates, causing a larger size at maturity.

In other studies where myliobatid and allied species reproductive characteristics have been derived, females are either the same size or larger at  $DW_{50}$  (Table 4.4.1). This study noted the largest size difference at maturity between males and females, while the lowest difference occurred with *M. freminvillei* where the  $DW_{50}$  maturity of both males and females was 533mm (Tagliafico et al., 2016). This species is also the smallest  $DW_{50}$  for both males and females among myliobatids, whereas *M. tenuicaudatus* had the highest documented  $DW_{50}$  for males (Jones et al., 2010). When considering allied families, female *M. birostris* reached the largest  $DW_{50}$  of >3,00 mm, while *M. birostris* had the largest value for males of 3,752 mm (White et al., 2006; Marshall & Bennett, 2010).

**Table 4.4.1.** Reproductive characteristics for various species of myliobatids and allies, including disk width at maturity ( $DW_{50}$ ), age at maturity, litter size, gonadosomatic index (GSI), gestation period and functionality of the uterus.

	Male $DW_{50}$ (mm)	Female $DW_{50}$ (mm)	Male age at maturity	Female age at maturity	Litter size	GSI peak	HSI peak	Gestation Period (months)	Functionality of uteri	Sex ratio (M:F)	Location
<b>Myliobatidae</b>											
<i>Myliobatis californica</i> <sub>1</sub>	662	881	2	5	2-5			9-12	Both	1.25:1	
<i>Myliobatis freminvillei</i> <sub>2</sub>	533	533			6						Margarita Island (Venezuela)
<i>Myliobatis goodei</i> <sub>3</sub>	NA	683			4-5	Spring	Autumn		Left	1:2.95	Southern Brazil
<i>Myliobatis ridens</i> <sub>3</sub>	NA	662			1-8	Spring	Summer	4-6	Left	1:6.29	Southern Brazil
<i>Myliobatis tenuicaudatus</i> <sub>4</sub>	689	879								1:1.28	Western Australia
<b><i>Myliobatis tenuicaudatus</i></b>	<b>595</b>	<b>833</b>	<b>5.1</b>	<b>8.9</b>	<b>1-3</b>	<b>Summer</b>	<b>Winter</b>		<b>Both</b>	<b>1:1.33</b>	<b>Swan-Canning Estuary (WA)</b>
<b>Aetobatidae</b>											
<i>Aetobatus narinari</i> <sub>5</sub>	1150- 1325	1250- 1350	14.2	15.4	1-5				Left	1:0.75	Gulf of Mexico
<i>Aetobatus narinari</i> <sub>6</sub>	1156	1234							Left		Paraiba (Brazil)
<i>Aetobatus narutobiei</i> <sub>7</sub>	764	952	3.5	6	1-7	Summer	Winter	12	Both		Japan
<b>Rhinopterae</b>											
<i>Rhinoptera bonasus</i> <sub>8</sub>	850-860	850-860	6-7	7-8	1			11-12	Left		Chesapeake Bay (USA)
<i>Rhinoptera bonasus</i> <sub>9</sub>	642	653	4-5	4-5	1			11-12			Gulf of Mexico
<i>Rhinoptera bonasus</i> <sub>10</sub>	681	701			1			11-12			Charlotte Harbor, Florida
<i>Rhinoptera bonasus</i> <sub>11</sub>	764	891			1			12			Gulf of Mexico
<i>Rhinoptera steindachneri</i> <sub>12</sub>		744	3.72	3.92				7-9	Left	1:1	Gulf of California (USA)
<b>Mobulidae</b>											
<i>Mobula alfredi</i> <sub>13</sub>		>3m			1-2			12		1:2.96	S. Mozambique
<i>Mobula japonica</i> <sub>14</sub>	2016										Indonesia
<i>Mobula tarapacana</i> <sub>14</sub>	2486										Indonesia
<i>Mobula birostris</i> <sub>14</sub>	3752										Indonesia
<i>Mobula thurstoni</i> <sub>14</sub>	1538										Indonesia

(Martin, 1982), 2. (Tagliafico et al., 2016), 3. (Araújo et al., 2016), 4. (Jones et al., 2010), 5. (Dubick, 2000), 6. (Araújo et al., 2022) 7. (Yamaguchi et al., 2021), 8. (Fisher et al., 2013), 9. (Neer & Thompson, 2005), 10. (Poulakis, 2013) 11. (Pérez-Jiménez, 2011), 12.(Pabón-Aldana et al., 2022), 12. (Marshall & Bennett, 2010), 13. (White et al., 2006). This study is bolded.

Both uteri were found to be fully functional in *M. tenuicaudatus*. This trait is similar to other myliobatid species, including *M. aquila* and *M. californica* (Martin, 1982; Capapé et al., 2007). However, unlike other Myliobatiformes, this trait is accompanied by a functional left ovary and a partially functional right ovary. One or two pups were commonly observed during the current study, however, there was a single case where three pups were aborted. It is thought that they all came from one mother as there was only one female present in the sample. The average litter size for *M. tenuicaudatus* is the smallest among myliobatids (range = 1- 3), but not among the allied species. The species with the highest litter size is *M. ridens* (8 pups), and the lowest in *Rhinoptera bonasus* at 1 pup (Table 4.4.1).

Martin (1982) noted that the number of embryos was limited by space within the body cavity, and as such, the number of uterine eggs ovulated is limited. It is suggested that by exceeding the limit, females would waste reproductive energy and constrain the nourishment of embryos, thereby diminishing the size of eggs. This is indicative that the nutrient supply provided by the mother can support only three *M. tenuicaudatus* embryos.

Through other existing biological programs in both the Peel-Harvey Estuary and Cockburn Sound, it has been noted that the smallest sized *M. tenuicaudatus* were found within the Swan-Canning Estuary (Murdoch, unpublished data). This, as well as the fact that newborn pups were found in most months, indicates that the Swan-Canning Estuary could act as a nursery area. However, it must also be noted that research sampling has been more intensive within the Swan-Canning Estuary.

The gestation period of the *M. tenuicaudatus* was unable to be fully determined in this study due to the limited number of pregnant females caught. However, between November 2022 and October 2023, pregnant individuals were found in all months except March, recognising this was limited to the capture of a single specimen. Yamaguchi et al. (2021) noted a unique reproductive trait of *A. narutobiei*, which has a diapause period, in which females hold the ovulated eggs for nine months. This is during the colder months when they migrate out of the Ariake Bay (Japan), before moving back into the bay where the embryos rapidly develop within the three warmer months. It was also suggested that mating, ovulation and fertilisation occurs directly after or at a similar time as parturition (Yamaguchi et al., 2021). *Myliobatis californica* shows similar traits as *M. tenuicaudatus* as they both have two fully functional uteri, as well as a small litter size of up to five pups (Table 4.4.1). It was also noted that this species, as well as two other species with limited pup numbers, i.e., *R. bonasus* and *M. alfredi* have a gestation period of 9-12 months.

#### 4.5 Diets

Of the 157 stomachs analysed, 24 were provided by the commercial fisher, which were all empty. This may be due to the longer set times by the fisher and thus although individual may have died, digestion continues due to the low stomach pH (Clark et al., 2022). It is thus relevant that the stomachs of elasmobranchs contains highly acidic gastric juices and as such digestion could still occur after death unless preserved (Babkin et al., 1935). As the specimens collected in this study by DPIRD were immediately frozen or processed, the acids had limited impacts on the digestion rate after death.

The dietary composition determined in this study were compared to those for *M. tenuicaudatus* in other locations and it was noted that diets from individuals caught in the Swan-Canning Estuary contained the greatest volume of penaeid prawns. It has been documented that penaeid use coastal and estuarine habitats as nursery areas for postlarvae and juveniles (De Freitas, 1986; Tweedley et al., 2017). There are two prominent species of prawns found within the Swan-Canning Estuary namely the Western School Prawn (*Melapenaeus dalli*) and the Western King Prawn (*Melicertus latisulcatus*). It is likely that most penaeids documented in the dietary composition were *M. dalli* which are found in shallows in spring and summer while being offshore in autumn and winter (Poh et al., 2019). It was also noted that the Western School Prawn, *Melapenaeus dalli*, preferred finer sediment noted in Dalkeith than the courser sediment located in Garrett Road Bridge (Tweedley et al., 2017). Basin estuarine area typically have finer grain sizes than ocean sediment and as such, penaeid prawns are more likely to reside in the estuarine areas (Valesini et al., 2009).

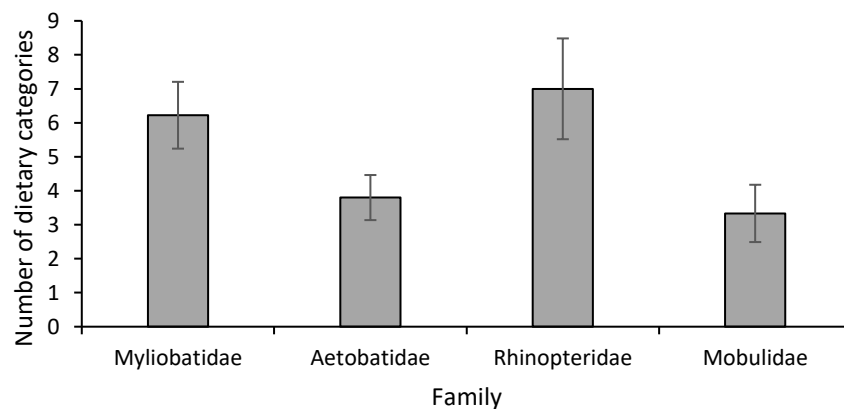
There was an abrupt dietary shift between disk widths of 200 and 400 mm due to the increase in volume of various prey items, while still maintaining high polychaete and penaeid presence. At ~600 mm DW, all dietary categories, with the exception of teleosts appeared to exhibit similar volumes. There was a decrease in volume of most categories between 800 and 1,000 mm DW, apart from brachyuran crabs. There was a notable difference of jaw sizes between size classes, indicating that larger specimen can feed on larger and harder prey groups. Sommerville et al. (2011) found a similar trend with larger rays predated on harder prey items, and suggested the reason for shift was that larger rays could target, handle and process larger prey items, which was not influenced by ontogeny.

The diet of *M. tenuicaudatus* changed progressively over spring to winter. Polychaetes were the dominant prey in spring, but their volume decreased in summer and

there was an corresponding increase in penaeid prawns. It has been noted that *M. dalli* spawn and reside within the Swan-Canning Estuary during the warmer summer and autumn months, and as such, provide an increased population for the *M. tenuicaudatus* to feed (Tweedley et al., 2017). It was also noted that the spawning season for the mytilid mussel, an abundant bivalve within the Swan-Canning Estuary, occurs in summer (Maus et al., 2024). This could explain the increase in bivalve presence and abundance within the autumn months.

Despite having a lower number of prey categories, the myliobatid species has a large breadth in composition ( $\sim 1.3$ ), with minimal variance, and as such, demonstrates that they feed on a variety of different food sources (Fig 4.5.1). Rhinopterids have a larger diversity than aetobatids have a limited breadth in composition ( $\sim 1.0$  in comparison to  $\sim 0.7$ , respectively). Species belonging to the mobulid family have the lowest dietary breadth ( $\sim 0.1$ ) feeding predominantly on one category has highlighted previously.

(a)



(b)

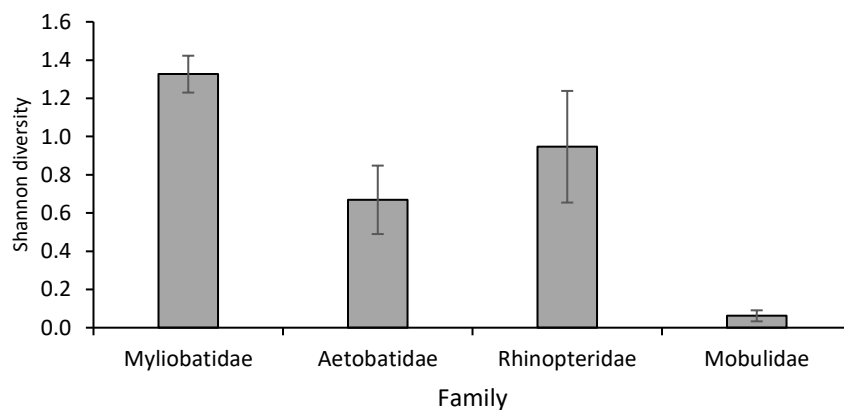


**Figure 4.5.1.** Means values ( $\pm 1$  SE) of (a) the number of prey items and (b) Shannon diversity as a proxy for dietary breadth the four families belonging to the Myliobatiformes order. Data taken from papers listed in Fig 4.5.4.

Meta-analyses were conducted only using published studies that measure diets using a volumetric or weighted method (i.e., V% or W%). Despite previously once being considered as one family, ANOSIM detected a significant difference between the dietary composition of myliobatids, aetobatid, rhinopterid and mobulid species (Global R = 0.63 P = 0.1%) and at a pairwise level the diet of each family was different from all others (R = 0.32 – 9.5 ; P = 0.1 - 2.4%). This is shown on the nMDS plot where the points representing each family are largely discrete (Figure 4.5.2).

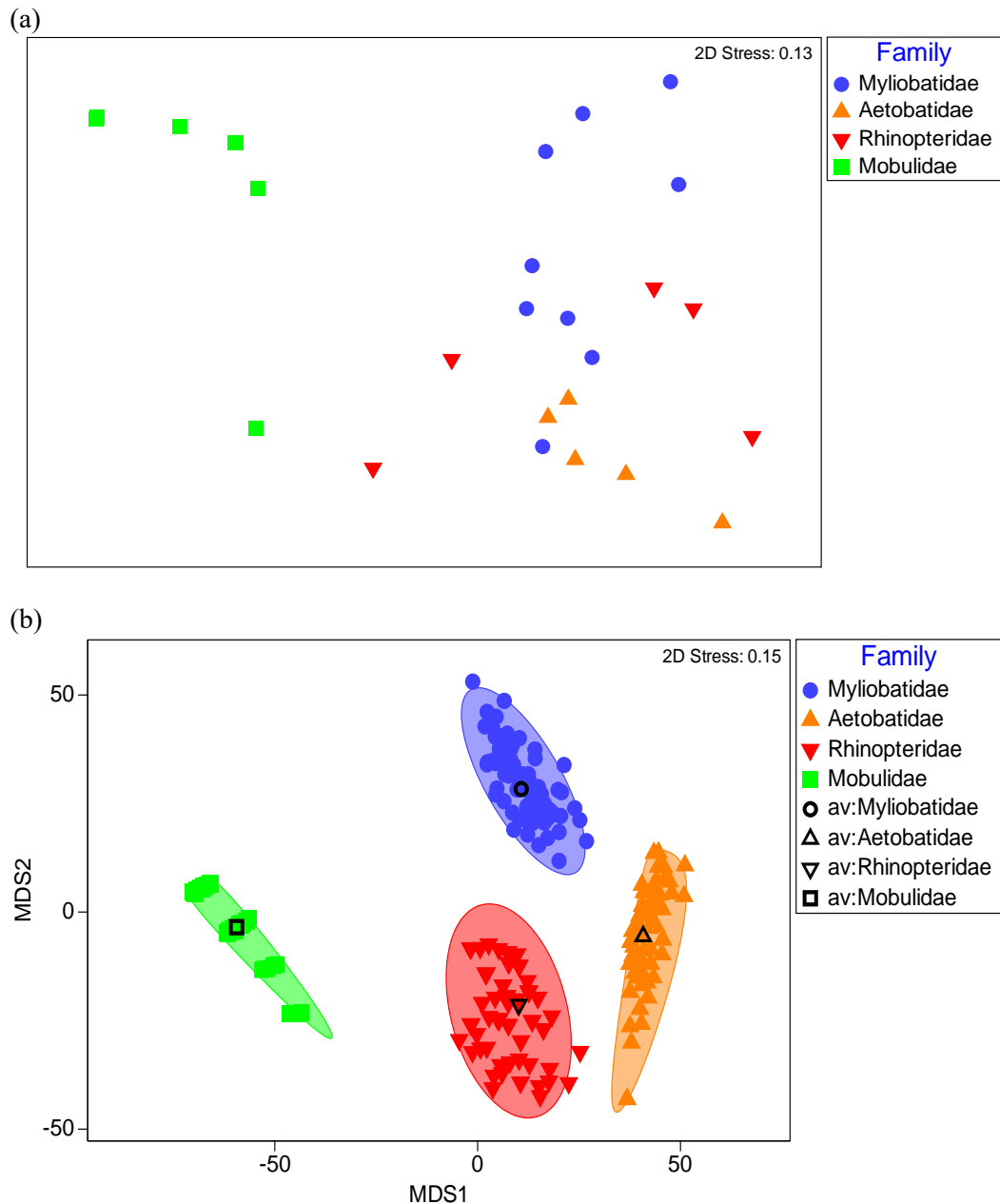


**Figure 4.5.2.** (a) non-metric and (b) metric MDS plots of dietary composition of various Myliobatid and allied species; i.e. Myliobatidae (●), Aetobatidae (▲), Rhinopteridae (▼) and Mobulidae (■). Data taken from papers listed in Fig. 4.5.4.

Aetobatids feed prominently on benthic hard-shelled items with no prey categories identified as soft or pelagic within the diets (Fig 4.5.4). In contrast, mobulids fed only on prey items that were rated as medium hardness. These prey items were found to be located primarily within the pelagic range with some prey being found in the demersal area. Myliobatids and rhinopterids were noted to feed on all hardness levels at similar increments. These prey items were spread between benthic and demersal habitats. It was noted that there were more benthic items found in rhinopterids species in comparison to myliobatids (25, compared to 50, respectively).

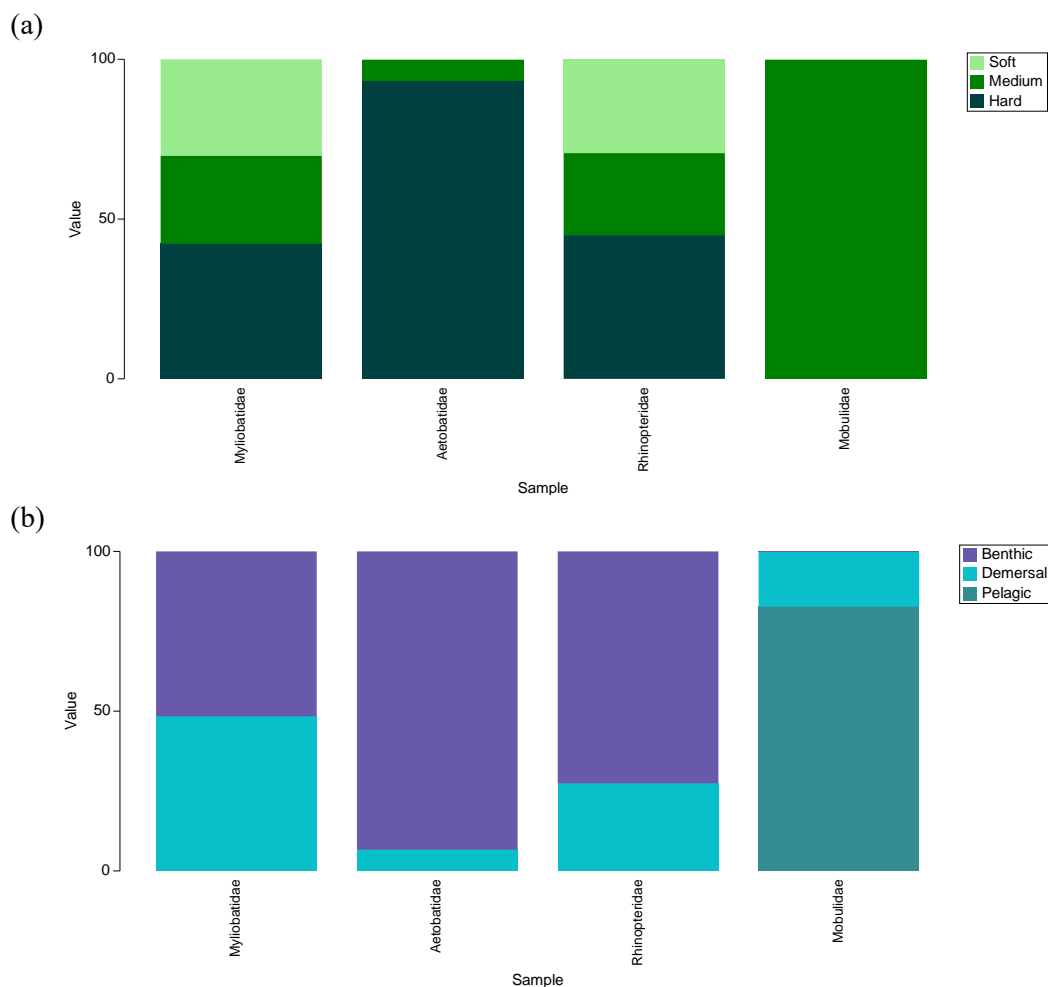


**Figure 4.5.3.** Prey items categorised by (a) hardness level and (b) habitat for the four Myliobatiformes families. Data taken from papers listed in Fig 4.5.4.

Myliobatid species fed predominantly on large benthic crustaceans, teleost, and shelled molluscs identified as gastropods (Fig 4.5.4). Shelled molluscs categorised by gastropods and bivalves were the most prominent prey categories of aetobatids, whereas rhinopterids were documented to feed on bivalves, echinoderms and annelids. The diets of mobulids have the greatest dissimilarity to other families as they feed on pelagic crustaceans (Table 4.5.1).

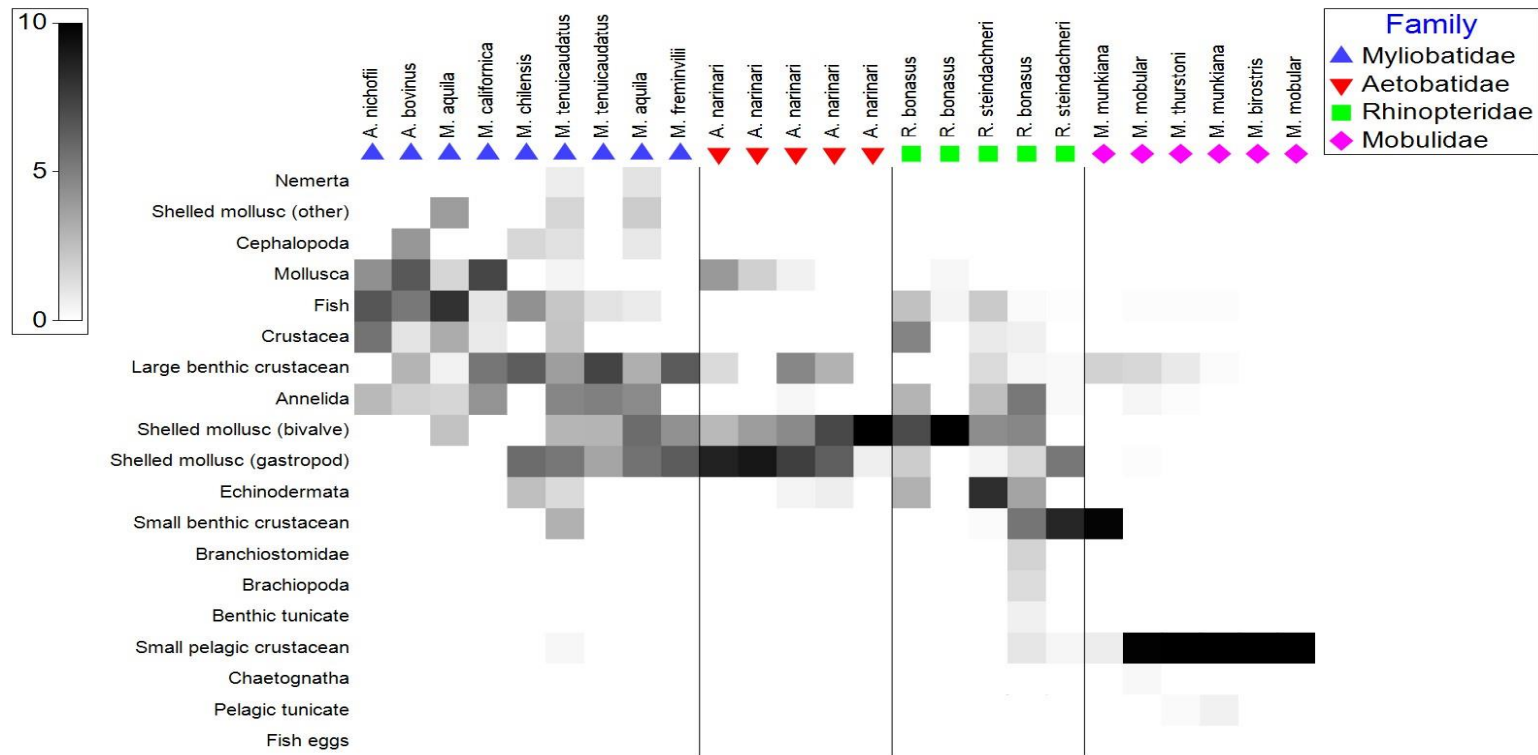


**Figure 4.5.4.** Shade plot indicating different prey items consumed by species in each family i.e. Myliobatidae (▲), Aetobatidae (▼), Rhinopteridae (■) and Mobulidae (◆). *Myliobatis aquila* (Jardas et al., 2004; Gül & Demirel, 2020), *M. californica* (Talent, 1982; Gray et al., 1997; Fernández-Aguirre et al., 2022; Reyes-Ramírez et al., 2022), *M. chilensis* (Gonzalez-Pestana et al., 2021), *M. freminvillii* (Szczepanski & Bengtson, 2014), *M. tenuicaudatus* (Sommerville et al., 2011). *Aetoylaeus bovinus* (Capapé, 1977), *A. narinari* (Schluessel et al., 2010; Ajemian et al., 2012). *Rhinoptera bonasus* (Collins, 2005; Ajemian et al., 2012), *R. steindachneri* (Ehemann et al., 2019; Simental-Anguiano et al., 2022)., *M. birostris* (Medeiros et al., 2022), *Mobula mobular* (Notarbartolo-di-Sciara, 1988; Coasaca-Céspedes et al., 2018), *Mobula munkiana* (Notarbartolo-di-Sciara, 1988; Coasaca-Céspedes et al., 2018).

**Table 4.5.1.** Dietary categories that typified (grey) and distinguished (white) of species in each of the families within the Myliobatiformes based on SIMPER. The family in which each dietary category was most frequent is provided in superscript for each pairwise comparison. Bray-Curtis similarity (Sim) and dissimilarity (Dsim) values are also provided. LBC denotes large benthic crustacean, SPC represents small pelagic crustaceans.

	<b>Myliobatidae</b>	<b>Aetobatidae</b>	<b>Rhinopteridae</b>	<b>Mobulidae</b>
<b>Myliobatidae</b>	Sim: 41.76 LBC Fish Annelida			
<b>Aetobatidae</b>	Dsim: 66.84 Gastropod <sup>Aetobatidae</sup> Bivalve <sup>Aetobatidae</sup> Fish <sup>Myliobatidae</sup> LBC <sup>Myliobatidae</sup> Annelida <sup>Myliobatidae</sup>	Sim: 58.47 Gastropod Bivalve		
<b>Rhinopteridae</b>	Dsim: 72.27 Bivalve <sup>Rhinopteridae</sup> LBC <sup>Myliobatidae</sup>	Dsim: 65.39 Gastropod <sup>Aetobatidae</sup> Bivalve <sup>Aetobatidae</sup> Echinodermata <sup>Rhinopteridae</sup> Annelida <sup>Rhinopteridae</sup>	Sim: 33.04 Bivalve	
<b>Mobulidae</b>	Dsim: 95.34 SPC <sup>Mobulidae</sup> LBC <sup>Myliobatidae</sup> Fish <sup>Myliobatidae</sup> Annelida <sup>Myliobatidae</sup>	Dsim: 96.94 SPC <sup>Mobulidae</sup> Gastropod <sup>Aetobatidae</sup> Bivalve <sup>Aetobatidae</sup>	Dsim: 93.41 SPC <sup>Mobulidae</sup> Bivalve <sup>Rhinopteridae</sup> Echinodermata <sup>Rhinopteridae</sup>	Sim: 65.62 SPC

Species of myliobatid and rhinopterid are durophagous benthic feeders, with a hard, fused grinding plates of flat teeth that interlock in rigid jaws that are used to crush hard-shelled organisms (Summers, 2000; Kolmann et al., 2015). They are deemed to be generalists in which they feed on a variety of organisms. These include shelled molluscs, teleosts, echinoderms and crustaceans.

Despite the pelagic nature of the aetobatids, they feed on predominantly benthic material and similar to myliobatids and rhinopterids, are durophagous. It has been documented that such species predate on predominantly molluscs with a smaller portion of the dietary composition to be crustaceans (~76% and ~18-22% of their diets, respectively) (Schluessel et al., 2010; Jacobsen & Bennett, 2013). As can be inferred and

seen throughout the literature, they have a limited range of prey and will often feed on only one type or species of prey (Chan et al., 2022).

On the other hand, mobulids fed on small crustacean, with the majority being pelagic. There is limited other prey items. This is due to the pelagic nature of the devil and manta rays. The predominant prey items of the mobulids, have documented over 90% of their diet to be Euphausiids (krill) or other zooplankton (Jacobsen & Bennett, 2013; Coasaca-Céspedes et al., 2018). Mobulids use cephalic lobes to guide prey into the mouth. While they have a tooth plate, it is not used in feeding. *Mobula munkiana* is the one species that shows different prey items, with the point representing this sampling being widely separated from those of the other mobulids (Fig. 3.5.6) as it specialises on feeding on small benthic crustacean (i.e., mysids) rather than pelagic ones (e.g. copepods; Fig. 3.5.7). Despite seeming like an outlier, this species feed in depths of 75cm of water off the coast, where waves consistently break. Due to this turbulent water movement, the mysids are resuspended in the water column for the *M. munkiana* to feed on (Porsiel et al., 2021).

#### **4.6 Limitations**

Sampling for this study occurred over two or three nights each month dependent on weather. Consequently, each site was sampled once a month, causing conservative interpretation which may not be representative of the population. However, this sampling regime was implemented due to funding and staffing limitations, and as such, fulfilling these issues proved improbable. Abundance of the *M. tenuicaudatus* may also be impacted by the tides, as seen in other batoid species (Brinton & Curran, 2017). However, due to the variability of sampling each month, tidal influence was not recorded or measured and as such may have impacted the catch rates.

During this project, very few mature females were sampled, causing discrepancies and limited information to be gathered on the reproductive system. Due to this the gestation period as well as embryonic development of this species remains undefined. As there were unidentified materials found while studying the dietary composition, some prey items such as soft-bodied prey were not considered, altering the percentage volume for some items, as well as impacting the overall analysis.

#### ***4.7 Implications and further research***

Stock assessments to assist in the sustainable management of various fish species with robust abundance estimates and values for a range of biological characteristics e.g. age, growth, size at maturity and fecundity required for accurate analytical interpretation. In addition to dietary analyses the findings of this project will be used to inform future management of this species. Due to the annual presence of neonates (juveniles and pregnant females year round, it suggests that the Swan-Canning Estuary may be an important nursery area for *M. tenuicaudatus*.

As noted, Myliobatiformes and other batoids are prone to high abortion rates. *M. tenuicaudatus* are no exception to this behavioural trait, with 14 females noted to have aborted eggs. Due to the frequency of abortions by pregnant females following capture during this study, methods to reduce stress should be considered, such as a short set time of nets to promote retention of fetuses. To ensure the sustainability of this species consideration should be given to changing gear type and protecting nursery areas and aggregation sites (Adams et al., 2018).

Furthermore, the publication of these characteristics improves the knowledge of this species in the scientific literature, enabling further comparisons between species to be documented. The methodology conducted during this project can be used in future studies as well as further continuous monitoring of this species. Further monitoring is essential to ensure a sustainable population remains within the Swan-Canning Estuary.

Further research on the influence of diel and tidal movements on this species as well as acoustic tracking to assess movements of *M. tenuicaudatus* in and out of the estuary would prove to be valuable. Additional investigations on the reproductive systems, including embryonic development of this species are crucial to further understand the unique reproduction of this species. This information is important to determine the movement patterns of *M. tenuicaudatus* and determine if they leave the estuary and migrate to other coastal areas such as Cockburn Sounds. If these rays are found to remain within the Swan-Canning Estuary annually with no migration patterns, the guild classification of “marine stragglers” could be altered (Tweedley et al., 2022)

## 5. Conclusion

This study described the patterns in the spatial and temporal abundance of the Southern Eagle Ray, *Myliobatis tenuicaudatus* in the Swan-Canning Estuary, produced estimate for a range of biological characteristics and determined its dietary composition. In a broader context, this study also compared the data obtained for *M. tenuicaudatus* with literature values for other closely related species. There was no significant relationship between catch rates and all environmental parameters, however, it was significantly affected by the month and site sampled. There was a significantly strong relationship between all morphological components, with females growing to a larger size than males. The size range of this species is intermediate between other similar species. Aging techniques noted that females grow to an older age than males (15.8 and 9.92 years, respectively) and while females had a larger  $DW_{\infty}$ , males had a greater  $k$  ( $DW_{\infty}$ = 1,033.38, 1,836.47 mm, males and females, respectively;  $k$ = 0.012, 0.05). It was discerned that both uteri of the *M. tenuicaudatus* were functional, with a litter size of one to three. There was a peak of GSI in summer, indicating that childbirth and copulation occur during this time, with an increase of lipids within the liver (HSI) occurring in the winter period. Maturity was reached at a larger size and older age for females than for males ( $DW_{50}$ = 851 and 620 mm, respectively; age: 9.4, 7.2 years). It was determined that there were a variety of prey items, indicating that this species is a generalist feeder, similar to that of other Myliobatid species. The main prey categories that were documented include prawns, polychaetes, gastropods and crabs (F%: 48%, 32%, 24%, 23%, respectively). Further research on the movement patterns as well as reproductive cycle of *M. tenuicaudatus* need to be undertaken to fully understand this species for accurate application in stock assessments. Furthermore, the construction of sound and informed management practices needs to be implemented to ensure a sustainable population of Southern Eagle Rays in the Swan-Canning Estuary.

## 6. References

- Adams, K. R., Fetterplace, L. C., Davis, A. R., Taylor, M. D., & Knott, N. A. (2018). Sharks, rays and abortion: the prevalence of capture-induced parturition in elasmobranchs. *Biological Conservation*, 217, 11-27.
- Adnet, S., Cappetta, H., Guinot, G., & NOTARBARTOLO DI SCIARA, G. (2012). Evolutionary history of the devilrays (Chondrichthyes: Myliobatiformes) from fossil and morphological inference. *Zoological Journal of the Linnean Society*, 166(1), 132-159.
- Ajemian, M. J., Powers, S. P., & Murdoch, T. J. (2012). Estimating the potential impacts of large mesopredators on benthic resources: integrative assessment of spotted eagle ray foraging ecology in Bermuda. *PloS one*, 7(7), e40227.
- Anderson, M. (2008). PERMANOVA+ for PRIMER: guide to software and statistical methods. *Primer-E Limited*.
- Araújo, P., Oddone, M., & Velasco, G. (2016). Reproductive biology of the stingrays, *Myliobatis goodei* and *Myliobatis ridens* (Chondrichthyes: Myliobatidae), in southern Brazil. *Journal of Fish Biology*, 89(1), 1043-1067.
- Araújo, P. R. V., Oddone, M. C., Evêncio-Neto, J., & Lessa, R. (2022). Reproductive biology of the whitespotted eagle ray *Aetobatus narinari* (Myliobatiformes) captured in the coast of Paraíba and Pernambuco, Brazil. *Journal of Fish Biology*, 100(4), 944-957.
- Aschliman, N. C. (2014). Interrelationships of the durophagous stingrays (Batoidea: Myliobatidae). *Environmental Biology of Fishes*, 97, 967-979.
- Babkin, B., Chaisson, A., & Friedman, M. (1935). Factors determining the course of the gastric secretion in elasmobranchs. *Journal of the Biological Board of Canada*, 1(4), 251-259.
- Ballantyne, J., & Fraser, D. (2012). Euryhaline elasmobranchs. In *Fish physiology* (Vol. 32, pp. 125-198). Elsevier.
- Başusta, N., & Aslan, E. (2018). Age and growth of bull ray *Aetomylaeus bovinus* (Chondrichthyes: Myliobatidae) from the northeastern Mediterranean coast of Turkey. *Cah. Biol. Mar*, 59, 107-114.
- Başusta, N., & Özbek, E. Ö. (2017). New record of giant devil ray, *Mobula mobular* (Bonnaterre, 1788) from the Gulf of Antalya (Eastern Mediterranean Sea). *Journal of the Black Sea/Mediterranean Environment*, 22, 162-169.
- Beck, M. W., Heck, K. L., Able, K. W., Childers, D. L., Eggleston, D. B., Gillanders, B. M., Halpern, B., Hays, C. G., Hoshino, K., & Minello, T. J. (2001). The identification, conservation, and management of estuarine and marine nurseries for fish and invertebrates: a better understanding of the habitats that serve as nurseries for marine species and the factors that create site-specific variability in nursery quality will improve conservation and management of these areas. *Bioscience*, 51(8), 633-641.
- Bishop, J., Moore, A., Alsaffar, A., & Abdul Ghaffar, A. (2016). The distribution, diversity and abundance of elasmobranch fishes in a modified subtropical estuarine system in Kuwait. *Journal of applied ichthyology*, 32(1), 75-82.
- Boggio-Pasqua, A., Bassos-Hull, K., Aeberhard, W. H., Hoopes, L. A., Swider, D. A., Wilkinson, K. A., & Dureuil, M. (2022). Whitespotted eagle ray (*Aetobatus narinari*) age and growth in wild (in situ) versus aquarium-housed (ex situ) individuals: Implications for conservation and management. *Frontiers in Marine Science*, 9, 960822.
- Brearley, A. (2005). *Ernest Hodgkin's Swanland: estuaries and coastal lagoons of South-western Australia*. UWA Publishing.
- Brinton, C. P., & Curran, M. C. (2017). Tidal and diel movement patterns of the Atlantic stingray (*Dasyatis sabina*) along a stream-order gradient. *Marine and Freshwater Research*, 68(9), 1716-1725.
- Brown, J. H., Gillooly, J. F., Allen, A. P., Savage, V. M., & West, G. B. (2004). Toward a metabolic theory of ecology. *Ecology*, 85(7), 1771-1789.
- Cailliet, G. M., Smith, W. D., Mollet, H. F., & Goldman, K. J. (2006). Age and growth studies of chondrichthyan fishes: the need for consistency in terminology, verification, validation, and growth function fitting. *Environmental Biology of Fishes*, 77, 211-228.
- Campbell, T. I., Tweedley, J. R., Johnston, D. J., & Loneragan, N. R. (2021). Crab diets differ between adjacent estuaries and habitats within a sheltered marine embayment. *Frontiers in Marine Science*, 8, 564695.

- Capapé, C. (1977). Etude du régime alimentaire de la Mourine vachette, *Pteromylaeus bovinus* (Geoffroy Saint-Hilaire, 1817)(Pisces, Myliobatidae) des côtes tunisiennes. *ICES Journal of Marine Science*, 37(3), 214-220.
- Capapé, C., Guélorget, O., Vergne, Y., & Quignard, J. (2007). Reproductive biology of the common eagle ray, *Myliobatis aquila* (Chondrichthyes: Myliobatidae) from the coast of Languedoc (Southern France, northern Mediterranean). *Vie et Milieu/Life & Environment*, 125-130.
- Carrier, J. C., Musick, J. A., & Heithaus, M. R. (2012). *Biology of sharks and their relatives*. CRC press.
- Cerrato, R. M. (1990). Interpretable statistical tests for growth comparisons using parameters in the von Bertalanffy equation. *Canadian Journal of Fisheries and Aquatic Sciences*, 47(7), 1416-1426.
- Chan, A. J., Raoult, V., Jaine, F. R., Peddemors, V. M., Broadhurst, M. K., & Williamson, J. E. (2022). Trophic niche of Australian cownose rays (*Rhinoptera neglecta*) and whitespotted eagle rays (*Aetobatus ocellatus*) along the east coast of Australia. *Journal of Fish Biology*, 100(4), 970-978.
- Chubb, C. F. (1979). *Fish Fauna of the Swan Estuary* Murdoch University].
- Clark, B., Chaumel, J., Johanson, Z., Underwood, C., Smith, M. M., & Dean, M. N. (2022). Bricks, trusses and superstructures: Strategies for skeletal reinforcement in batoid fishes (rays and skates). *Frontiers in Cell and Developmental Biology*, 10, 932341.
- Clarke, K., & Gorley, R. (2015). Getting started with PRIMER v7. *PRIMER-E: Plymouth, Plymouth Marine Laboratory*, 20(1).
- Clarke, K. R., Tweedley, J. R., & Valesini, F. J. (2014). Simple shade plots aid better long-term choices of data pre-treatment in multivariate assemblage studies. *Journal of the Marine Biological Association of the United Kingdom*, 94(1), 1-16.
- Coasaca-Céspedes, J. J., Segura-Cobeña, E., Montero-Taboada, R., Gonzalez-Pestana, A., Alfaro-Córdova, E., Alfaro-Shigueto, J., & Mangel, J. C. (2018). Preliminary analysis of the feeding habits of batoids from the genera *Mobula* and *Myliobatis* in Northern Peru. *Revista de Biología Marina y Oceanografía*, 53(3), 367-374.
- Collins, A. B. (2005). An examination of the diet and movement patterns of the Atlantic cownose ray *Rhinoptera bonasus* within a southwest Florida estuary.
- Cuevas-Zimbrón, E., Sosa-Nishizaki, O., Pérez-Jiménez, J. C., & O'Sullivan, J. B. (2013). An analysis of the feasibility of using caudal vertebrae for ageing the spinetail devilray, *Mobula japonica* (Müller and Henle, 1841). *Environmental Biology of Fishes*, 96, 907-914.
- Davey, J., Clarke, T. M., Niella, Y., Dennis, J. D., & Huveneers, C. (2023). Seasonal variation in space use and residency of the southern eagle ray *Myliobatis tenuicaudatus* in a temperate ecosystem. *Marine Ecology Progress Series*, 705, 77-94.
- Davy, L. E., Simpfendorfer, C. A., & Heupel, M. R. (2015). Movement patterns and habitat use of juvenile mangrove whiprays (*Himantura granulata*). *Marine and Freshwater Research*, 66(6), 481-492.
- De Freitas, A. (1986). Selection of nursery areas by six southeast African Penaeidae. *Estuarine, Coastal and Shelf Science*, 23(6), 901-908.
- Dubick, J. D. (2000). *Age and growth of the spotted eagle ray, Aetobatus narinari (Euphrasen, 1790), from southwest Puerto Rico with notes on its biology and life history*. University of Puerto Rico, Mayaguez (Puerto Rico).
- Dulvy, N. K., Fowler, S. L., Musick, J. A., Cavanagh, R. D., Kyne, P. M., Harrison, L. R., Carlson, J. K., Davidson, L. N., Fordham, S. V., & Francis, M. P. (2014). Extinction risk and conservation of the world's sharks and rays. *elife*, 3, e00590.
- Dulvy, N. K., Pacoureau, N., Rigby, C. L., Pollom, R. A., Jabado, R. W., Ebert, D. A., Finucci, B., Pollock, C. M., Cheok, J., & Derrick, D. H. (2021). Overfishing drives over one-third of all sharks and rays toward a global extinction crisis. *Current Biology*, 31(21), 4773-4787. e4778.
- Ebert, D. A., & Cowley, P. D. (2009). Reproduction and embryonic development of the blue stingray, *Dasyatis chrysonota*, in southern African waters. *Journal of the Marine Biological Association of the United Kingdom*, 89(4), 809-815.

- Ehemann, N., Abitia-Cardenas, L., Navia, A., Mejía-Falla, P., & Cruz-Escalona, V. (2019). Zeros as a result in diet studies, is this really bad? *Rhinoptera steindachneri* as a case study. *Journal of the Marine Biological Association of the United Kingdom*, 99(7), 1661-1666.
- Eschmeyer, W., Fricke, R., & Laan, R. (2021). Eschmeyer's catalog of fishes: genera, species, references. Accessed: March 04, 2023, 26, 2021.
- Essington, T. E., Kitchell, J. F., & Walters, C. J. (2001). The von Bertalanffy growth function, bioenergetics, and the consumption rates of fish. *Canadian Journal of Fisheries and Aquatic Sciences*, 58(11), 2129-2138.
- Fernández-Aguirre, E., Galván-Magaña, F., Sánchez-González, A., González-Armas, R., Abitia-Cárdenas, L. A., Elorriaga-Verplancken, F. R., Villalejo-Fuerte, M. T., Tripp-Valdéz, A., Barajas-Calderón, A. V., & Delgado-Huertas, A. (2022). Changes in the feeding habits of the bat ray *Myliobatis californica* (Gill 1865) during climatic anomalies off the west coast of the Baja California Peninsula, Mexico. *Regional Studies in Marine Science*, 53, 102462.
- Fisher, R. A., Call, G. C., & Grubbs, R. D. (2013). Age, growth, and reproductive biology of cownose rays in Chesapeake Bay. *Marine and Coastal Fisheries*, 5(1), 224-235.
- Flowers, K. I., Heithaus, M. R., & Papastamatiou, Y. P. (2021). Buried in the sand: Uncovering the ecological roles and importance of rays. *Fish and Fisheries*, 22(1), 105-127.
- Fricke, R., Eschmeyer, W., & Van der Laan, R. (2020). Eschmeyers Catalog of Fishes: genera, species, references. . In.
- Frisk, M. G. (2010). *Life history strategies of batoids. Sharks and their Relatives. II. Biodiversity, adaptive physiology, and conservation*. CRC Press, Boca Raton, Florida.
- Froese, R., & Pauly, D. (2023). *Myliobatidae Bonaparte, 1835*. In FishBase (Ed.). World Register of Marine Species.
- García-Salinas, P., Gallego, V., & Asturiano, J. F. (2021). Reproductive Anatomy of Chondrichthyans: Notes on Specimen Handling and Sperm Extraction. I. Rays and Skates. *Animals*, 11(7), 1888.
- Goldman, K. J. (2005). Age and growth of elasmobranch fishes. *FAO Fisheries Technical Paper*, 474, 76.
- Gonzalez-Pestana, A., Mangel, J. C., Alfaro-Córdova, E., Acuña-Perales, N., Córdova-Zavaleta, F., Segura-Cobeña, E., Benites, D., Espinoza, M., Coasaca-Céspedes, J., & Jiménez, A. (2021). Diet, trophic interactions and possible ecological role of commercial sharks and batoids in northern Peruvian waters. *Journal of Fish Biology*, 98(3), 768-783.
- Gray, A. E., Mulligan, T. J., & Hannah, R. W. (1997). Food habits, occurrence, and population structure of the bat ray, *Myliobatis californica*, in Humboldt Bay, California. *Environmental Biology of Fishes*, 49, 227-238.
- Greenwell, C. N., Loneragan, N. R., Tweedley, J. R., & Wall, M. (2019). Diet and trophic role of octopus on an abalone sea ranch. *Fisheries management and ecology*, 26(6), 638-649.
- Grey, D. L., Dall, W., & Baker, A. (1983). A guide to the Australian penaeid prawns. *A guide to the Australian penaeid prawns*.
- Gül, G., & Demirel, N. (2020). Trophic interactions of uncommon batoid species in the sea of Marmara. *J. Black Sea/Mediterranean Environment*, 26, 294-309.
- Hallett, C. S., Hobday, A. J., Tweedley, J. R., Thompson, P. A., McMahon, K., & Valesini, F. J. (2018). Observed and predicted impacts of climate change on the estuaries of south-western Australia, a Mediterranean climate region. *Regional Environmental Change*, 18, 1357-1373.
- Hallett, C. S., Trayler, K. M., & Valesini, F. J. (2019). The Fish Community Index: A practical management tool for monitoring and reporting estuarine ecological condition. *Integrated Environmental Assessment and Management*, 15(5), 726-738.
- Hismayasari, I. B., Marhendra, A. P. W., Rahayu, S., Saidin, S. D., & Supriyadi, D. (2015). Gonadosomatic index (GSI), hepatosomatic index (HSI) and proportion of oocytes stadia as an indicator of rainbowfish *Melanotaenia boesemani* spawning season. *International Journal of Fisheries and Aquatic Studies*, 2(5), 359-362.
- Hodgkin, E. P., & Hesp, P. (1998). Estuaries to salt lakes: Holocene transformation of the estuarine ecosystems of south-western Australia. *Marine and Freshwater Research*, 49(3), 183-201.

- Hogan-West, K., Tweedley, J. R., Coulson, P. G., Poh, B., & Loneragan, N. R. (2019). Abundance and distribution of the non-indigenous *Acentrogobius pflaumii* and native gobiids in a temperate Australian estuary. *Estuaries and Coasts*, 42, 1612-1631.
- Holmes, B. J., Williams, S. M., Barnett, A., Awruch, C. A., Currey-Randall, L. M., Ferreira, L. C., Huveneers, C., Jones, R. L., Nowland, S. J., & Taylor, A. (2022). 13 Research methods for marine and estuarine fishes. *Wildlife Research in Australia: Practical and Applied Methods*, 257.
- Hume, J. B. (2019). Higher temperatures increase developmental rate & reduce body size at hatching in the small-eyed skate *Raja microocellata*: implications for exploitation of an elasmobranch in warming seas. *Journal of Fish Biology*, 95(2), 655-658.
- Jabado, R. W., Ebert, D. A., & Al Dhaheri, S. S. (2022). Resolution of the *Aetomylaeus nichofii* species complex, with the description of a new eagle ray species from the northwest Indian Ocean and a key to the genus *Aetomylaeus* (Myliobatiformes: Myliobatidae). *Marine Biodiversity*, 52(2), 15.
- Jacobsen, I. P., & Bennett, M. B. (2013). A comparative analysis of feeding and trophic level ecology in stingrays (Rajiformes; Myliobatoidei) and electric rays (Rajiformes: Torpedinoidei). *PloS one*, 8(8), e71348.
- Jardas, I., Santic, M., & Pallaoro, A. (2004). Diet composition of the eagle ray, *Myliobatis aquila* (Chondrichthyes: Myliobatidae), in the Eastern Adriatic Sea. *Cybiurn (Paris)*, 28(4), 372-374.
- Jones, A. A., Hall, N. G., & Potter, I. C. (2010). Species compositions of elasmobranchs caught by three different commercial fishing methods off southwestern Australia, and biological data for four abundant bycatch species.
- Jones, C. M., Hoffmayer, E. R., Hendon, J. M., Quattro, J. M., Lewandowski, J., Roberts, M. A., Poulakis, G. R., Ajemian, M. J., Driggers, W. B., & De Carvalho, M. R. (2017). Morphological conservation of rays in the genus *Rhinoptera* (Elasmobranchii, Rhinopteridae) conceals the occurrence of a large batoid, *Rhinoptera brasiliensis* Müller, in the northern Gulf of Mexico. *Zootaxa*, 4286(4), 499-514.
- Jones, D. S., & Morgan, G. J. (1994). *Field guide to crustaceans of Australian waters*. Reed.
- Karpouzi, V. S., & Stergiou, K. (2003). The relationships between mouth size and shape and body length for 18 species of marine fishes and their trophic implications. *Journal of Fish Biology*, 62(6), 1353-1365.
- Khan, S., & Khan, M. A. (2020). Importance of age and growth studies in fisheries management. Reviewed Proceedings of National Seminar on NGSV. Next Generation Sciences: Vision,
- Knoblauch, K. (2023). psyphy: Functions for Analyzing Psychophysical Data in R. In.
- Kolmann, M. A., Crofts, S. B., Dean, M. N., Summers, A. P., & Lovejoy, N. R. (2015). Morphology does not predict performance: jaw curvature and prey crushing in durophagous stingrays. *Journal of Experimental Biology*, 218(24), 3941-3949.
- Kyne, P. M. (2016). *Myliobatis tenuicaudatus*. In. The IUCN Red List of Threatened Species 2016.
- Lang, D. T. (2023). RCurl: General Network (HTTP/FTP/...) Client Interface for R. In.
- Last, P., Naylor, G., Séret, B., White, W., de Carvalho, M., & Stehmann, M. (2016). *Rays of the World*. CSIRO publishing.
- Last, P. R., & Stevens, J. D. (2009). *Sharks and rays of Australia*.
- Lek, E., Fairclough, D., Platell, M., Clarke, K., Tweedley, J., & Potter, I. (2011). To what extent are the dietary compositions of three abundant, co-occurring labrid species different and related to latitude, habitat, body size and season? *Journal of Fish Biology*, 78(7), 1913-1943.
- Lessa, R., Santana, F. M., & Duarte-Neto, P. (2006). A critical appraisal of marginal increment analysis for assessing temporal periodicity in band formation among tropical sharks. *Environmental Biology of Fishes*, 77, 309-315.
- Marcotte, M. M. (2013). Homing in the New Zealand eagle ray *Myliobatis tenuicaudatus*. *Marine and Freshwater Research*, 65(4), 306-311.
- Marshall, A., & Bennett, M. (2010). Reproductive ecology of the reef manta ray *Manta alfredi* in southern Mozambique. *Journal of Fish Biology*, 77(1), 169-190.

- Marshall, A. D., Compagno, L. J., & Bennett, M. B. (2009). Redescription of the genus *Manta* with resurrection of *Manta alfredi* (Krefft, 1868)(Chondrichthyes; Myliobatoidei; Mobulidae). *Zootaxa*, 2301(1), 1-28.
- Martin, L. K. (1982). *Growth and reproduction of the bat ray, Myliobatis californica Gill, in California* San Jose State University San Jose].
- Martin, L. K., & Cailliet, G. M. (1988). Age and growth determination of the bat ray, *Myliobatis californica* Gill, in central California. *Copeia*, 762-773.
- Martins, A., Heupel, M., Chin, A., & Simpfendorfer, C. (2018). Batoid nurseries: definition, use and importance. *Marine Ecology Progress Series*, 595, 253-267.
- Maschette, D., Fromont, J., Platell, M., Coulson, P., Tweedley, J., & Potter, I. (2020). Characteristics and implications of spongivory in the Knifefaw *Oplegnathus woodwardi* (Waite) in temperate mesophotic waters. *Journal of Sea Research*, 157, 101847.
- Maus, C., Cottingham, A., Bossie, A., & Tweedley, J. R. (2024). Assessing the Efficacy of a Bouchot-Style Shellfish Reef as a Restoration Option in a Temperate Estuary. *Journal of marine science and engineering*, 12(1), 87.
- Medeiros, A. M., Bersano, J. G. F., Ari, C., & de Araujo Monteiro-Filho, E. L. (2022). Endangered mobulids within sustainable use protected areas of southeastern Brazil: occurrence, fisheries impact, and a new prey item. *Environmental Biology of Fishes*, 105(6), 775-786.
- Meloni, C. J., Cech Jr, J. J., & Katzman, S. M. (2002). Effect of brackish salinities on oxygen consumption of bat rays (*Myliobatis californica*). *Copeia*, 2002(2), 462-465.
- Microsoft Corporation. (2018). *Microsoft Excel*. In
- Molina, J. M., & Cazorla, A. L. (2015). Biology of *Myliobatis goodei* (Springer, 1939), a widely distributed eagle ray, caught in northern Patagonia. *Journal of Sea Research*, 95, 106-114.
- Moral-Flores, L. F. D., Meza-Abundio, I., & Pérez-España, H. (2020). First confirmed record of the occurrence of the lesser devil ray, *Mobula hypostoma* (Elasmobranchii, Mobulidae), in the southwestern Gulf of Mexico. *Latin american journal of aquatic research*, 48(4), 696-699.
- Musick, J. A., Ellis, J. K., & Hamlett, W. (2005). Reproductive evolution of chondrichthyans. *Reproductive biology and phylogeny of chondrichthyes: sharks, batoids and chimaeras*, 3, 45-80.
- Neer, J. A., & Thompson, B. A. (2005). Life history of the cownose ray, *Rhinoptera bonasus*, in the northern Gulf of Mexico, with comments on geographic variability in life history traits. *Environmental Biology of Fishes*, 73, 321-331.
- Notarbartolo-di-Sciara, G. (1988). Natural history of the rays of the genus *Mobula* in the Gulf of California. *Fishery Bulletin*, 86(1), 45-66.
- Ogle, D. H., Doll, J. C., Wheeler, A. P., & Dinno, A. (2023). FSA: Simple Fisheries Stock Assessment Methods. In
- Pabón-Aldana, K. A., Melo-Barrera, F. N., Pérez-Palafox, X. A., Navia, A. F., Cruz-Escalona, V. H., & Mejía-Falla, P. A. (2022). Age and growth of Pacific cownose ray, *Rhinoptera steindachneri*: a species with intermediate growth and shorter lifespan than expected. *Marine and Freshwater Research*, 73(8), 1011-1024.
- Pardo, S. A., Kindsvater, H. K., Cuevas-Zimbrón, E., Sosa-Nishizaki, O., Pérez-Jiménez, J. C., & Dulvy, N. K. (2016). Growth, productivity and relative extinction risk of a data-sparse devil ray. *Scientific reports*, 6(1), 33745.
- Pérez-Jiménez, J. C. (2011). Reproductive biology of the cownose ray *Rhinoptera bonasus* (Elasmobranchii) in the Southeastern Gulf of Mexico. *Hidrobiológica*, 21(2), 159-167.
- Platell, M., Maschette, D., Coulson, P., Tweedley, J., & Potter, I. (2022). Dietary characteristics of the ecologically-important fish species *Centroberyx gerrardi*, including discussion of resource partitioning among species of Berycidae in Australia. *Estuarine, Coastal and Shelf Science*, 275, 107975.
- Platell, M. E., Hayward, M. W., & Tweedley, J. R. (2024). Demystification of multivariate approaches for dietary data. In *Unravelling the Food Web: Quantitative approaches to describing wildlife feeding relationships*. . CSIRO Publishing.



- Poh, B., Tweedley, J. R., Chaplin, J. A., Trayler, K. M., Crisp, J. A., & Loneragan, N. R. (2019). Influence of physico-chemical and biotic factors on the distribution of a penaeid in a temperate estuary. *Estuarine, Coastal and Shelf Science*, 218, 70-85.
- Porsiel, N., Hernández, S., Cordier, D., & Heidemeyer, M. (2021). The devil is coming: Feeding behavior of juvenile Munk's devil rays (*Mobula munkiana*) in very shallow waters of Punta Descartes, Costa Rica. *Revista de Biología Tropical*, 69, 256-266.
- Potter, I., & Hyndes, G. (1994). Composition of the fish fauna of a permanently open estuary on the southern coast of Australia, and comparisons with a nearby seasonally closed estuary. *Marine Biology*, 121, 199-209.
- Poulakis, G. R. (2013). Reproductive biology of the cownose ray in the Charlotte Harbor estuarine system, Florida. *Marine and Coastal Fisheries*, 5(1), 159-173.
- Pratt, H. L., & Carrier, J. C. (2001). A review of elasmobranch reproductive behavior with a case study on the nurse shark, *Ginglymostoma cirratum*. *Environmental Biology of Fishes*, 60, 157-188.
- R Core Team. (2023). R: A Language and Environment for Statistical Computing. In (4.1.3 ed.). Vienna, Austria: R Foundation for Statistical Computing.
- Reyes-Ramírez, H., Tripp-Valdez, A., Elorriaga-Verplancken, F. R., Piñón-Gimate, A., Zetina Rejón, M. J., & Galván-Magaña, F. (2022). Feeding guilds among batoids in the northwest coast of the Baja California Sur, Mexico. *Marine Ecology*, e12728.
- Rohner, C. A., Burgess, K. B., Rambahiniarison, J. M., Stewart, J. D., Ponzio, A., & Richardson, A. J. (2017). Mobulid rays feed on euphausiids in the Bohol Sea. *Royal Society Open Science*, 4(5), 161060.
- Rossouw, G. (1987). Function of the liver and hepatic lipids of the lesser sand shark, *Rhinobatos annulatus* (Müller & Henle). *Comparative Biochemistry and Physiology. B, Comparative Biochemistry*, 86(4), 785-790.
- Schieber, J. J., Fahy, D. P., Carlson, J. K., & Kerstetter, D. W. (2023). Age, growth and maturity of the yellow stingray (*Urobatis jamaicensis*), a biannually reproductive tropical batoid. *Journal of Fish Biology*.
- Schluessel, V., Bennett, M., & Collin, S. (2010). Diet and reproduction in the white-spotted eagle ray *Aetobatus narinari* from Queensland, Australia and the Penghu Islands, Taiwan. *Marine and Freshwater Research*, 61(11), 1278-1289.
- Schneider, C. A., Rasband, W. S., & Eliceiri, K. W. (2012). NIH Image to ImageJ: 25 years of image analysis. *Nature methods*, 9(7), 671-675.
- Serra-Pereira, B., Farias, I., Moura, T., Gordo, L. S., Santos, M., & Figueiredo, I. (2010). Morphometric ratios of six commercially landed species of skate from the Portuguese continental shelf, and their utility for identification. *ICES Journal of Marine Science*, 67(8), 1596-1603.
- Simental-Anguiano, M. D., Torres-Rojas, Y. E., Galván-Magaña, F., & Tripp-Quezada, A. (2022). Importance of Shellfish in the Diet of Two Ray Species (*Rhinoptera steindachneri* and *Hypanus dipterurus*) in the Upper Gulf of California. *Journal of Shellfish Research*, 41(2), 291-299.
- Sommerville, E., Platell, M., White, W., Jones, A., & Potter, I. (2011). Partitioning of food resources by four abundant, co-occurring elasmobranch species: relationships between diet and both body size and season. *Marine and Freshwater Research*, 62(1), 54-65.
- Springer, S. (1967). Social organization of shark population. *Sharks, skate and rays*, 149-174.
- Summers, A. P. (2000). Stiffening the stingray skeleton—an investigation of durophagy in myliobatid stingrays (Chondrichthyes, Batoidea, Myliobatidae). *Journal of morphology*, 243(2), 113-126.
- Svanbäck, R., Bolnick, D. I., Jorgensen, S., & Fath, B. (2008). Food specialization. *Encyclopedia of ecology*, 2, 1636-1642.
- Szczepanski, J. A., & Bengtson, D. A. (2014). Quantitative food habits of the bullnose ray, *Myliobatis freminvillii*, in Delaware Bay. *Environmental Biology of Fishes*, 97, 981-997.
- Tagliafico, A., Butcher, P. A., Colefax, A. P., Clark, G. F., & Kelaher, B. P. (2020). Variation in cownose ray *Rhinoptera neglecta* abundance and group size on the central east coast of Australia. *Journal of Fish Biology*, 96(2), 427-433.




- Tagliafico, A., Ehemann, N., Rangel, M. S., & Rago, N. (2016). Exploitation and reproduction of the bullnose ray (*Myliobatis freminvillei*) caught in an artisanal fishery in La Pared, Margarita Island, Venezuela.
- Talent, L. (1982). Food habits of the gray smoothhound, *Mustelus californicus*, the brown smoothhound, *Mustelus henlei*, the shovelnose guitarfish, *Rhinobatos productus*, and the bat ray, *Myliobatis californica*, in Elkhorn Slough, California. *Calif. Fish Game*, 68, 224-234.
- Torrejon-Magallanes, J. (2020). sizeMat: Estimate Size at Sexual Maturity. In.
- Trayler, K., Taljaard, E., Maus, C., Cottingham, A., Johnston, D., & Tweedley, J. (2024). Ray of white. *Landscape*, 39(3), 25-27.
- Tweedley, J., Krispyn, K., & Hallett, C. (2022). Swan Canning Estuary condition assessment based on fish communities-2022. *Murdoch University, Perth, Western Australia, Final report to the Department of Biodiversity, Conservation and Attractions*, 59.
- Tweedley, J., Loneragan, N., Crisp, J., Poh, B., Broadley, A., Bennett, A., Hodson, K., Trayler, K., Jenkins, G., & Chaplin, J. (2017). Restocking of the Western School Prawn (*Metapenaeus dalli*) in the Swan Canning Riverpark.
- Tweedley, J. R., Hallett, C. S., Warwick, R. M., Clarke, K. R., & Potter, I. C. (2015). The hypoxia that developed in a microtidal estuary following an extreme storm produced dramatic changes in the benthos. *Marine and Freshwater Research*, 67(3), 327-341.
- Tweedley, J. R., Warwick, R. M., & Potter, I. C. (2016). The contrasting ecology of temperate macrotidal and microtidal estuaries. In *Oceanography and Marine Biology* (pp. 81-180). CRC Press.
- Uchida, S. (1990). Reproduction of the elasmobranchs in captivity. *NOAA/Tech. REP. NMFS*, 90, 211-237.
- Valesini, F., Coen, N., Wildsmith, M., Hourston, M., Tweedley, J., Hallett, C., Linke, T., & Potter, I. (2009). Relationships between fish faunas and habitat type in south-western Australian estuaries. Fisheries Research and Development Corporation Final Report, July 2009.
- Valesini, F., Cottingham, A., Hallett, C., & Clarke, K. (2017). Interdecadal changes in the community, population and individual levels of the fish fauna of an extensively modified estuary. *Journal of Fish Biology*, 90(5), 1734-1767.
- Valetta, M. (2010). Report of the Workshop on Sexual Maturity Staging of Elasmobranchs (WKMSSEL).
- Venables, W. N., & Ripley, B. D. (2002). *Modern Applied Statistics with S* (Fourth ed.). Springer.
- Visser, I. (1999). Benthic foraging on stingrays by killer whales (*Orcinus orca*) in New Zealand waters. *Marine Mammal Science*, 15(1), 220-227.
- Walker, T. I. (2020). Chapter 10 Reproduction of Chondrichthyans. *Reproduction in Aquatic Animals: From Basic Biology to Aquaculture Technology*, 193-223.
- Weir, C. R., Macena, B. C., & di Sciara, G. N. (2012). Records of rays of the genus *Mobula* (Chondrichthyes: Myliobatiformes: Myliobatidae) from the waters between Gabon and Angola (eastern tropical Atlantic). *Marine Biodiversity Records*, 5, e26.
- White, W., & Dharmadi. (2007). Species and size compositions and reproductive biology of rays (Chondrichthyes, Batoidea) caught in target and non-target fisheries in eastern Indonesia. *Journal of Fish Biology*, 70(6), 1809-1837.
- White, W. T. (2014). A revised generic arrangement for the eagle ray family Myliobatidae, with definitions for the valid genera. *Zootaxa*, 3860(2), 149-166.
- White, W. T., Corrigan, S., Yang, L., Henderson, A. C., Bazinet, A. L., Swofford, D. L., & Naylor, G. J. (2018). Phylogeny of the manta and devilrays (Chondrichthyes: Mobulidae), with an updated taxonomic arrangement for the family. *Zoological Journal of the Linnean Society*, 182(1), 50-75.
- White, W. T., Giles, J., & Potter, I. C. (2006). Data on the bycatch fishery and reproductive biology of mobulid rays (Myliobatiformes) in Indonesia. *Fisheries Research*, 82(1-3), 65-73.
- White, W. T., & Naylor, G. (2016). Resurrection of the family Aetobatidae (Myliobatiformes) for the pelagic eagle rays, genus *Aetobatus*. *Zootaxa*, 4139(3), 435-438.
- Wickham, H. (2016). *ggplot2: Elegant Graphics for Data Analysis*. Springer-Verlag New York.
- Wickham, H., Averick, M., Bryan, J., Chang, W., McGowan, L. D. A., Romain François, G. G., Hayes, A., Henry, L., Hester, J., Kuhn, M., Pedersen, T. L., Miller, E., Bache, S. M.,

- Müller, K., Ooms, J., Robinson, D., Seidel, D. P., Spinu, V., Takahashi, K., . . . Yutani, H. (2019). Welcome to the tidyverse. *Journal of Open Source Software*, 4, 1686. <https://doi.org/10.21105/joss.01686>
- Wickham, H., François, R., Henry, L., Müller, K., & Vaughan, D. (2023). dplyr: A Grammar of Data Manipulation. In.
- Wosnick, N., Awruch, C. A., Adams, K., Gutierre, S., Bornatowski, H., Prado, A., & Freire, C. (2019). Impacts of fisheries on elasmobranch reproduction: high rates of abortion and subsequent maternal mortality in the shortnose guitarfish. *Animal Conservation*, 22(2), 198-206.
- Wosnick, N., Leite, R. D., Balanin, S., Chaves, A. P., de Senna Gastal, E. R., Hauser-Davis, R. A., & Giareta, E. P. (2023). Behavioral and visual stress-induced proxies in elasmobranchs. *Reviews in Fish Biology and Fisheries*, 33(1), 175-199.
- Yamaguchi, A., Furumitsu, K., & Wyffels, J. (2021). Reproductive Biology and Embryonic Diapause as a Survival Strategy for the East Asian Endemic Eagle Ray *Aetobatus narutobiei*. *Frontiers in Marine Science*, 1830.
- Yamaguchi, A., Kawahara, I., & Ito, S. (2005). Occurrence, growth and food of longheaded eagle ray, *Aetobatus flagellum*, in Ariake Sound, Kyushu, Japan. *Environmental Biology of Fishes*, 74, 229-238.

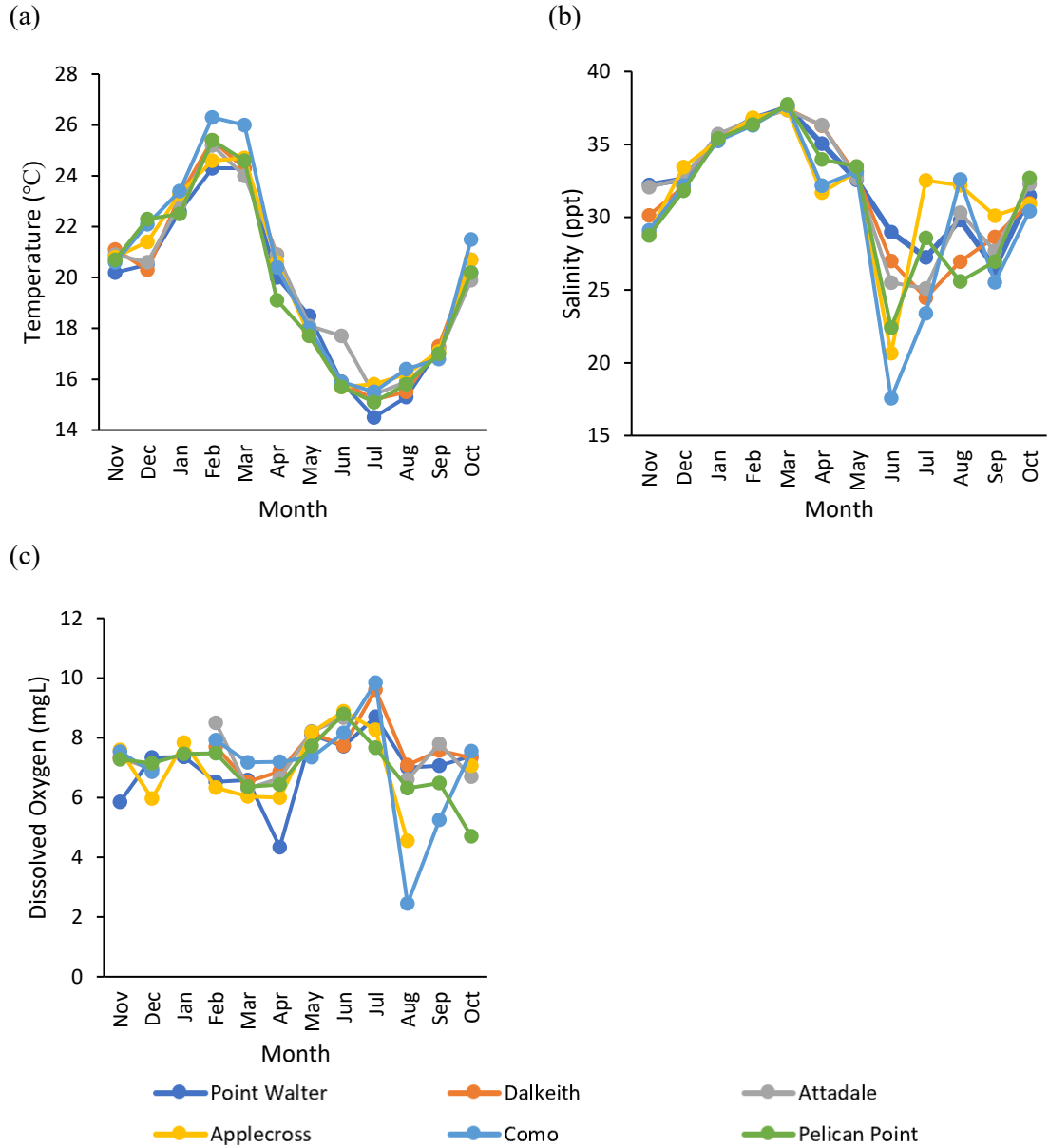
## 7. Appendices

**Appendix 1.** Species and maximum size of each species in each family as well as common names and taxonomic authority. Common names and images taken from (Last et al., 2016; Jabado et al., 2022). \* indicates species that originally was part of *Manta* genus before becoming part of the *Mobuila* genus.

Family	Genus	Species	Common name	Authority
Myliobatidae- Eagle Ray	<i>Myliobatis</i> 	<i>M. aquila</i>	Common Eagle Ray	Linnaeus, 1758
		<i>M. californica</i>	Bat Eagle Ray	Gill, 1865
		<i>M. chilensis</i>	Chilean Eagle Ray	Philippi, 1892
		<i>M. freminvillei</i>	Bullnose Eagle Ray	Lesueur, 1824
		<i>M. goodei</i>	Southern Eagle Ray	Garman, 1885
		<i>M. hamlyni</i>	Purple Eagle Ray	Ogilby, 1911 Applegate & Fitch, 1964
		<i>M. longirostris</i>	Snouted Eagle Ray	
		<i>M. peruvianus</i>	Peruvian Eagle Ray	Garman, 1913
		<i>M. ridens</i>	Shortnose Eagle Ray	Ruocco, et al., 2012
		<i>M. tenuicaudatus</i>	Southern Eagle Ray	Hector, 1877
	<i>Aetomylaeus</i> 	<i>M. tobije</i>	Japanese Eagle Ray	Bleeker, 1854
		<i>A. asperrimus</i>	Rough Eagle Ray	Gilbert, 1898
		<i>A. bovinus</i>	Bull Ray	Geoffroy Saint-Hilaire, 1817 White, Last & Baje, 2015
		<i>A. caeruleofasciatus</i>	Blue-banded Eagle Ray	
		<i>A. maculatus</i>	Mottled Eagle Ray	Gray, 1834
		<i>A. milvus</i>	Ocellate Eagle Ray	Muller & Henle, 1841 Bloch & Schneider, 1801
		<i>A. nichofii</i>	Banded Eagle Ray	
		<i>A. vespertilio</i>	Ornate Eagle Ray	Bleeker, 1852
		<i>A. wafickii</i>	Wafc's Eagle Ray	Jabado, et al., 2022

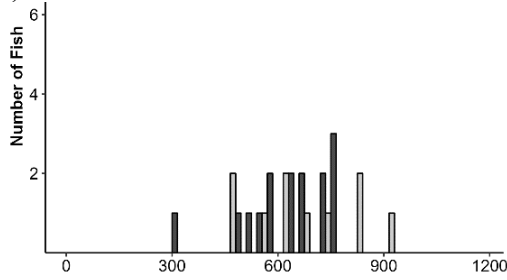
Family	Genus	Species	Common name	Authority
Aetobatidae- pelagic Eagle Rays	<i>Aetobatus</i>  <u><i>A. narinari</i></u>	<i>A. flagellum</i>	Longhead eagleray	Bloch & Schneider, 1801
		<i>A. laticeps</i>	Pacific Eagle Ray	Gill, 1865
		<i>A. narinari</i>	Whitespot Eagle Ray	Euphrasen, 1790
		<i>A. narutobiei</i>	Naru Eagle Ray	White, et al., 2013
		<i>A. ocellatus</i>	Spotted Eagle Ray	Kuhl, 1823
Rhinopteridae- Cownose Rays	<i>Rhinoptera</i>  <u><i>R. neglecta</i></u>	<i>R. bonasus</i>	Cownose Ray	Mitchill, 1815
		<i>R. brasiliensis</i>	Brazilian Cownose Ray	Muller, 1836
		<i>R. javanica</i>	Flapnose ray	Muller & Henle, 1841
		<i>R. jayakari</i>	Oman Cownose Ray	Boulenger, 1895
		<i>R. marginata</i>	Lusitanian Cownose Ray	Geoffroy Saint-Hillaire, 1817
		<i>R. neglecta</i>	Australian Cownose Ray	Ogilby, 1912
		<i>R. steindachneri</i>	Pacific Cownose Ray	Evermann & Jenkins, 1891
Mobulidae- manta and devil rays	<i>Mobula</i>  <u><i>M. kuhlii</i></u>	<i>M. alfredi</i> *	Alfred Manta	Kreffft, 1868
		<i>M. birostris</i> *	Giant Manta	Walbaum, 1792
		<i>M. hypostoma</i>	Lesser Devil Ray	Bancroft, 1831
		<i>M. kuhlii</i>	Shortfin Devil Ray	Muller & Henle, 1841
		<i>M. mobular</i>	Devil Fish	Bonnaterre, 1788
		<i>M. munkiana</i>	Munk's Devil Ray	Notarbarto-di-Sciara, 1987
		<i>M. tarapacana</i>	Chilean Devil Ray	Philippi, 1892
		<i>M. thurstoni</i>	Smoothtail Mobula	Lloyd, 1908

**Appendix 2.** (a) Water temperature, (b) salinity, and (c) dissolved oxygen concentrations at the bottom of the water column at each sample site in the Swan-Canning Estuary in each month between November 2022 and October 2023.

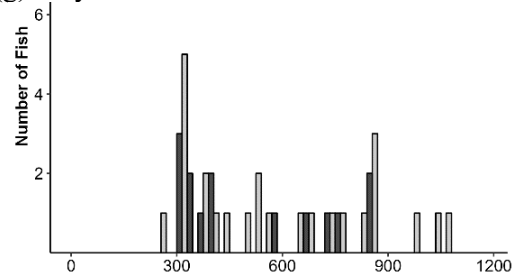


**Appendix 3.** Count of male (■) and female (□) *Myliobatis tenuicaudatus* of various disk widths in the Swan-Canning Estuary each month sampled.

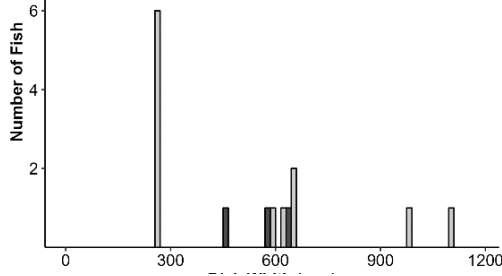
(a) November 2022



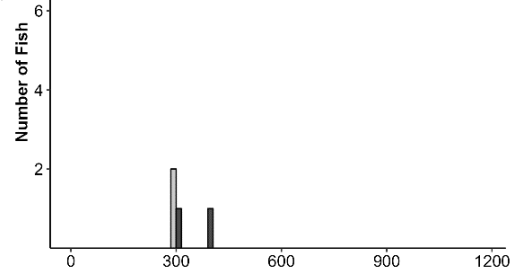
(g) May 2023



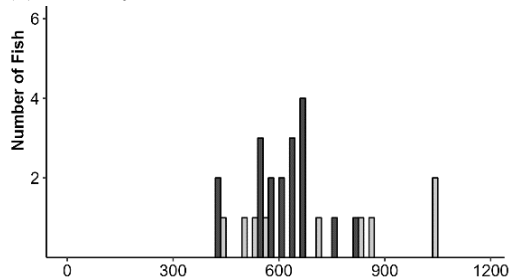
(b) December 2022



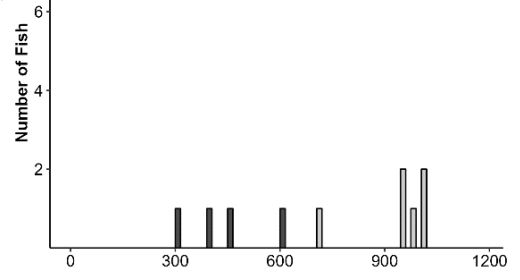
(h) June 2023



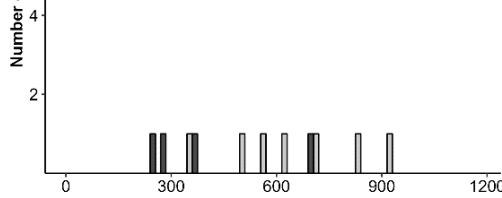
(c) January 2023



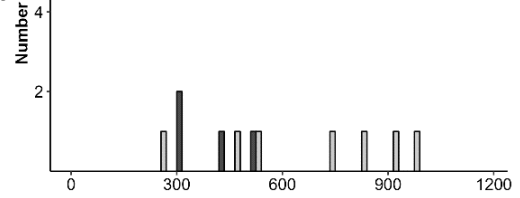
(i) July 2023



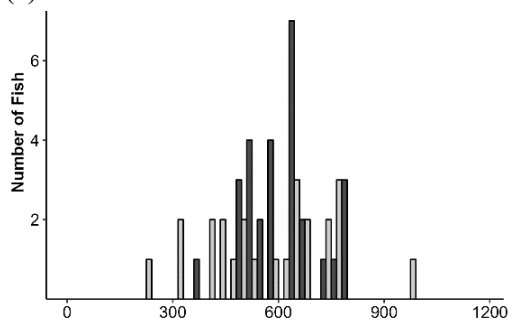
(d) February 2023



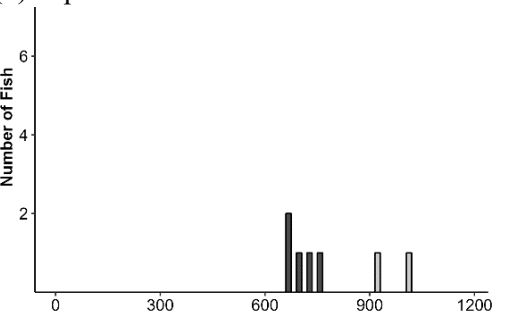
(j) August 2023



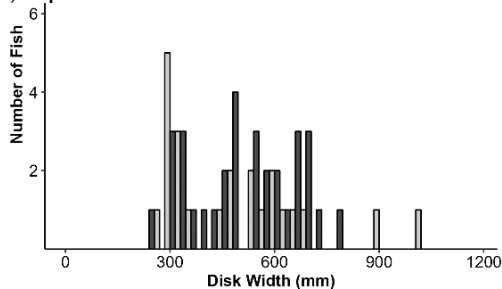
(e) March 2023



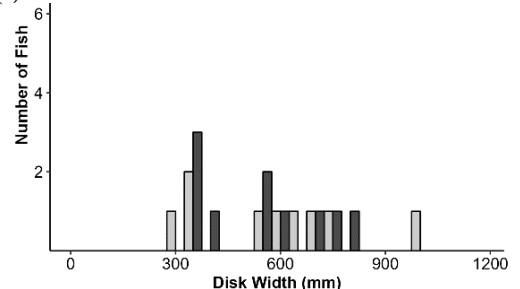
(k) September 2023



(f) April 2023

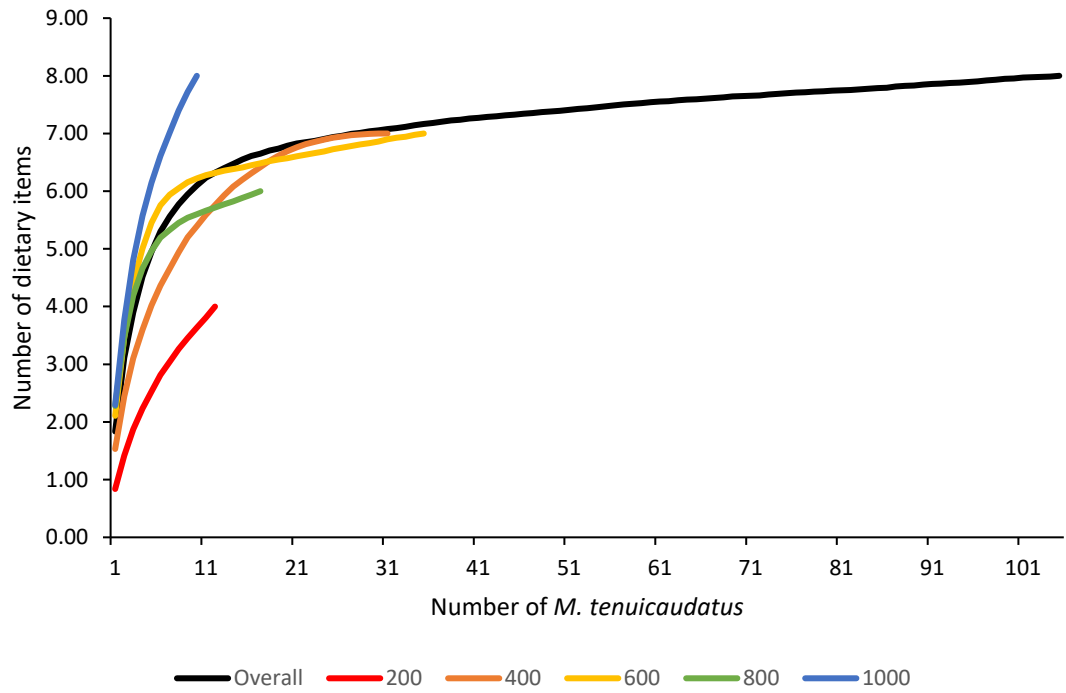


(l) October 2023



**Appendix 4.** Species accumulation curve for each (a) 200 mm disk width class and (b) season for dietary items of *Myliobatis tenuicaudatus*.

(a)



(b)

